NASA TECHNICAL MEMORANDUM

NASA TM X-1015

NASA TM X-1015

c 2

AERODYNAMIC CHARACTERISTICS OF A MANNED LIFTING ENTRY VEHICLE AT MACH NUMBERS FROM 0.2 TO 1.2

by Robert W. Rainey and Charles L. Ladson

Langley Research Center
Langley Station, Hampton, Va.

NATIONAL AERONAUTICS AND SPACE ADMINISTRATION • WASHINGTON, D. C. • SEPTEMBER 1964

AERODYNAMIC CHARACTERISTICS OF A MANNED LIFTING ENTRY VEHICLE AT MACH NUMBERS FROM 0.2 TO 1.2

By Robert W. Rainey and Charles L. Ladson

Langley Research Center
Langley Station, Hampton, Va.

NATIONAL AERONAUTICS AND SPACE ADMINISTRATION

AERODYNAMIC CHARACTERISTICS OF A MANNED LIFTING ENTRY VEHICLE AT MACH NUMBERS FROM 0.2 TO 1.2*

By Robert W. Rainey and Charles L. Ladson
Langley Research Center

SUMMARY

A research study is underway at the Langley Research Center of a blunt-leading-edge, negative-camber, delta-planform entry vehicle with horizontal-landing capability, designated HL-10. As part of this study, the aerodynamic characteristics of the vehicle have been obtained at Mach numbers from 0.2 to 1.2 at angles of attack from 0° to about 24°. The performance and static longitudinal, directional, and lateral stability and control parameters of the entry vehicle were measured. In general, the vehicle was stable and controllable and had favorable yaw due to roll and unfavorable roll due to yaw (correctable by use of roll controls) throughout the test range of Mach numbers and angles of attack. Effects of tip-fin removal, center-line dorsal-fin size, and the close proximity of a launch-vehicle adapter section upon the aerodynamic characteristics have been determined.

INTRODUCTION

Studies of manned lifting entry over a wide range of entry velocities at the Langley Research Center (ref. 1) and at other research facilities (for instance, ref. 2) have indicated that a vehicle with a hypersonic maximum lift-drag ratio of about 1 merits consideration as a future manned entry vehicle. Consequently, at the Langley Research Center an investigation of a manned lifting entry vehicle was initiated. In order that specific problems and probable solutions may be ascertained, a basic blunt body that showed considerable promise of meeting the main objectives was designed. This basic shape was studied, with and without negative camber, at hypersonic and subsonic speeds (refs. 3 and 4). From these results it was decided to use the horizontal landing version of the negative-camber basic body, designated HL-10, throughout the major portion of the initial detailed studies. (See, for instance, ref. 5.)

The purpose of this paper is to present the transonic aerodynamic characteristics of the negative-camber HL-10 vehicle with tip fin D and center-line dorsal fin E that were recommended in references 4 and 5. Tests were conducted at Mach numbers from 0.2 to 1.2 at Reynolds numbers ranging from about

*Title, Unclassified.

1.8×10^6 to about 5.1×10^6, based on body length. The entry-vehicle configuration modifications studied included removal of tip fin, changing the dorsal-fin size, installing a canopy, and deflecting the controls. In addition, the effects of a launch-vehicle adapter section in close proximity behind the entry vehicle equipped with abort rockets and windshield cover were determined. The longitudinal performance and the longitudinal, directional, and lateral stability and control data are presented without analysis.

SYMBOLS

b characteristic span for yawing- and rolling-moment coefficients

C_A axial-force coefficient, $\frac{\text{Axial force}}{qS}$

C_D drag coefficient, $\frac{\text{Drag}}{qS}$

C_L lift coefficient, $\frac{\text{Lift}}{qS}$

C_l rolling-moment coefficient, $\frac{\text{Rolling moment}}{qSb}$

$C_{l_\beta} = \frac{\partial C_l}{\partial \beta}$ per degree

C_m pitching-moment coefficient, $\frac{\text{Pitching moment}}{qSl}$

C_N normal-force coefficient, $\frac{\text{Normal force}}{qS}$

C_n yawing-moment coefficient, $\frac{\text{Yawing moment}}{qSb}$

$C_{n_\beta} = \frac{\partial C_n}{\partial \beta}$ per degree

C_Y side-force coefficient, $\frac{\text{Side force}}{qS}$

$C_{Y_\beta} = \frac{\partial C_Y}{\partial \beta}$ per degree

L/D	lift-drag ratio
l	length of vehicle
M	free-stream Mach number
q	free-stream dynamic pressure
R	Reynolds number based on vehicle length l
S	reference area equal to projected planform area with elevons
X,Y,Z	body axes
x,y,z	ordinates along body axes
α	angle of attack, deg
β	angle of sideslip, deg
δ_e	elevon deflection angle, positive with trailing edge down, deg
δ_r	rudder deflection, positive with trailing edge to left, deg
δ_a	aileron deflection angle, equal to right elevon deflection angle minus left elevon deflection angle, deg

MODEL AND DESIGNATIONS

Three-view drawings showing details of the basic HL-10 configuration and most of the various components tested are presented in figure 1. The fins, canopy, and adapter section are identified by letter designations as follows:

Fin D-1: Tip dorsal fins toed in 16° and rolled up 64.5° from the horizontal

Fin E: Center-line dorsal fin mounted either on the body with canopy off or on the canopy

Fin O: Center-line dorsal fin E mounted on the body and partially submerged in the canopy

Canopy D: Center-line canopy extending from vehicle nose to trailing edge

Launch-vehicle adapter section A: Conical section between launch vehicle and spacecraft having a semivertex angle of 45°

These model designations are a continuation of those presented in reference 5. The rolled-up tip dorsal fin is designated fin D in reference 5 and D-1 in this

report to show that there were minor angular and dimensional differences between the fins of the two models. Nondimensional cross-section ordinates for the HL-10 configuration with tip fins off are presented in table I.

The 16-inch-long model was constructed of molded fiber glass with a steel core and was equipped with interchangeable fins, elevons, and canopy. The tip fins and canopy were constructed of fiber glass, the center-line dorsal fin of aluminum, and the abort rockets and launch-vehicle adapter section of wood. The adapter section was mounted on the balance support sting with about 1/16-inch clearance between it and the model.

All coefficients are based on the total projected planform area (tip fins excluded), the span, and the length of the model. The moment center is located $0.53l$ behind the vehicle nose and $0.0125l$ below the reference center line. The reference areas and lengths are as follows:

$$S = 0.6344 \text{ sq ft}$$

$$b = 10.31 \text{ in.}$$

$$l = 16.00 \text{ in.}$$

APPARATUS, TESTS, AND PROCEDURE

The investigation was conducted in the Langley 8-foot transonic pressure tunnel. The test section of this facility has a rectangular cross section. The upper and lower walls are slotted longitudinally to allow continuous operation throughout the transonic speed range with negligible effects of choking and blockage. The dewpoint of the tunnel air was held constant at about 0° F, and the stagnation temperature of the tunnel air was automatically held at about 120° F. Control of both dewpoint and stagnation temperature minimized humidity effects. Details of the test section are presented in reference 6.

Most of the tests were conducted at Mach numbers from 0.6 to 1.2 at angles of attack from 0° to about 24°; one test was made at $M = 0.2$. The tunnel stagnation pressure was varied with Mach number and also with configuration changes due to balance overloading. A summary of the maximum and minimum dynamic pressure for each Mach number, with the corresponding Reynolds number based on model length, is presented in the following table:

M	q, lb/sq ft	R
0.2	115	3.25×10^6
0.6	421	4.24×10^6
0.8	626	5.13×10^6
	483	3.96×10^6
0.9	639	4.77×10^6
	410	3.06×10^6
1.0	353	2.48×10^6
	260	1.82×10^6
1.2	280	1.81×10^6

The angle of attack of the model was determined by measuring the angle of the support sting and adjusting it for both the tunnel airflow misalinement and the deflection of model and sting support due to aerodynamic load. The pressure within the cavity of the model base was measured, and the axial-force coefficients were adjusted to a condition of free-stream static pressure within the cavity.

The forces and moments were measured on a six-component electrical strain-gage balance mounted in the model.

All lateral and directional stability data were obtained at sideslip angles between 0° and about 6°. All longitudinal performance data are referred to the stability-axis system (see fig. 2); whereas, the directional, lateral, and longitudinal stability results are referred to the body-axis system. The longitudinal performance and stability results at sideslip angles other than 0° are in close agreement with those at $\beta = 0^\circ$ and are not presented.

ACCURACY OF RESULTS

Calibrations of the tunnel test section indicate that local deviations from the average free-stream Mach number are of the order of ± 0.005 at subsonic speeds. With increases in Mach number, these deviations increase but do not exceed 0.010 in the region of the model at $M = 1.2$. Several representative Mach number distributions along the center of the test section are presented in reference 6. The average free-stream Mach number was held to within ± 0.005 of the nominal value shown in the figures. The accuracy in angles of attack and sideslip was $\pm 0.2^\circ$. A summary of the balance accuracy in terms of the

aerodynamic coefficients for the maximum dynamic pressure at each test Mach number is presented in the following table:

M	Accuracy of static balance calibration in terms of -					
	C_N	C_A	C_m	C_l	C_n	C_Y
0.2	0.0247	0.0025	0.0021	0.0009	0.0009	0.0062
.6	.0067	.0007	.0006	.0003	.0003	.0017
.8	.0045	.0005	.0004	.0002	.0002	.0011
.9	.0044	.0004	.0004	.0002	.0002	.0011
1.0	.0080	.0008	.0007	.0003	.0003	.0020
1.2	.0101	.0010	.0009	.0004	.0004	.0025

RESULTS AND DISCUSSION

The basic data are presented in figures 3 to 17. An index of the data plots is given in table II. Although no detailed analysis of the results is presented, several pertinent areas are briefly discussed.

With tip fins D-1 either on or off and dorsal fin E installed, the vehicle is longitudinally stable and can be trimmed over a relatively large angle-of-attack range (figs. 6 and 11). No major deficiencies in longitudinal stability near trim are noted. With tip fins on and at $M = 0.8$, double reflexes in the C_m curve were obtained at several elevon deflection angles. (See figs. 3(a) to 3(d).) With $\delta_e = 0^\circ$, two stable trim points occurred at angles of attack of 7° and 13°. It is possible to alleviate this pitching-moment characteristic by differential deflection of upper and lower elevons (upper elevons at -5° and lower elevons at $+5^\circ$. (See fig. 3(h).) Removal of the tip fins eliminated most of the aforementioned C_m characteristic (figs. 10 and 11) as a result of the alteration of local flow characteristics in the vicinity of the body and fin juncture.

Large differences in the longitudinal characteristics of the entry vehicle are evident as a result of the placement of the launch-vehicle adapter section in close proximity with the vehicle and the installation of the canopy shield and abort rockets. (See figs. 14 and 15.) It is believed that large regions of separated flow existed over the aft portions of the upper and lower surfaces of the vehicle. The pressure increase in the separated-flow region reduced the drag significantly throughout the test Mach number range and reduced the slope of the lift curve at Mach numbers above about 0.8. These launch-vehicle interference effects should result in the alleviation of launch-vehicle bending moments created by the addition of this vehicle with relatively high-lift capability.

Whenever the center-line dorsal fin E is installed, the vehicle is, in general, directionally and laterally stable throughout the test ranges of Mach number and angle of attack. (See figs. 7, 12, and 17.) The negative values of C_{n_β} at $M = 1.2$ (figs. 7(b) and 7(c)) at $\alpha > 20^\circ$ are at angles of attack in excess of the trim values of 15° and 19° for the vehicle with $\delta_e = -5^\circ$ and $\delta_e = -10^\circ$, respectively. It is possible that with $\delta_e = -15^\circ$, the trim angle of attack of 22° may be high enough to cause the vehicle to approach a neutrally stable condition. The directional-stability data are not shown for this combination of angle of attack and elevon deflection in figure 7(d), since they were not available.

For most of the test conditions, roll control is positive and is accompanied by favorable yaw due to roll (fig. 8). However, the positive yaw produces an unfavorable roll due to yaw that may be offset by use of roll controls (fig. 9).

CONCLUDING REMARKS

The aerodynamic characteristics of a blunt-leading-edge, negative-camber, delta-planform entry vehicle with horizontal-landing capability, designated HL-10, have been obtained at Mach numbers from 0.2 to 1.2 and at angles of attack from 0° to about 24°. From these results it was determined that the vehicle, in general, has longitudinal, directional, and lateral static stability and is controllable with favorable yaw due to roll and unfavorable roll due to yaw; the latter can be corrected by use of roll controls. In addition, a launch-vehicle adapter section in close proximity with the entry vehicle reduced the drag and lift-curve slopes of the entry vehicle at transonic speeds.

Langley Research Center,
National Aeronautics and Space Administration,
Langley Station, Hampton, Va., April 24, 1964.

REFERENCES

1. Love, E. S., and Pritchard, E. B.: A Look at Manned Entry at Circular to Hyperbolic Velocities. 2nd Manned Space Flight Meeting (Dallas, Texas), American Inst. Aero. and Astronautics, Apr. 1963, pp. 167-180.

2. Syvertson, C. A., Swenson, B. L., Anderson, J. L., and Kenyon, G. C.: Some Considerations of the Performance of a Maneuverable, Lifting-Body, Entry Vehicle. Vol. 16, pt. one of Advances in Astronautical Sciences, Norman V. Petersen, ed., Western Periodicals Co. (N. Hollywood, Calif.), c.1963, pp. 898-918.

3. Rainey, Robert W., and Ladson, Charles L.: Preliminary Aerodynamic Characteristics of a Manned Lifting Entry Vehicle at a Mach Number of 6.8. NASA TM X-844, 1963.

4. Ware, George M.: Aerodynamic Characteristics of Models of Two Thick 74° Delta Manned Lifting Entry Vehicles at Low-Subsonic Speeds. NASA TM X-914, 1964.

5. Ladson, Charles L.: Aerodynamic Characteristics of a Manned Lifting Entry Vehicle at a Mach Number of 6.8. NASA TM X-915, 1964.

6. Mugler, John P., Jr.: Transonic Wind-Tunnel Investigation of the Aerodynamic Loading Characteristics of a 60° Delta Wing in the Presence of a Body With and Without Indentation. NACA RM L55G11, 1955.

TABLE I.- CROSS-SECTION ORDINATES FOR HL-10 WITH TIP FINS OFF

x/l = 0.042		x/l = 0.083		x/l = 0.125		x/l = 0.167	
z/l	y/l	z/l	y/l	z/l	y/l	z/l	y/l
0.0541	0	0.0681	0	0.0737	0	0.0771	0
.0532	.0083	.0668	.0083	.0729	.0083	.0763	.0083
.0503	.0167	.0637	.0167	.0702	.0167	.0744	.0167
.0441	.0250	.0579	.0250	.0660	.0250	.0712	.0250
.0375	.0306	.0502	.0333	.0594	.0330	.0664	.0333
.0333	.0338	.0417	.0392	.0505	.0417	.0597	.0417
.0250	.0390	.0330	.0444	.0417	.0477	.0512	.0500
.0167	.0431	.0250	.0487	.0333	.0528	.0417	.0565
.0083	.0459	.0167	.0521	.0250	.0571	.0333	.0618
0	.0476	.0083	.0547	.0167	.0604	.0250	.0664
-.0536	0	0	.0568	.0083	.0632	.0167	.0701
		-.0083	.0585	0	.0656	.0083	.0732
		-.0167	.0596	-.0083	.0675	0	.0757
		-.0752	0	-.0167	.0691	-.0083	.0778
				-.0250	.0704	-.0167	.0796
				-.0333	.0714	-.0250	.0811
				-.0904	0	-.0333	.0823
						-.0417	.0833
						-.0500	.0840
						-.1026	0

TABLE I.- CROSS-SECTION ORDINATES FOR HL-10 WITH TIP FINS OFF - Continued

x/l = 0.208		x/l = 0.250		x/l = 0.292		x/l = 0.333	
z/l	y/l	z/l	y/l	z/l	y/l	z/l	y/l
0.0792	0	0.0807	0	0.0817	0	0.0820	0
.0787	.0083	.0803	.0083	.0814	.0083	.0818	.0083
.0772	.0167	.0792	.0167	.0807	.0167	.0813	.0167
.0747	.0250	.0773	.0250	.0794	.0250	.0803	.0250
.0712	.0333	.0748	.0333	.0774	.0333	.0789	.0333
.0664	.0416	.0712	.0417	.0750	.0417	.0771	.0417
.0592	.0500	.0666	.0500	.0715	.0500	.0747	.0500
.0517	.0583	.0606	.0583	.0672	.0583	.0716	.0583
.0417	.0656	.0527	.0667	.0617	.0667	.0677	.0667
.0333	.0713	.0458	.0721	.0546	.0750	.0627	.0750
.0250	.0760	.0417	.0754	.0500	.0789	.0564	.0833
.0167	.0800	.0333	.0811	.0417	.0858	.0485	.0917
.0083	.0833	.0250	.0862	.0333	.0918	.0417	.0968
0	.0860	.0167	.0902	.0250	.0969	.0333	.1027
-.0083	.0882	.0083	.0937	.0167	.1010	.0250	.1078
-.0167	.0902	0	.0965	.0083	.1044	.0167	.1119
-.0250	.0919	-.0083	.0990	0	.1072	.0083	.1152
-.0333	.0933	-.0167	.1011	-.0083	.1098	0	.1179
-.0417	.0946	-.0250	.1027	-.0167	.1119	-.0083	.1204
-.0500	.0955	-.0333	.1044	-.0250	.1137	-.0167	.1227
-.0583	.0962	-.0417	.1057	-.0333	.1156	-.0250	.1250
		-.0500	.1067	-.0417	.1170	-.0333	.1267
-.1126	0	-.0583	.1076	-.0500	.1182	-.0417	.1282
		-.0667	.1083	-.0583	.1192	-.0500	.1296
		-.1205	0	-.0667	.1198	-.0583	.1306
				-.0750	.1202	-.0667	.1317
				-.1268	0	-.0750	.1321
						-.1312	0

TABLE I.- CROSS-SECTION ORDINATES FOR HL-10 WITH TIP FINS OFF - Continued

x/l = 0.375		x/l = 0.417		x/l = 0.458		x/l = 0.500	
z/l	y/l	z/l	y/l	z/l	y/l	z/l	y/l
0.0821	0	0.0814	0	0.0800	0	0.0782	0
.0820	.0083	.0813	.0083	.0799	.0083	.0782	.0167
.0816	.0167	.0811	.0167	.0797	.0167	.0780	.0250
.0809	.0250	.0805	.0250	.0794	.0250	.0776	.0333
.0799	.0333	.0797	.0333	.0788	.0333	.0770	.0417
.0783	.0417	.0786	.0417	.0780	.0417	.0762	.0500
.0766	.0500	.0772	.0500	.0768	.0500	.0751	.0583
.0744	.0583	.0755	.0583	.0755	.0583	.0738	.0667
.0714	.0667	.0733	.0667	.0739	.0667	.0723	.0750
.0679	.0750	.0706	.0750	.0720	.0750	.0705	.0833
.0633	.0833	.0674	.0833	.0694	.0833	.0682	.0917
.0576	.0917	.0633	.0917	.0664	.0917	.0655	.1000
.0503	.1000	.0582	.1000	.0629	.1000	.0620	.1083
.0415	.1083	.0517	.1083	.0581	.1083	.0579	.1167
.0333	.1136	.0437	.1167	.0526	.1167	.0529	.1250
.0250	.1187	.0375	.1211	.0453	.1250	.0467	.1333
.0167	.1229	.0333	.1241	.0363	.1333	.0390	.1417
.0083	.1262	.0250	.1296	.0292	.1379	.0333	.1458
0	.1292	.0167	.1339	.0250	.1407	.0250	.1521
-.0083	.1315	.0083	.1375	.0167	.1454	.0167	.1571
-.0167	.1337	0	.1406	.0083	.1491	.0083	.1612
-.0250	.1358	-.0083	.1431	0	.1521	0	.1643
-.0333	.1377	-.0167	.1453	-.0083	.1549	-.0083	.1672
-.0417	.1394	-.0250	.1472	-.0167	.1571	-.0167	.1694
-.0500	.1408	-.0333	.1492	-.0250	.1592	-.0250	.1715
-.0583	.1420	-.0417	.1508	-.0333	.1611	-.0333	.1733
-.0667	.1429	-.0500	.1523	-.0417	.1627	-.0417	.1750
-.0750	.1437	-.0583	.1536	-.0500	.1642	-.0500	.1763
-.0833	.1442	-.0667	.1546	-.0583	.1654	-.0583	.1775
-.1334	0	-.0750	.1554	-.0667	.1664	-.0667	.1785
		-.0833	.1559	-.0750	.1672	-.0750	.1792
		-.1340	0	-.0833	.1677	-.1285	0
				-.1322	0		

TABLE I.- CROSS-SECTION ORDINATES FOR HL-10 WITH TIP FINS OFF - Continued

x/l = 0.542		x/l = 0.583		x/l = 0.625		x/l = 0.667	
z/l	y/l	z/l	y/l	z/l	y/l	z/l	y/l
0.0759	0	0.0741	0	0.0716	0	0.0687	0
.0759	.0166	.0741	.0104	.0716	.0104	.0686	.0208
.0758	.0249	.0740	.0271	.0716	.0271	.0686	.0375
.0756	.0332	.0735	.0437	.0713	.0437	.0684	.0541
.0752	.0415	.0726	.0604	.0707	.0604	.0678	.0708
.0747	.0498	.0710	.0771	.0696	.0771	.0669	.0875
.0740	.0581	.0671	.0937	.0678	.0937	.0655	.1041
.0730	.0664	.0668	.1020	.0655	.1104	.0634	.1208
.0718	.0747	.0651	.1104	.0637	.1187	.0601	.1374
.0705	.0830	.0626	.1187	.0616	.1270	.0580	.1458
.0688	.0913	.0596	.1270	.0591	.1354	.0553	.1541
.0666	.0996	.0563	.1354	.0558	.1437	.0522	.1624
.0642	.1079	.0521	.1437	.0521	.1520	.0483	.1708
.0611	.1162	.0471	.1520	.0478	.1604	.0439	.1791
.0575	.1245	.0412	.1604	.0429	.1687	.0385	.1874
.0530	.1328	.0337	.1687	.0365	.1770	.0317	.1958
.0476	.1411	.0250	.1756	.0292	.1842	.0250	.2015
.0410	.1494	.0167	.1813	.0250	.1878	.0167	.2080
.0326	.1577	.0083	.1860	.0167	.1941	.0083	.2128
.0249	.1629	0	.1897	.0083	.1991	0	.2167
.0166	.1685	-.0083	.1926	0	.2028	-.0083	.2197
.0083	.1729	-.0167	.1949	-.0083	.2057	-.0167	.2218
0	.1764	-.0250	.1970	-.0167	.2080	-.0250	.2237
-.0083	.1790	-.0333	.1988	-.0250	.2101	-.0333	.2254
-.0166	.1815	-.0417	.2003	-.0333	.2118	-.0417	.2264
-.0249	.1834	-.0500	.2017	-.0417	.2132	-.0986	0
-.0332	.1853	-.0583	.2028	-.0500	.2143		
-.0415	.1869	-.1156	0	-.1073	0		
-.0498	.1882						
-.0581	.1893						
-.0664	.1902						
-.1229	0						

TABLE I.- CROSS-SECTION ORDINATES FOR HL-10 WITH TIP FINS OFF - Concluded

x/l = 0.708		x/l = 0.750		x/l = 0.792		x/l = 0.833	
z/l	y/l	z/l	y/l	z/l	y/l	z/l	y/l
0.0654	0	0.0617	0	0.0578	0	0.0536	0
.0653	.0417	.0616	.0625	.0577	.0937	.0534	.1666
.0651	.0583	.0615	.0791	.0576	.1104	.0532	.1833
.0650	.0750	.0611	.0958	.0573	.1270	.0528	.1999
.0643	.0916	.0606	.1125	.0569	.1437	.0521	.2166
.0634	.1083	.0596	.1291	.0561	.1604	.0510	.2332
.0617	.1250	.0581	.1458	.0549	.1770	.0482	.2499
.0596	.1416	.0561	.1624	.0532	.1937	.0455	.2582
.0582	.1499	.0533	.1791	.0506	.2103	.0400	.2666
.0563	.1583	.0488	.1958	.0486	.2187	.0333	.2707
.0542	.1666	.0458	.2041	.0460	.2270	.0250	.2736
.0517	.1749	.0421	.2124	.0425	.2353	.0167	.2749
.0487	.1833	.0372	.2207	.0375	.2437	.0083	.2753
.0446	.1916	.0333	.2256	.0333	.2481	0	.2753
.0398	.1999	.0292	.2307	.0250	.2551	-.0563	0
.0340	.2083	.0250	.2347	.0167	.2588		
.0292	.2130	.0167	.2409	.0083	.2611		
.0250	.2168	.0083	.2447	0	.2624		
.0167	.2235	0	.2470	-.0083	.2631		
.0083	.2283	-.0083	.2491	-.0167	.2634		
0	.2317	-.0167	.2504	-.0673	0		
-.0083	.2343	-.0250	.2511				
-.0167	.2363	-.0785	0				
-.0250	.2378						
-.0333	.2390						
-.0889	0						
x/l = 0.875		x/l = 0.917		x/l = 0.958		x/l = 1.000	
0.0487	0	0.0440	0	0.0392	0	0.0344	0
-.0452	0	-.0341	0	-.0227	0	-.0125	0

TABLE II.- INDEX TO DATA PLOTS

Figure	Tip fin	Center fin	Canopy	Adapter section A	δ_e, deg	δ_a, deg	δ_r, deg	Data plotted
3(a)	D-1	E	Off	Off	0	0	0	C_L, C_D, L/D, C_m against α
3(b)					-5			
3(c)					-10			
3(d)					-15			
3(e)					5			
3(f)					10			
3(g)					15			
3(h)					±5			
4(a)					0	-10		
4(b)					0	-20		
4(c)					0	-30		
4(d)					-10	-10		
4(e)					-10	-20		
4(f)					10	-10		
4(g)					10	-20		
5(a)					0	0	22.5	
5(b)					0		45.0	
6					Variable		0	C_m against C_N
7(a)					0			C_{l_β}, C_{n_β}, C_{Y_β} against α
7(b)					-5			
7(c)					-10			
7(d)					-15			
7(e)					10			
7(f)					15			
8(a)					0	-10		ΔC_l, ΔC_n, ΔC_Y against α
8(b)					0	-20		
8(c)					0	-30		
8(d)					-10	-10		
8(e)					-10	-20		
8(f)					10	-10		
8(g)					10	-20		
9(a)					0	0	22.5	
9(b)					0		45.0	
10(a)	Off				0		0	C_L, C_D, L/D, C_m against α
10(b)					-15			
10(c)					15			
11					Variable			C_m against C_N
12					0			C_{l_β}, C_{n_β}, C_{Y_β} against α
13(a)	D-1		D		0			C_L, C_D, L/D, C_m against α
13(b)					-10			
13(c)		0			0			
13(d)		Off			0			
14		E		On and off	0			
15		E			Variable			C_m against C_N
16		On and off		Off	0			C_m against C_N
17(a)		E						C_l, C_n, C_Y against β
17(b)		E						C_{l_β}, C_{n_β}, C_{Y_β} against α
17(c)		0						C_{l_β}, C_{n_β}, C_{Y_β} against α
17(d)		Off						C_l, C_n, C_Y against β
17(e)		Off						C_{l_β}, C_{n_β}, C_{Y_β} against α

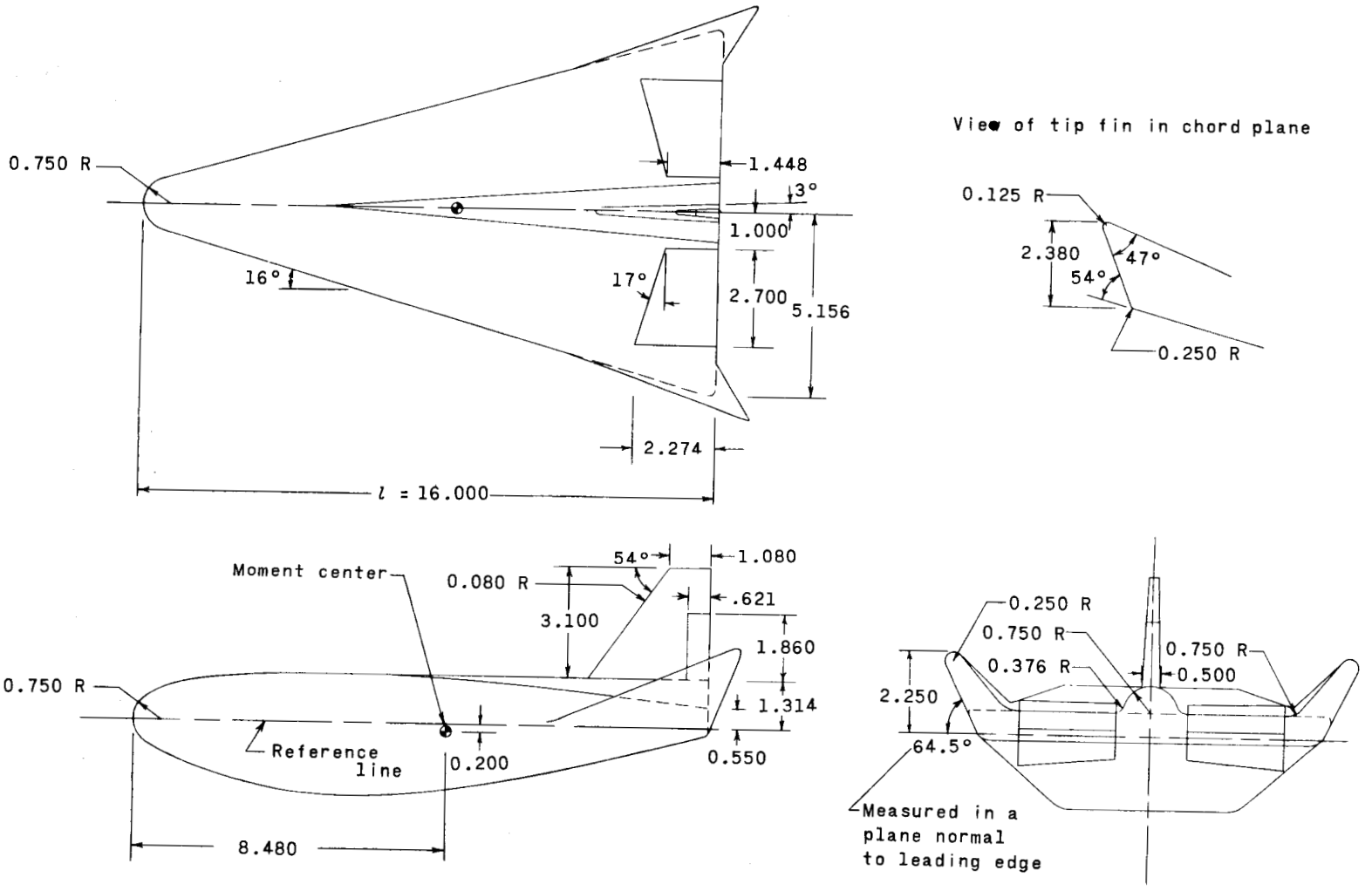

(a) HL-10 with tip fin D-1 and center fin E.

Figure 1.- Basic HL-10 model and components. (All dimensions are in inches unless otherwise noted.)

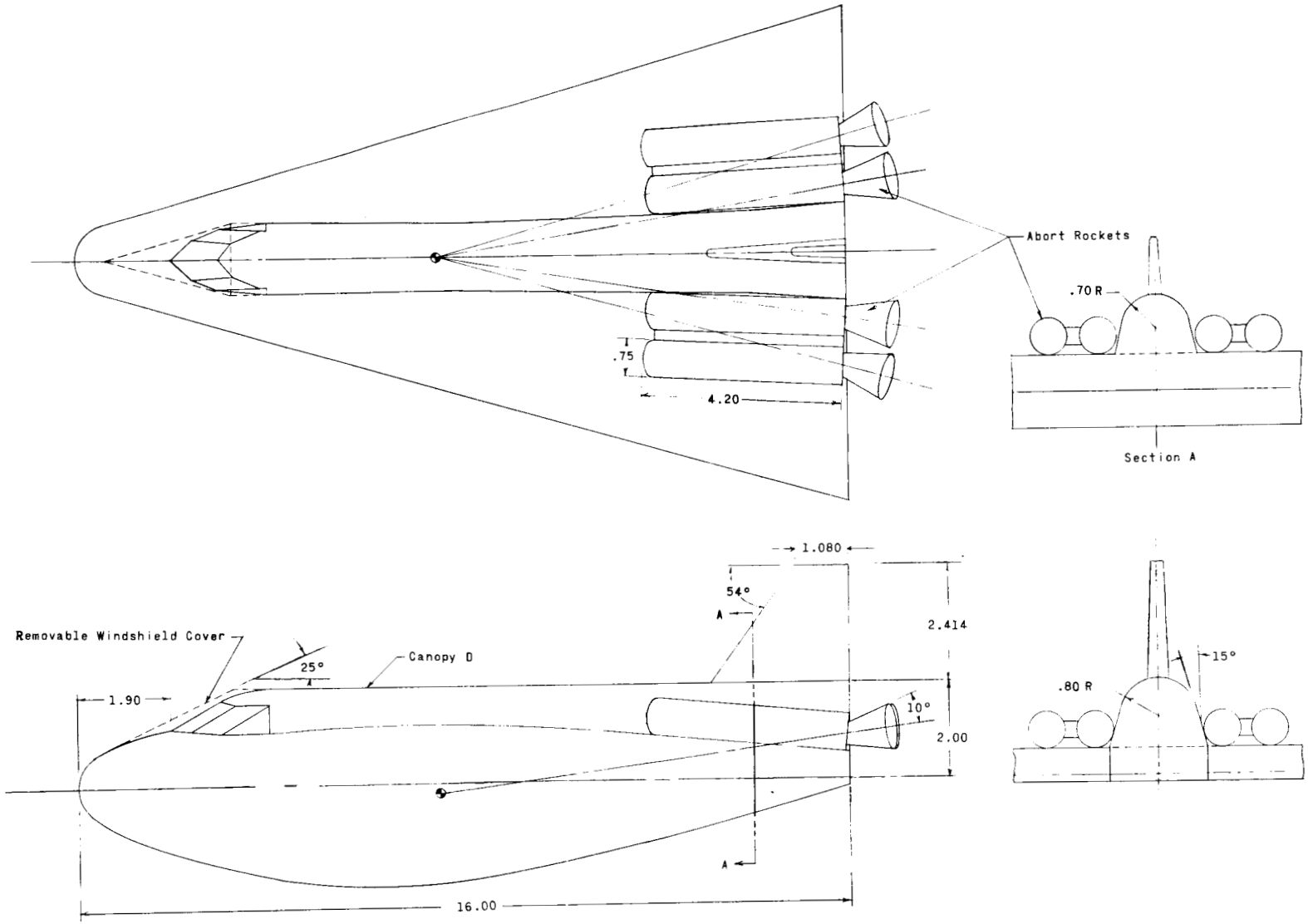

(b) Details of canopy, abort rockets, and center fin O.

Figure 1.- Continued.

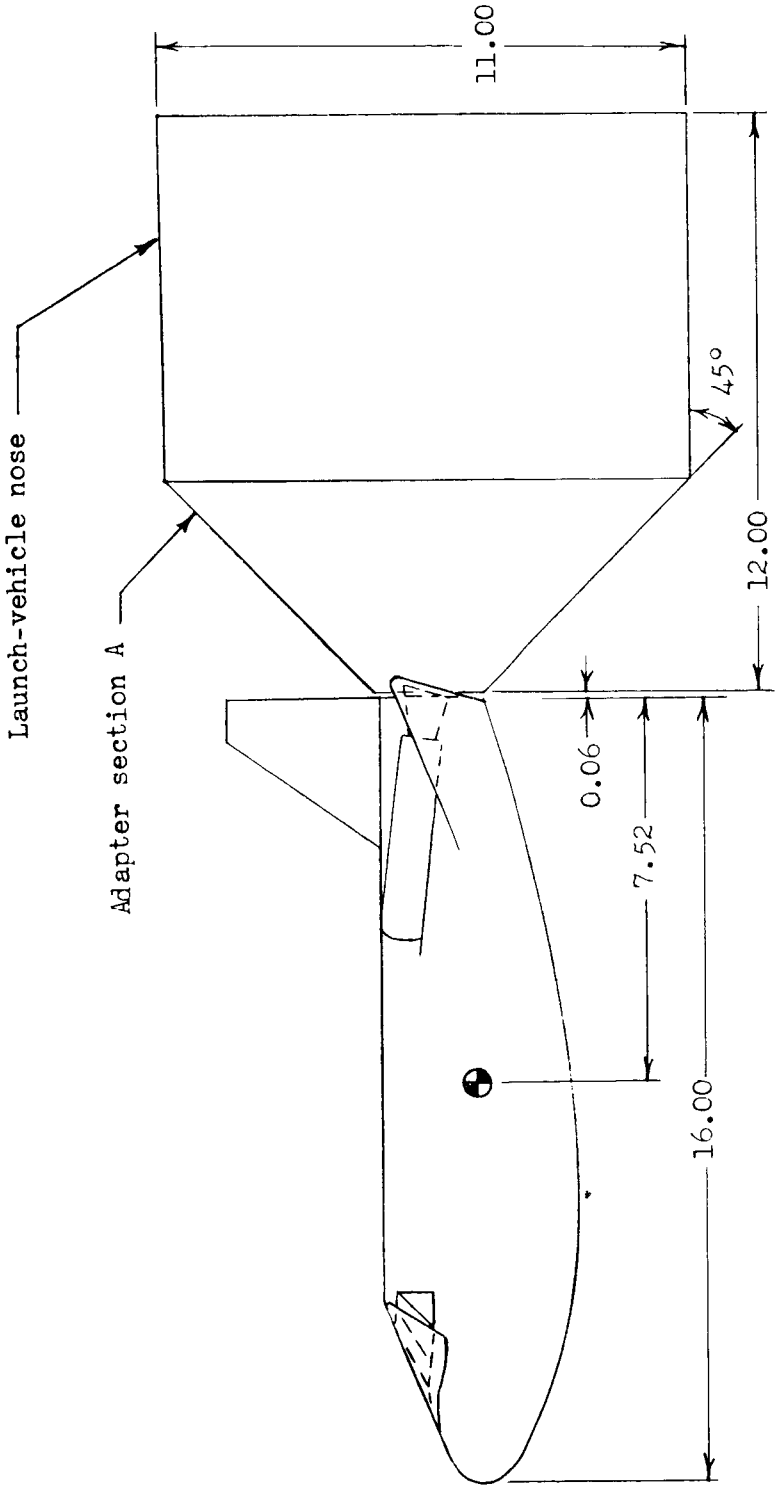

(c) HL-10 in close proximity with launch-vehicle adapter section A.

Figure 1.- Continued.

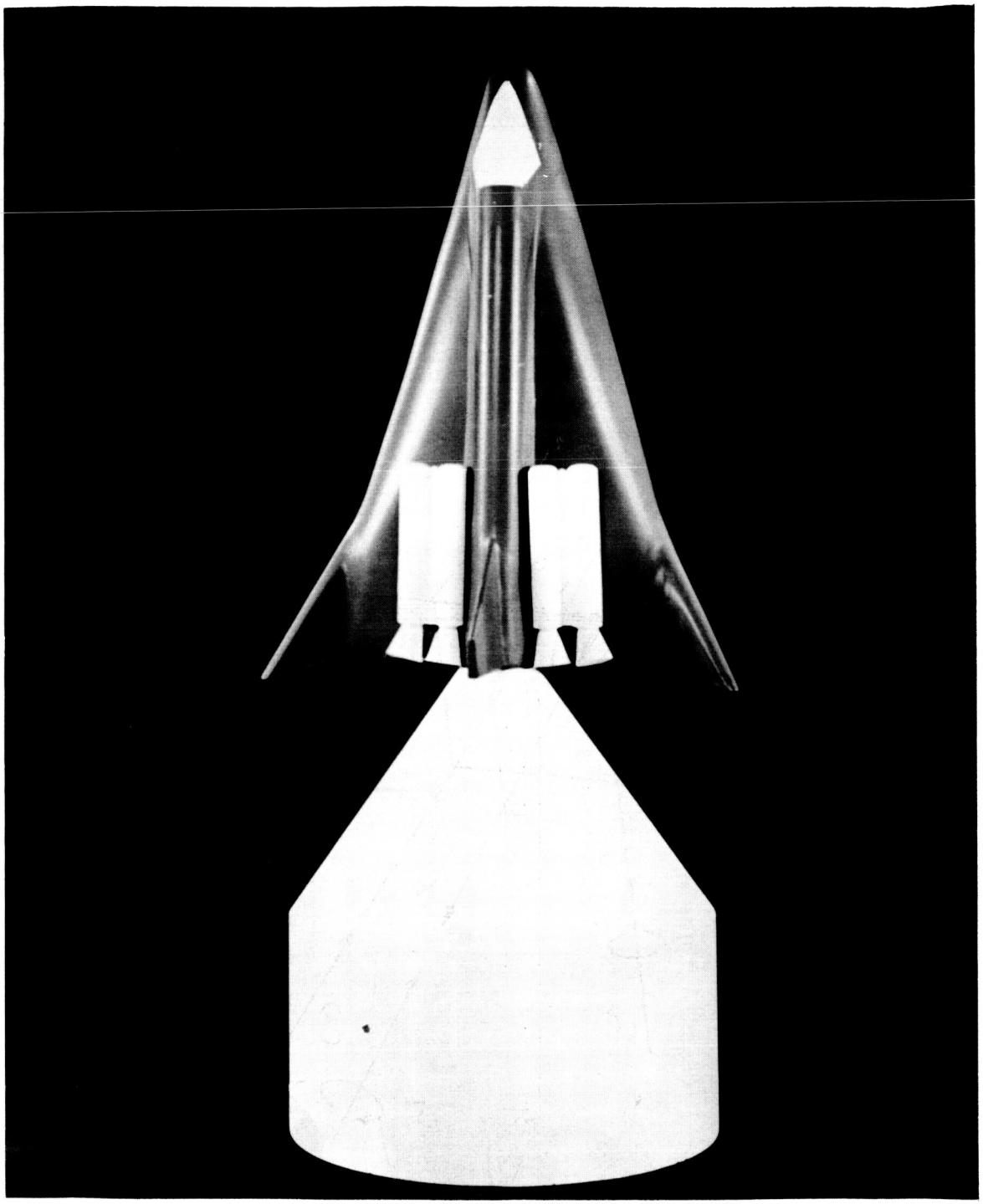

L-64-808

(d) HL-10 with canopy D, abort rockets, and launch-vehicle adapter section A.

Figure 1.- Concluded.

Figure 2.- Axes systems with positive directions of forces, moments, and angles indicated by arrows.

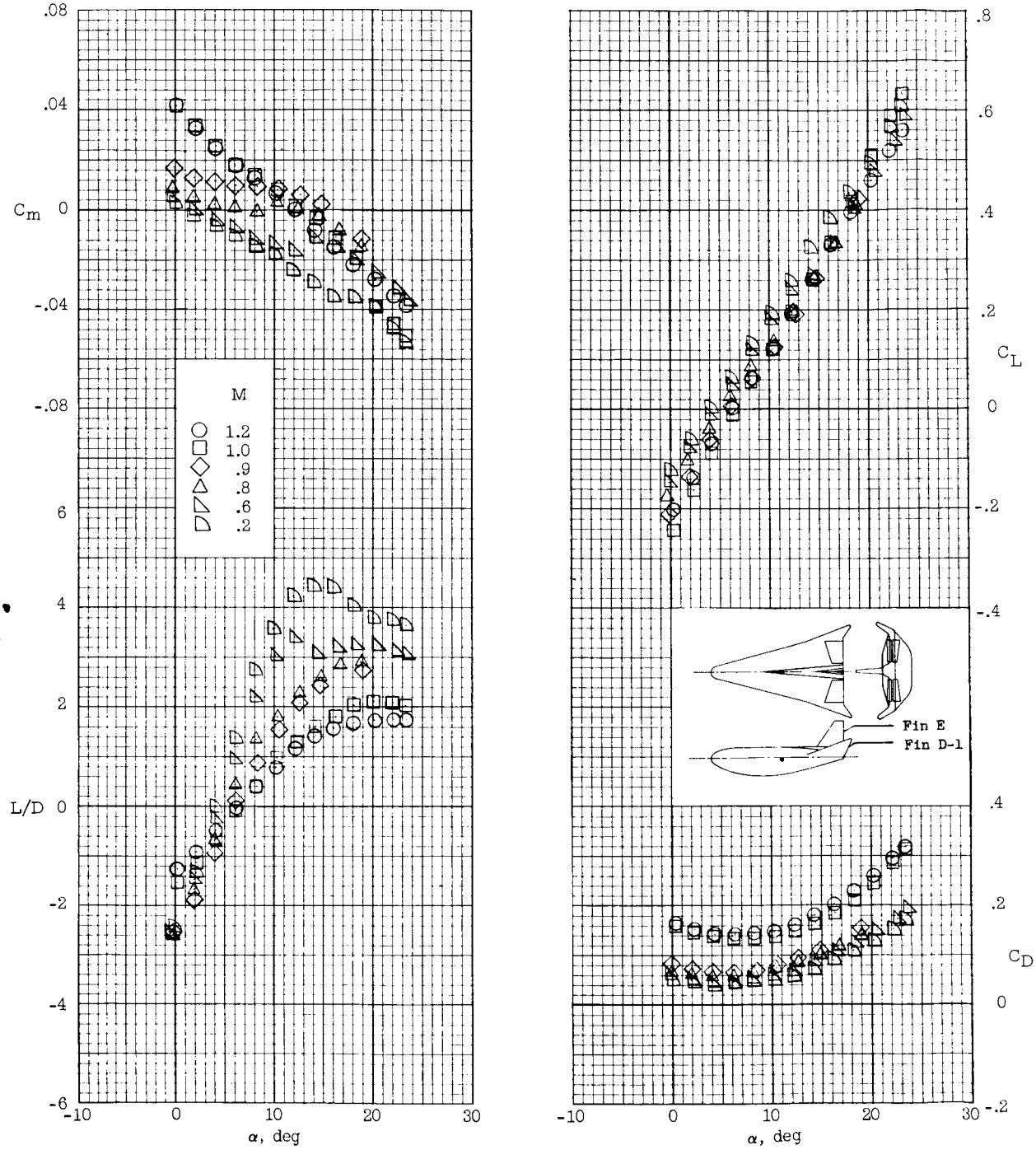

(a) $\delta_e = 0^o$.

Figure 3.- Longitudinal performance of HL-10 model with center fin E, tip fins D-1, $\beta = 0^o$, $\delta_a = 0^o$, and $\delta_r = 0^o$.

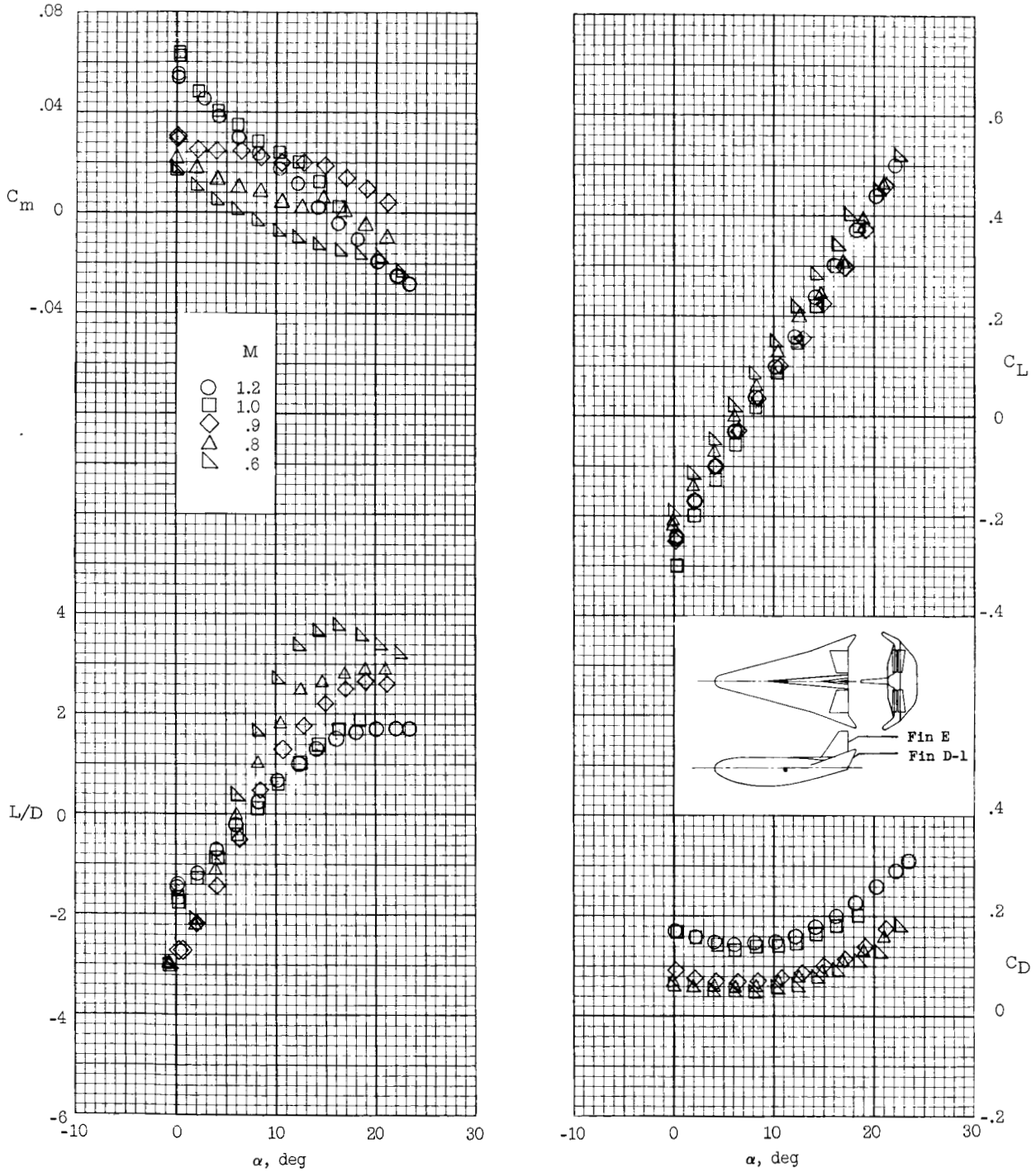

(b) $\delta_e = -5^\circ$

Figure 3.- Continued.

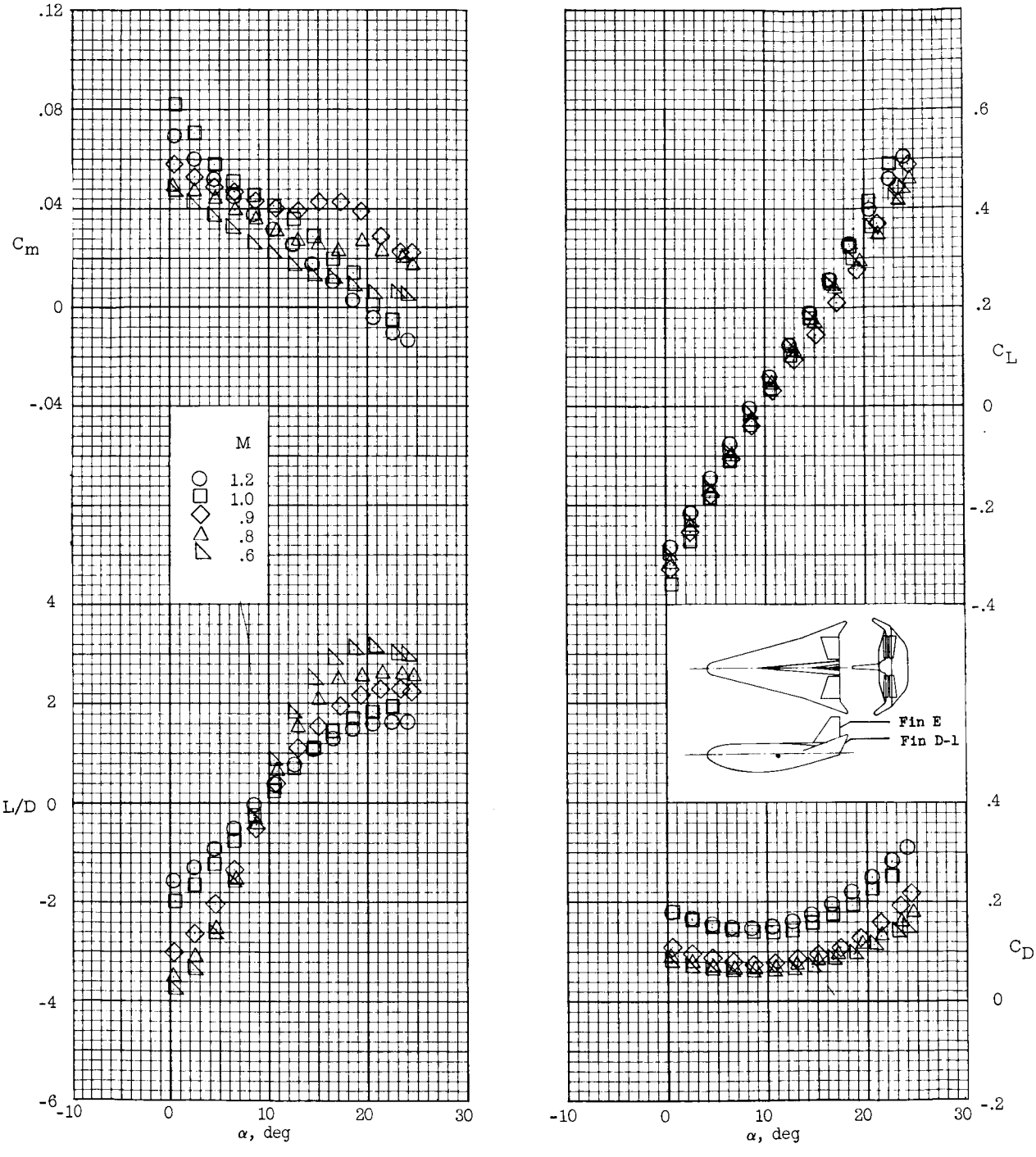

(c) $\delta_e = -10^\circ$.

Figure 3.- Continued.

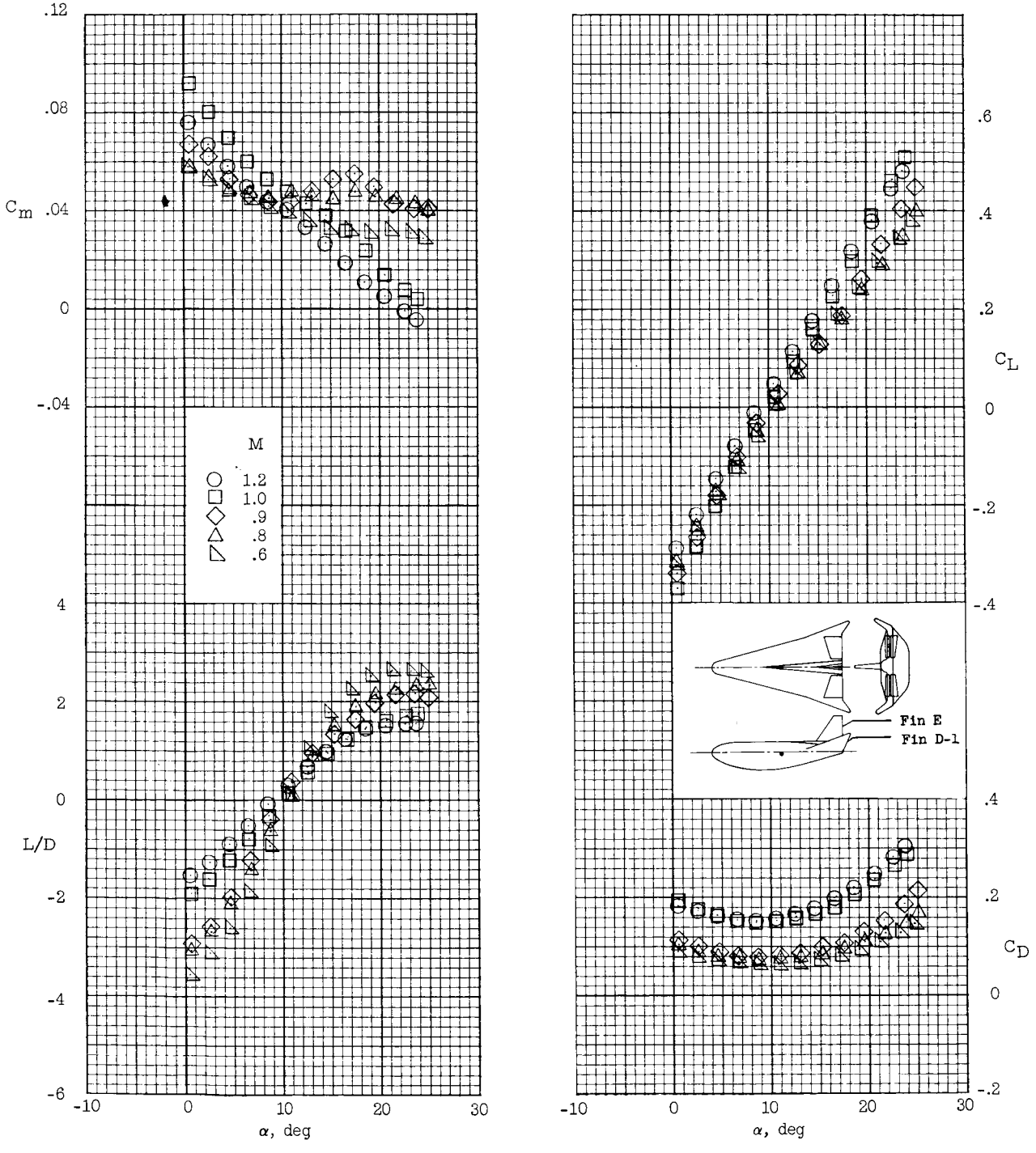

(d) $\delta_e = -15^\circ$.

Figure 3.- Continued.

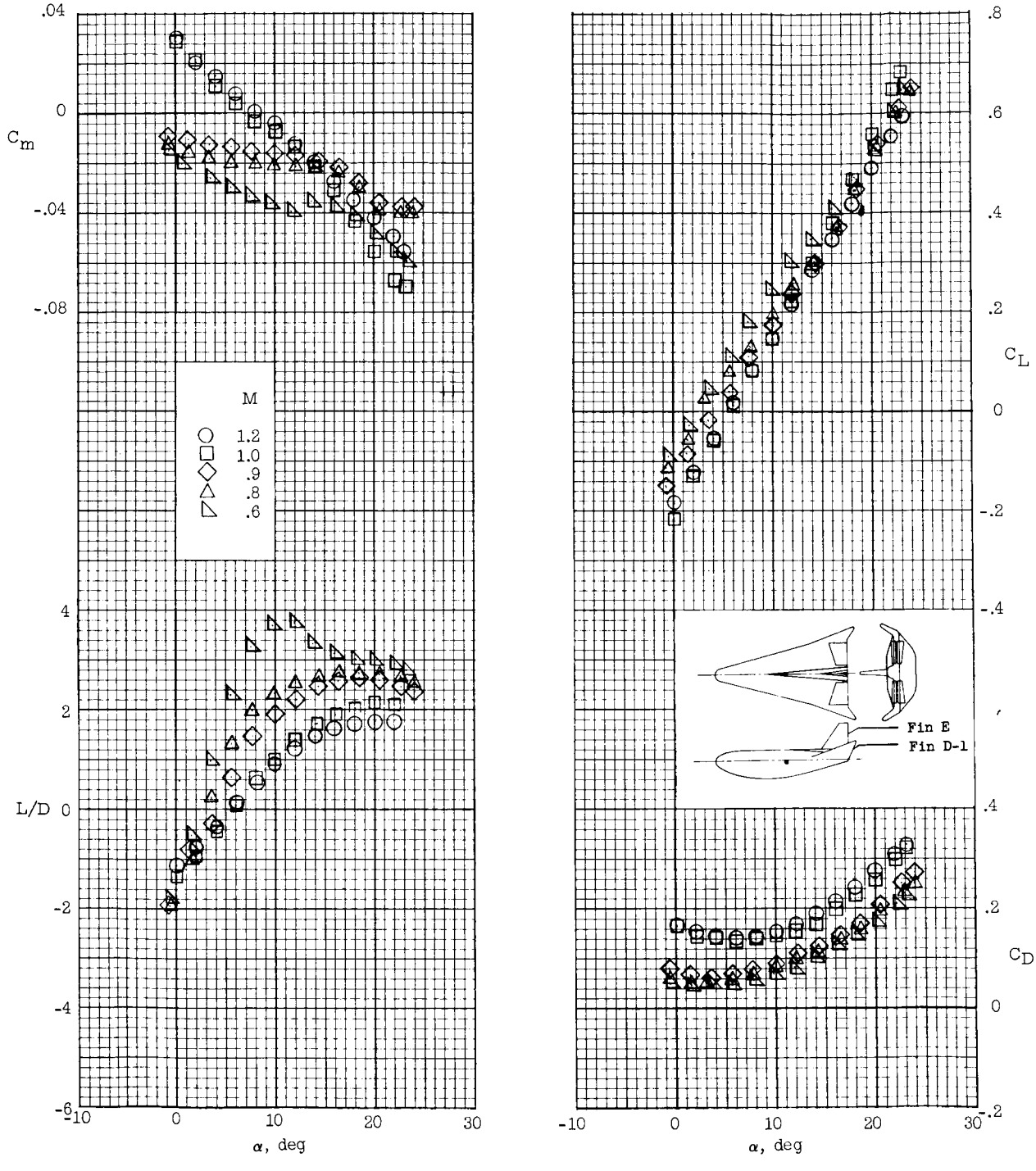

(e) $\delta_e = 5^\circ$.

Figure 3.- Continued.

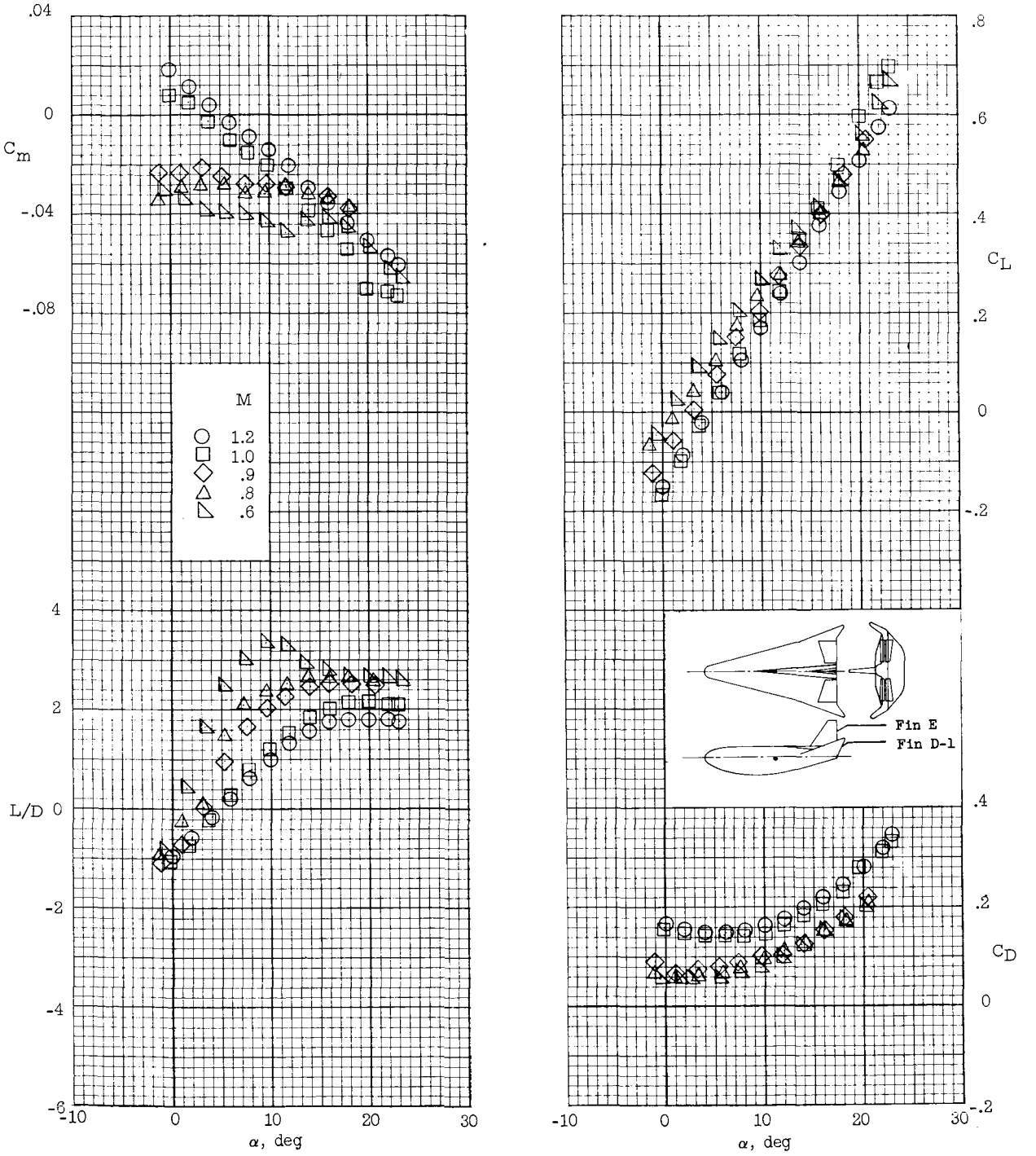

(f) $\delta_e = 10^\circ$.

Figure 3.- Continued.

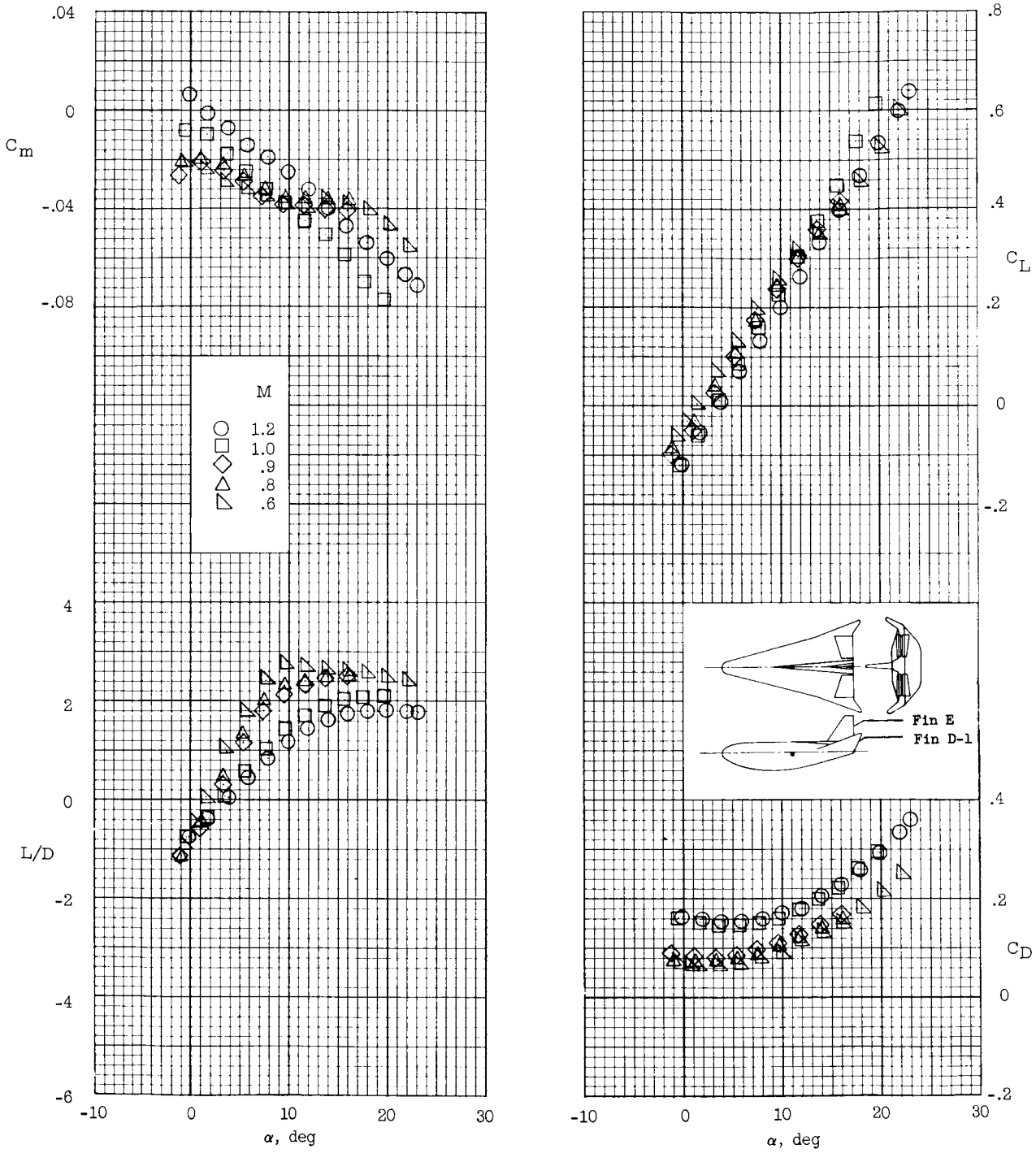

(g) $\delta_e = 15°$.

Figure 3.- Continued.

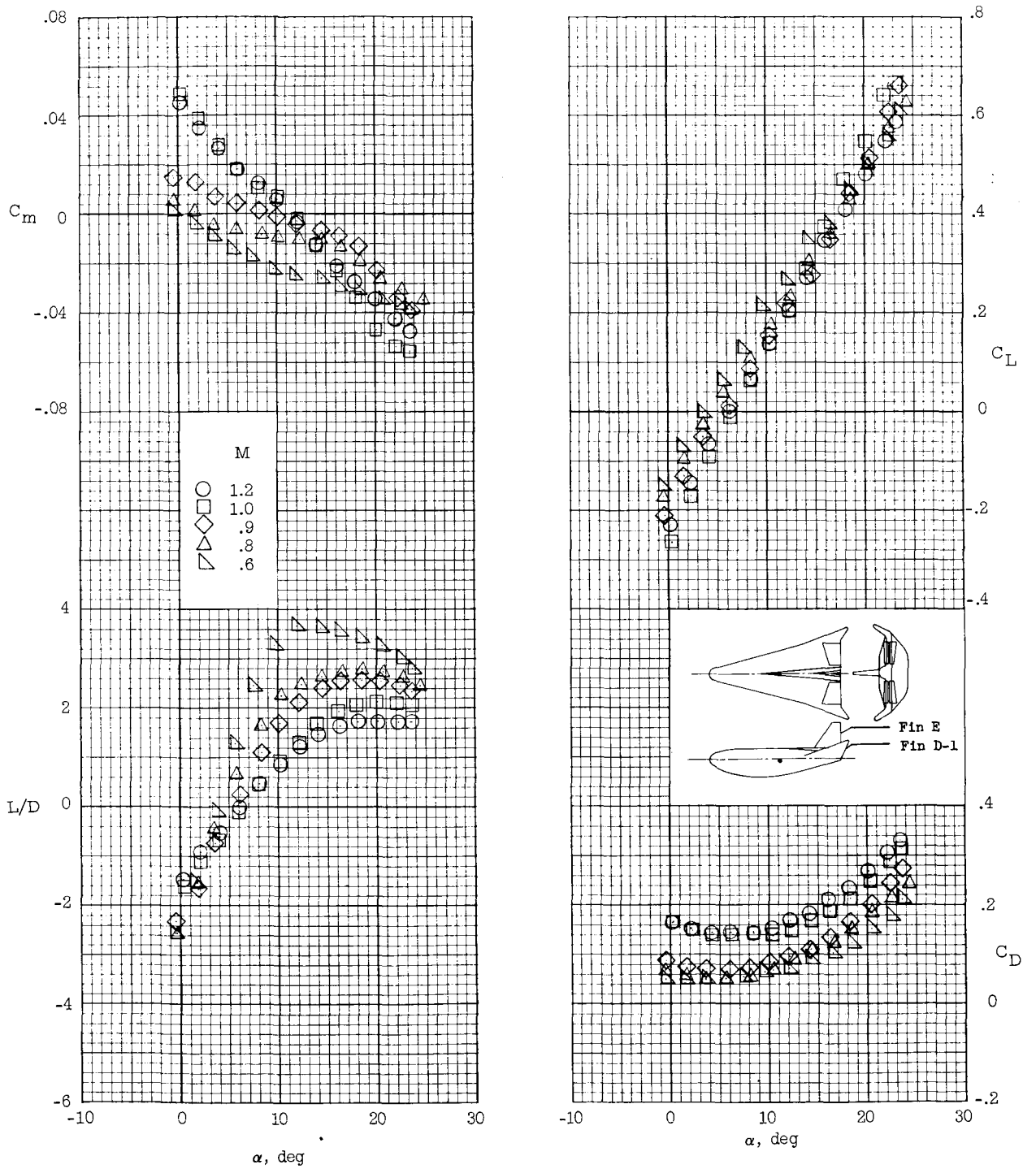

(h) $\delta_{e,upper} = -5^{\circ}$; $\delta_{e,lower} = 5^{\circ}$.

Figure 3.- Concluded.

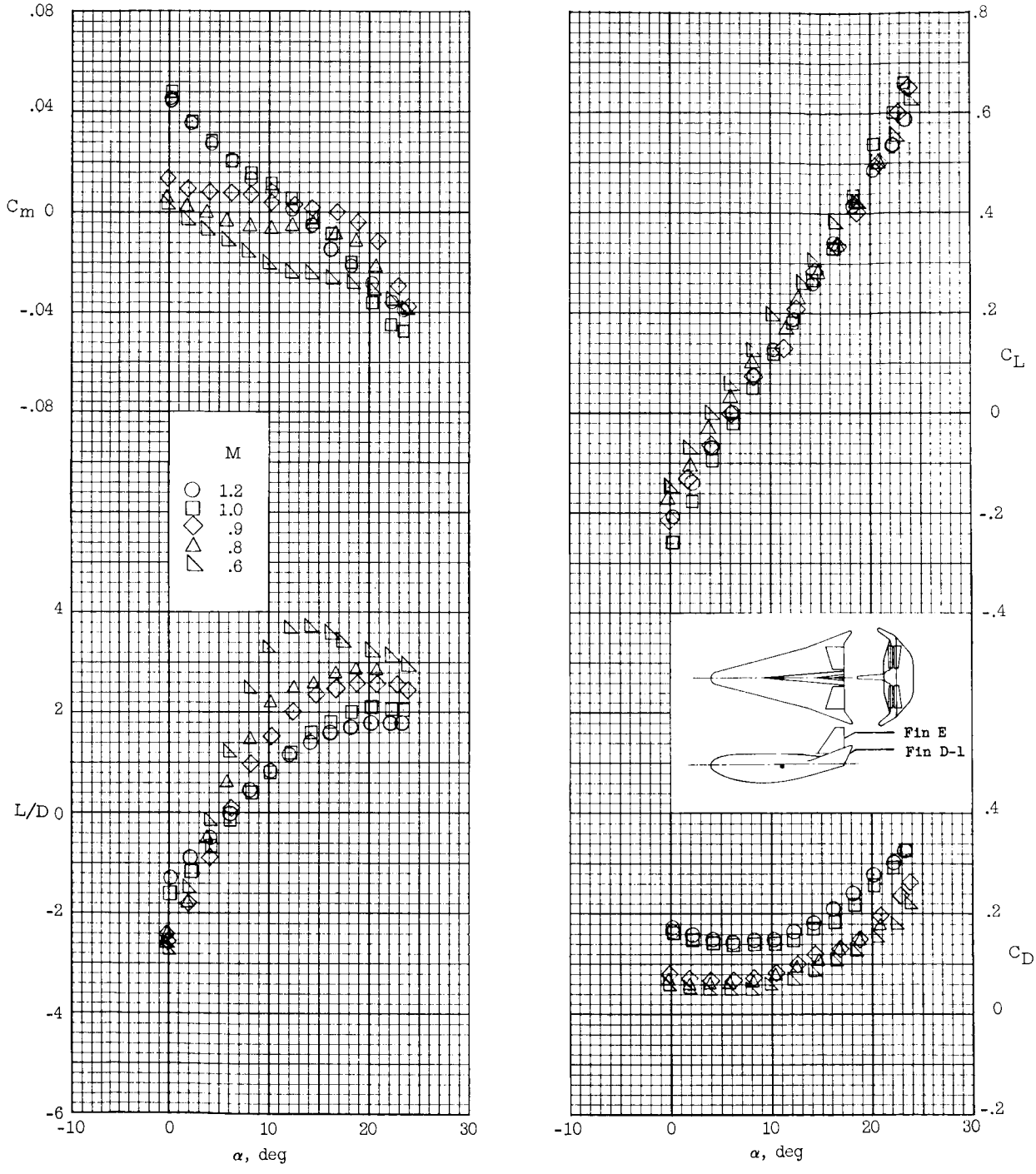

(a) $\delta_e = 0^o$; $\delta_a = -10^o$.

Figure 4.- Longitudinal performance of HL-10 model with center fin E, tip fins D-1, $\beta = 0^o$, and $\delta_r = 0^o$.

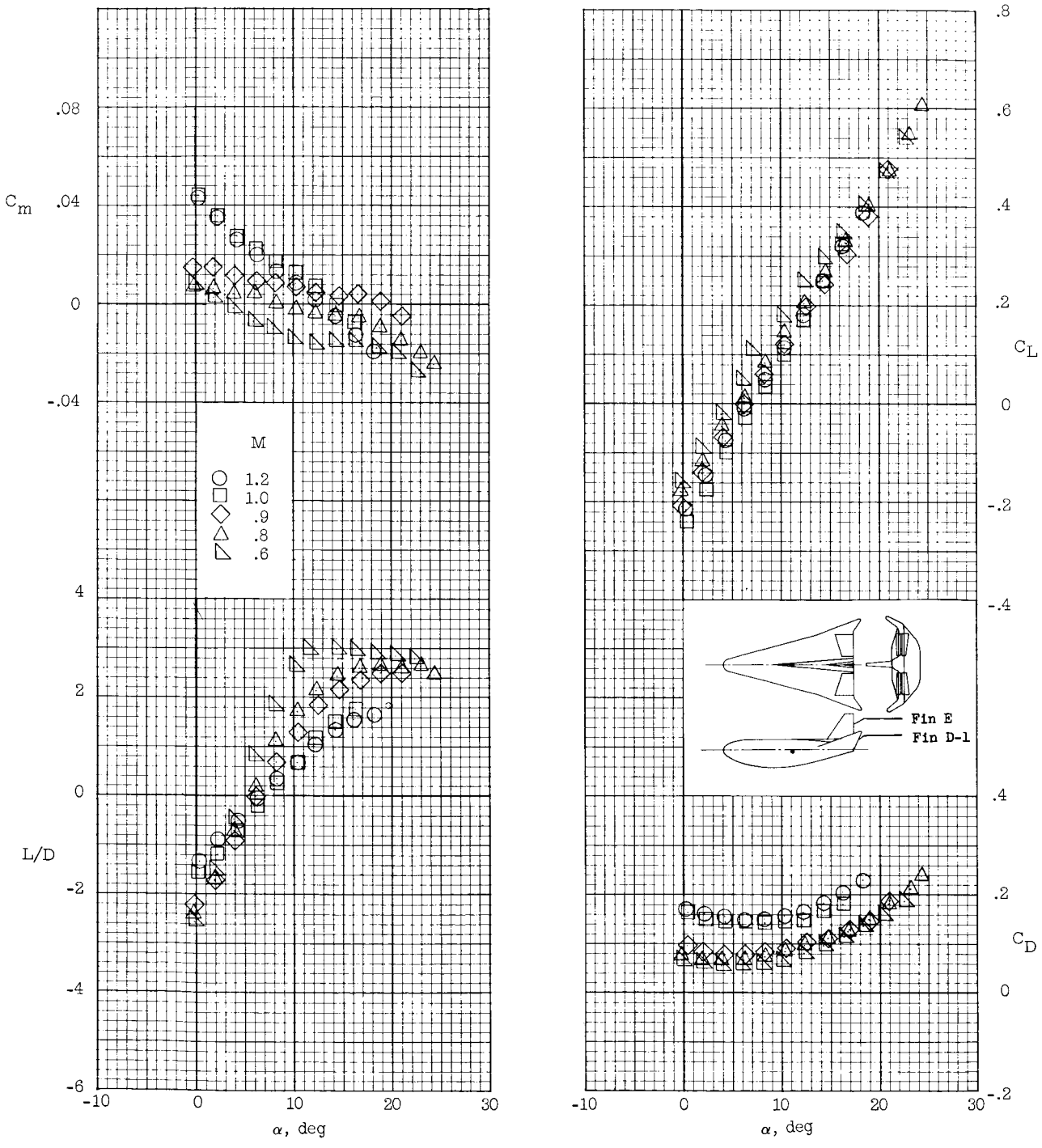

(b) $\delta_e = 0^o$; $\delta_a = -20^o$.

Figure 4.- Continued.

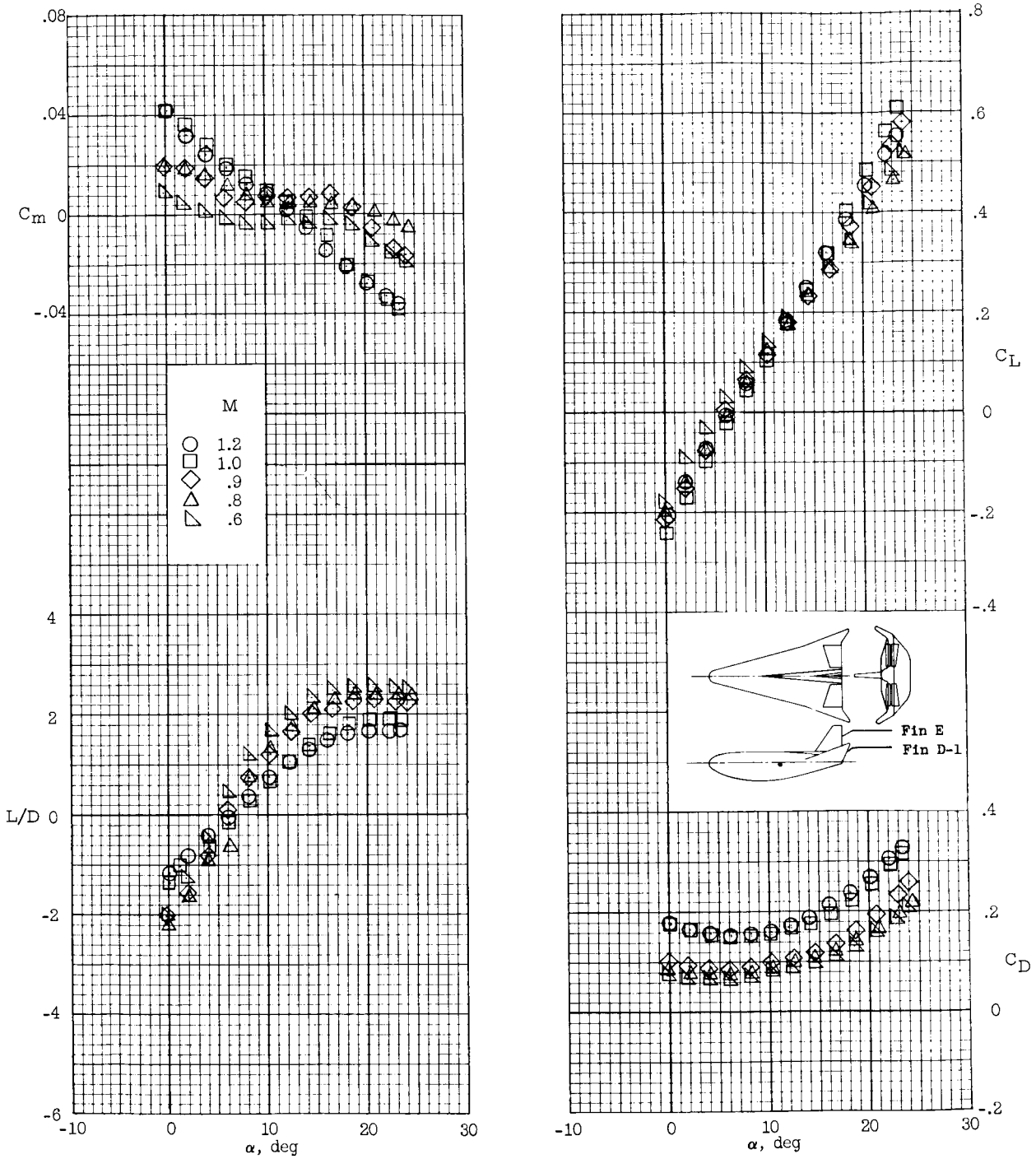

(c) $\delta_e = 0^\circ$; $\delta_a = -30^\circ$.

Figure 4.- Continued.

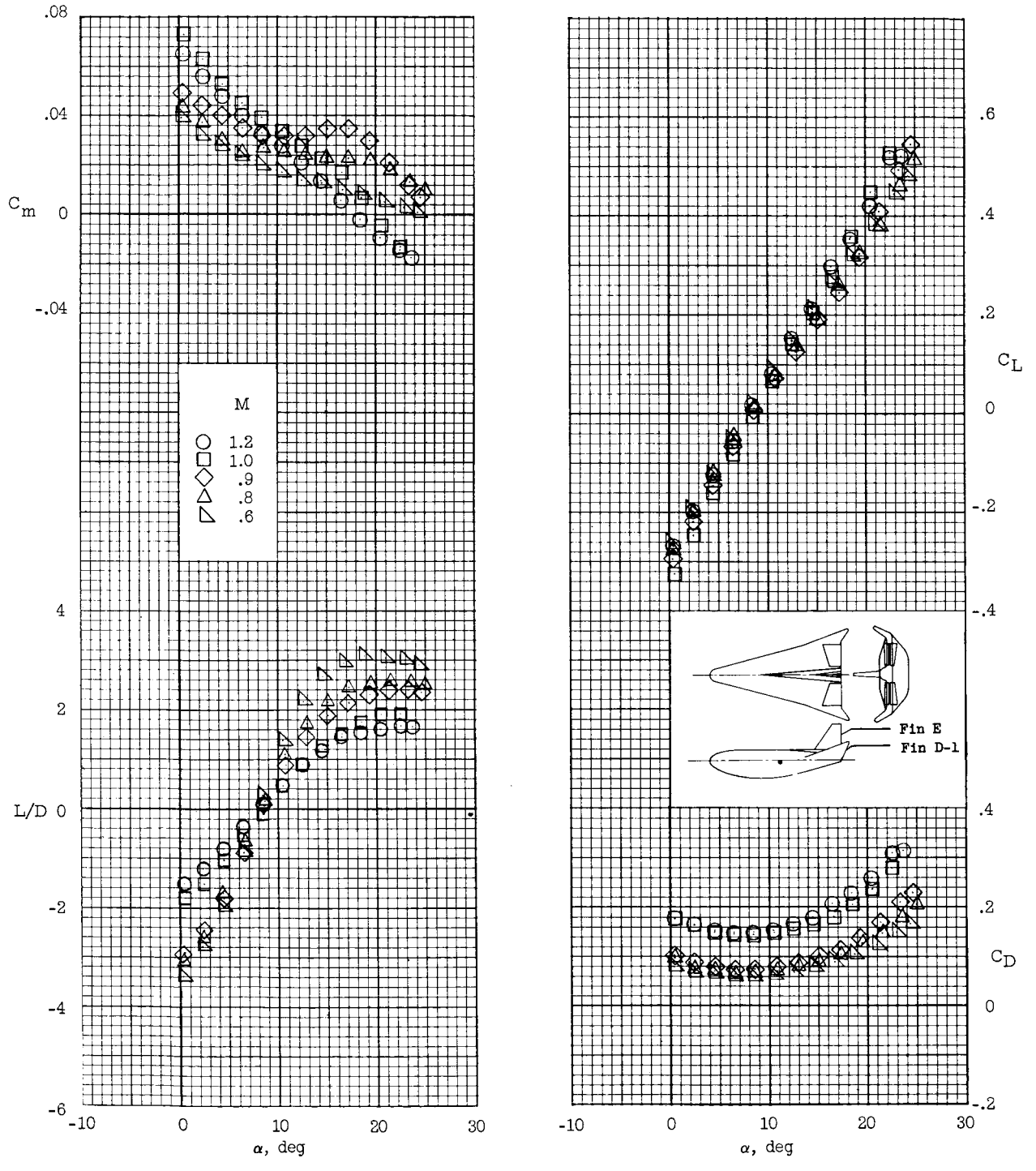

(d) $\delta_e = -10^o$; $\delta_a = -10^o$.

Figure 4.- Continued.

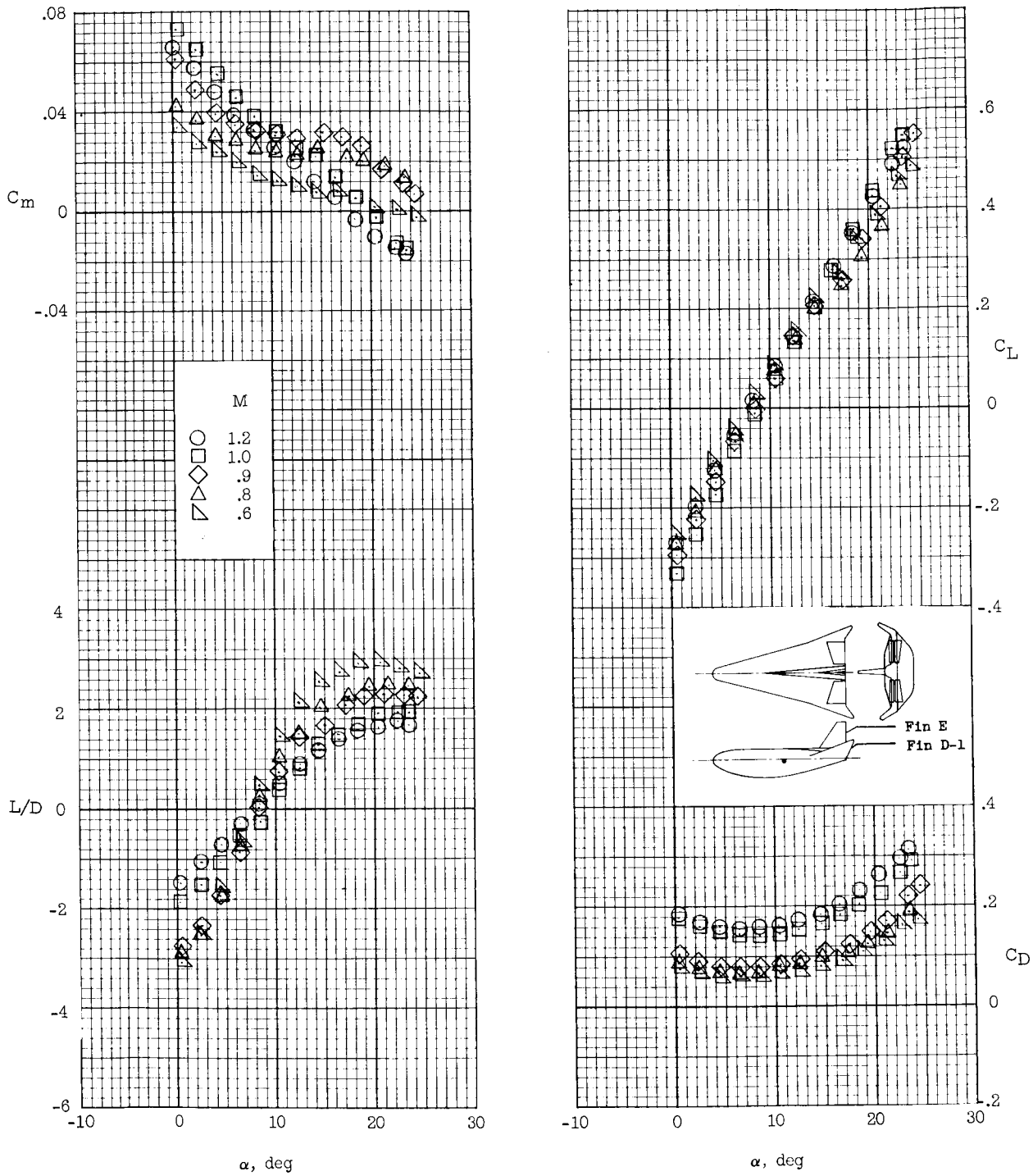

(e) $\delta_e = -10^\circ$; $\delta_a = -20^\circ$.

Figure 4.- Continued.

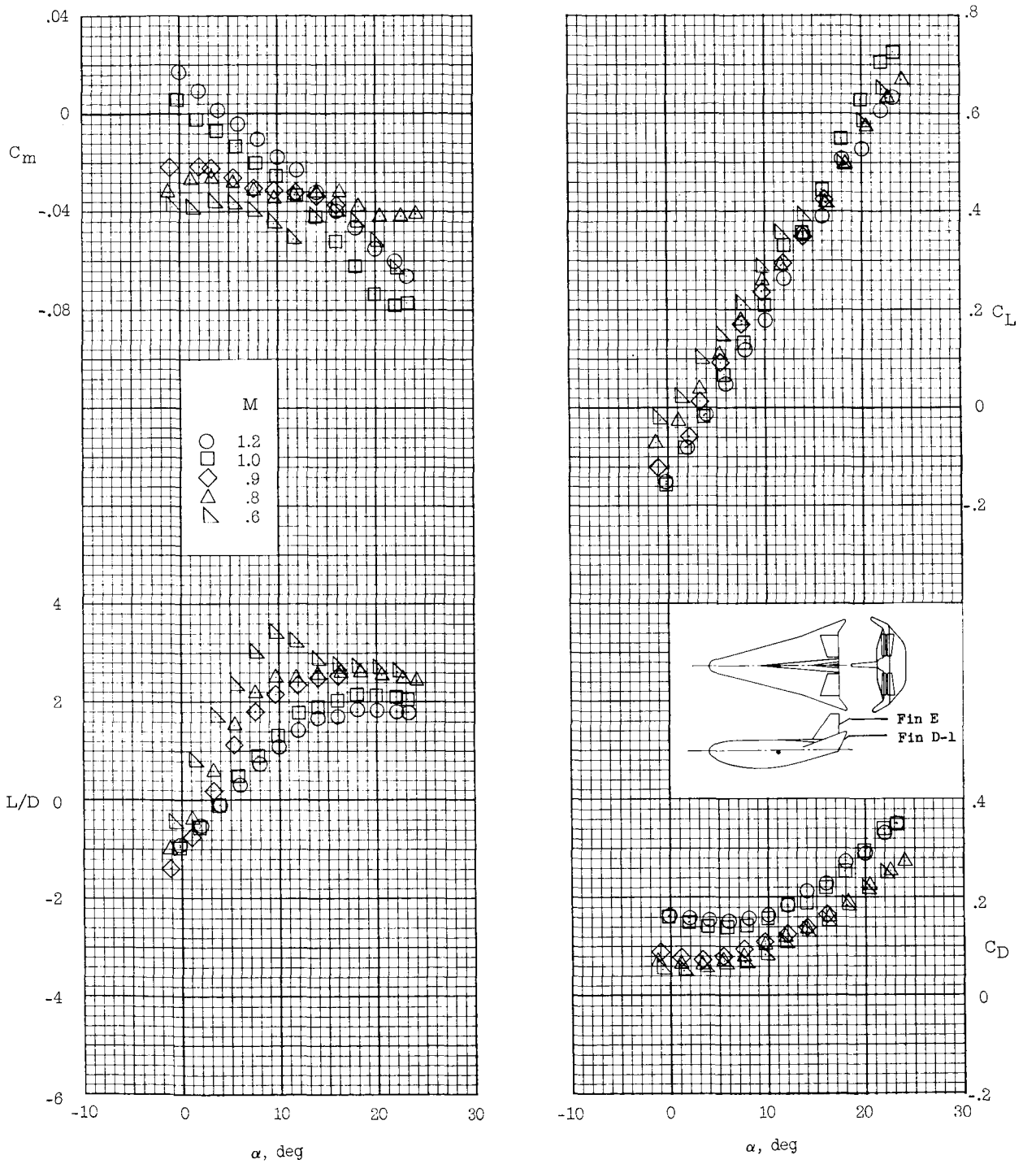

(f) $\delta_e = 10^\circ$; $\delta_a = -10^\circ$.

Figure 4.- Continued.

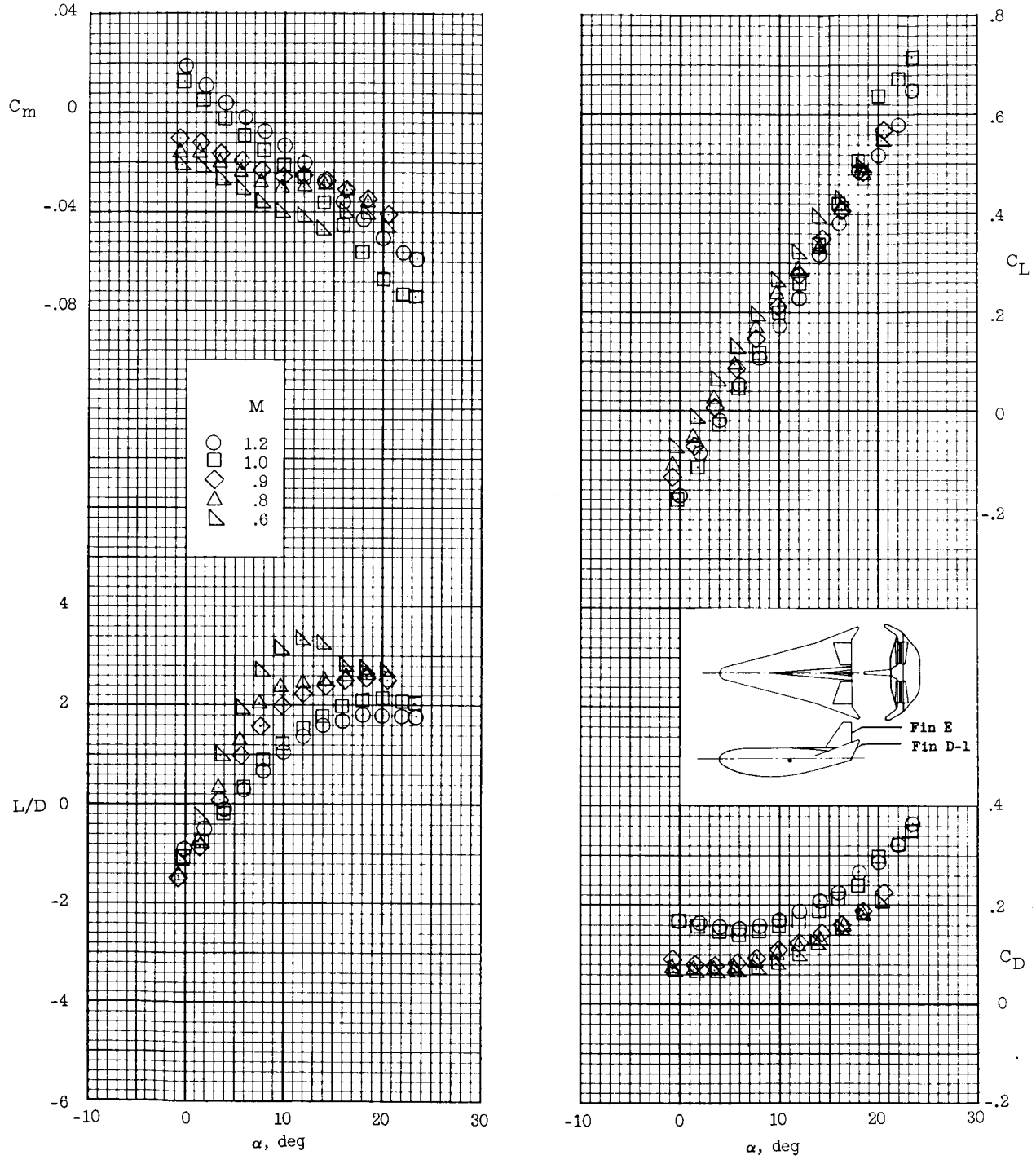

(g) $\delta_e = 10^\circ$; $\delta_a = -20^\circ$.

Figure 4.- Concluded.

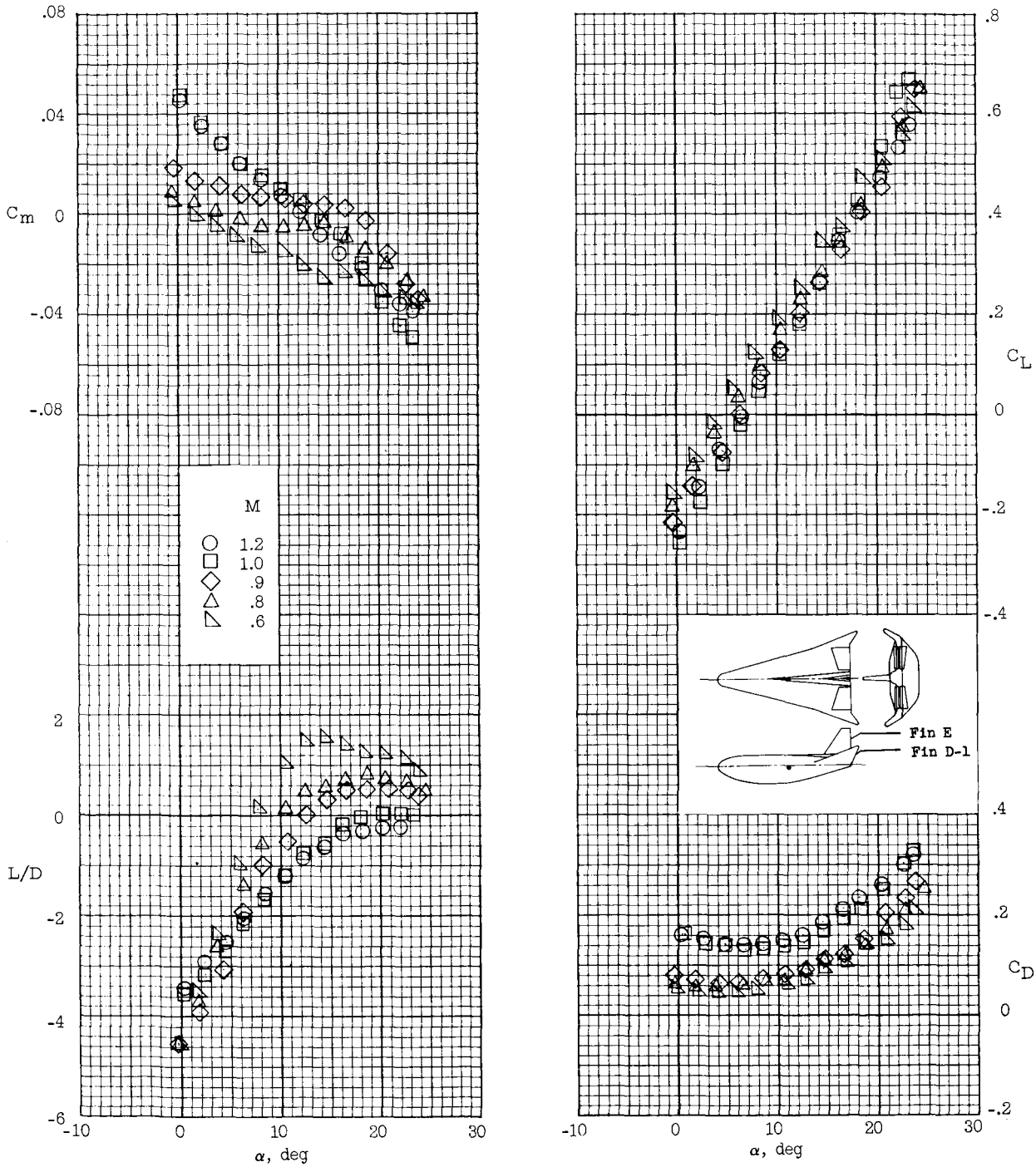

(a) $\delta_r = 22.5^\circ$.

Figure 5.- Longitudinal performance of HL-10 model with center fin E, tip fins D-1, $\beta = 0^\circ$, $\delta_e = 0^\circ$, and $\delta_a = 0^\circ$.

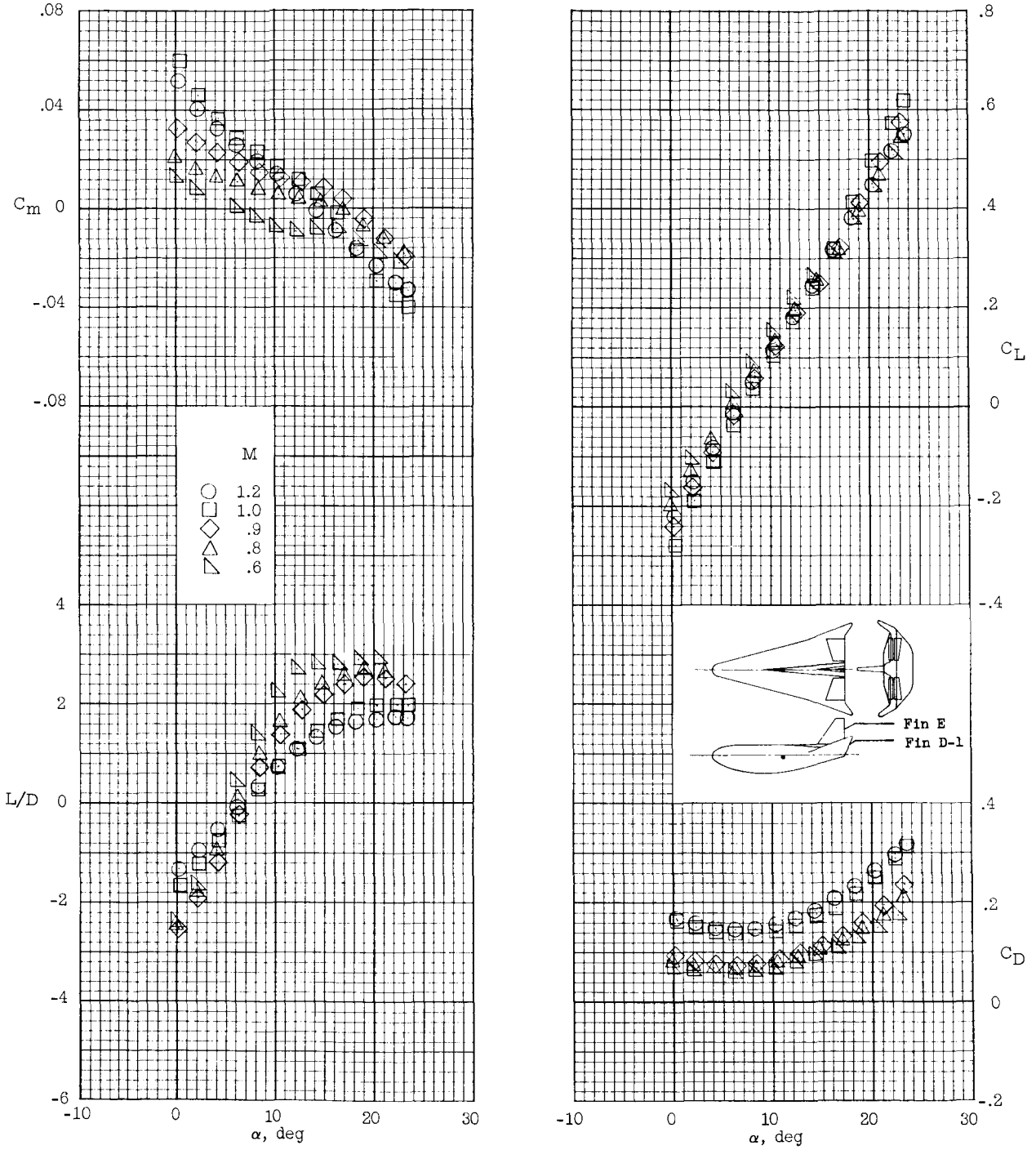

(b) $\delta_r = 45°$.

Figure 5.- Concluded.

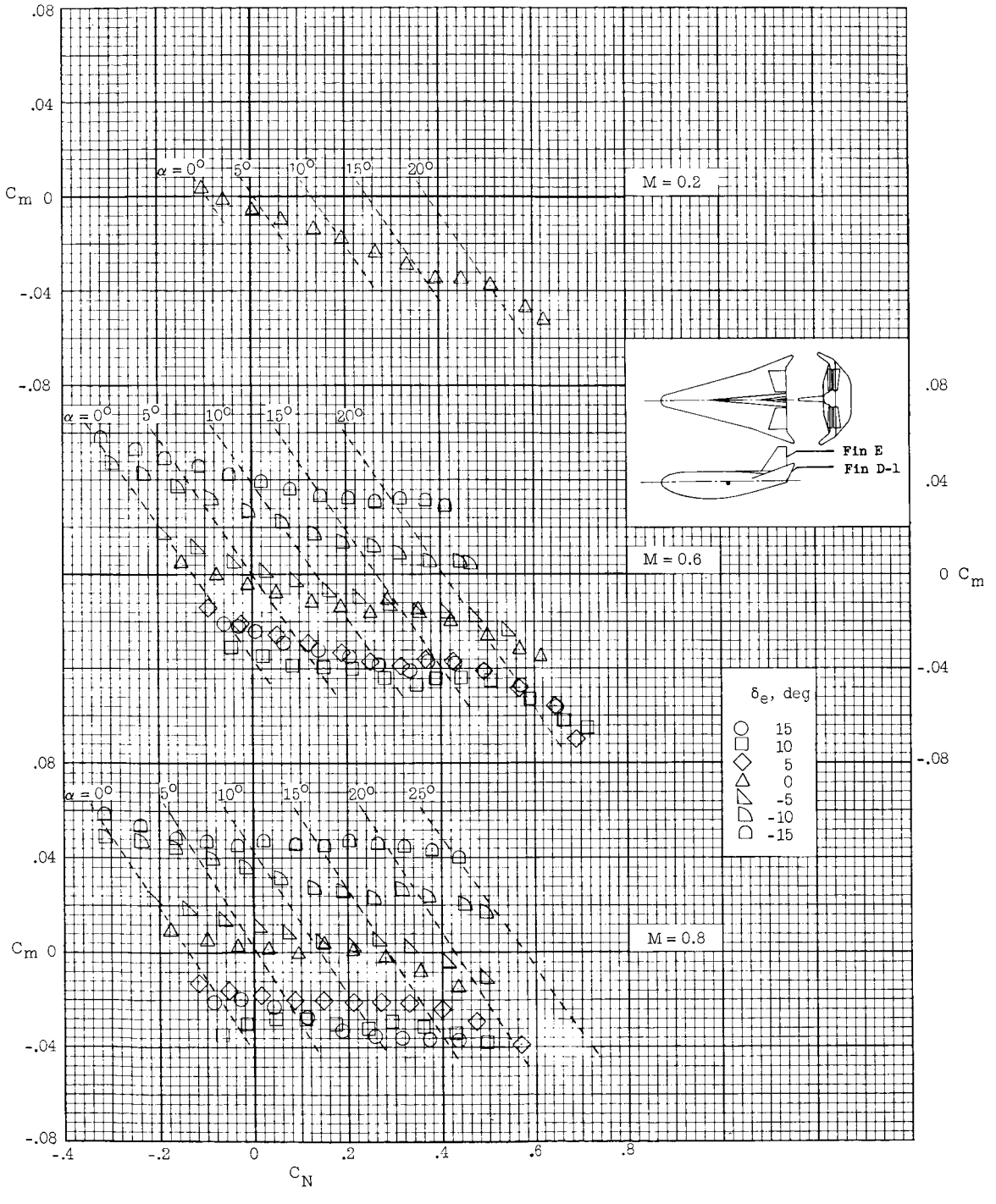

(a) M = 0.2, 0.6, and 0.8.

Figure 6.- Longitudinal stability of HL-10 model with center fin E, tip fins D-1, $\beta = 0^o$, $\delta_a = 0^o$, and $\delta_r = 0^o$.

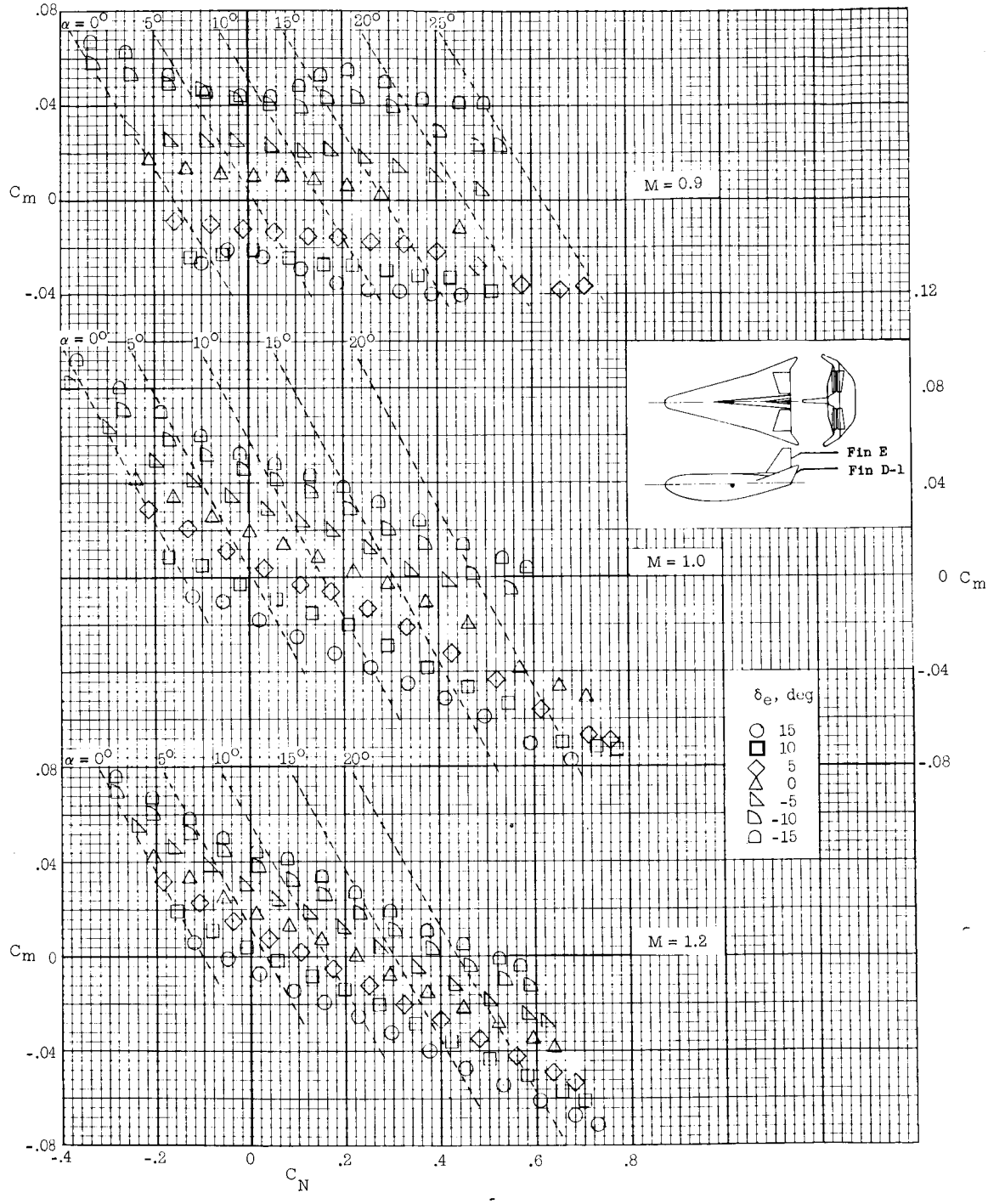

(b) M = 0.9, 1.0, and 1.2.

Figure 6.- Concluded.

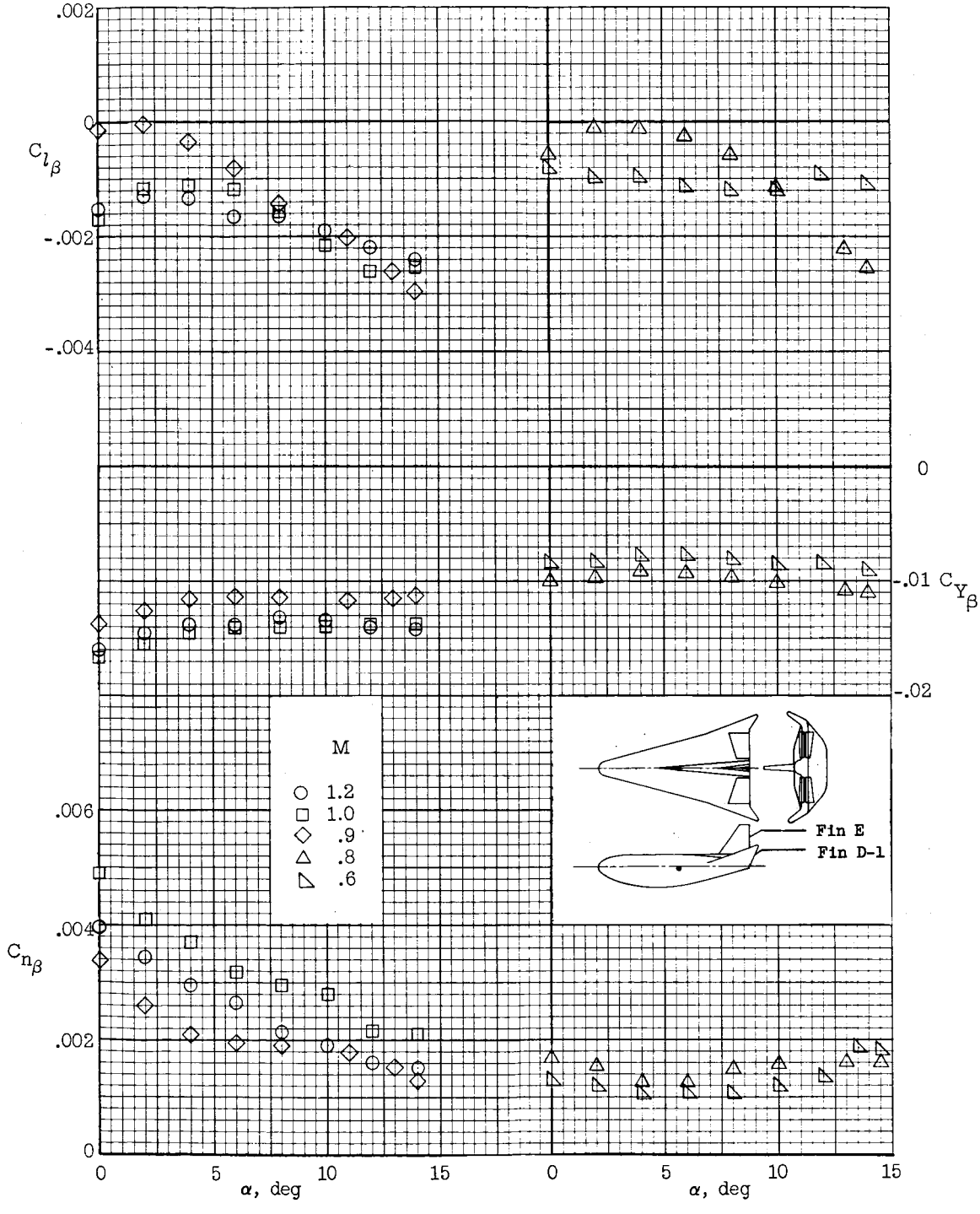

(a) $\delta_e = 0^o$.

Figure 7.- Directional-lateral stability of HL-10 model with center fin E, tip fins D-1, $\delta_a = 0^o$, and $\delta_r = 0^o$.

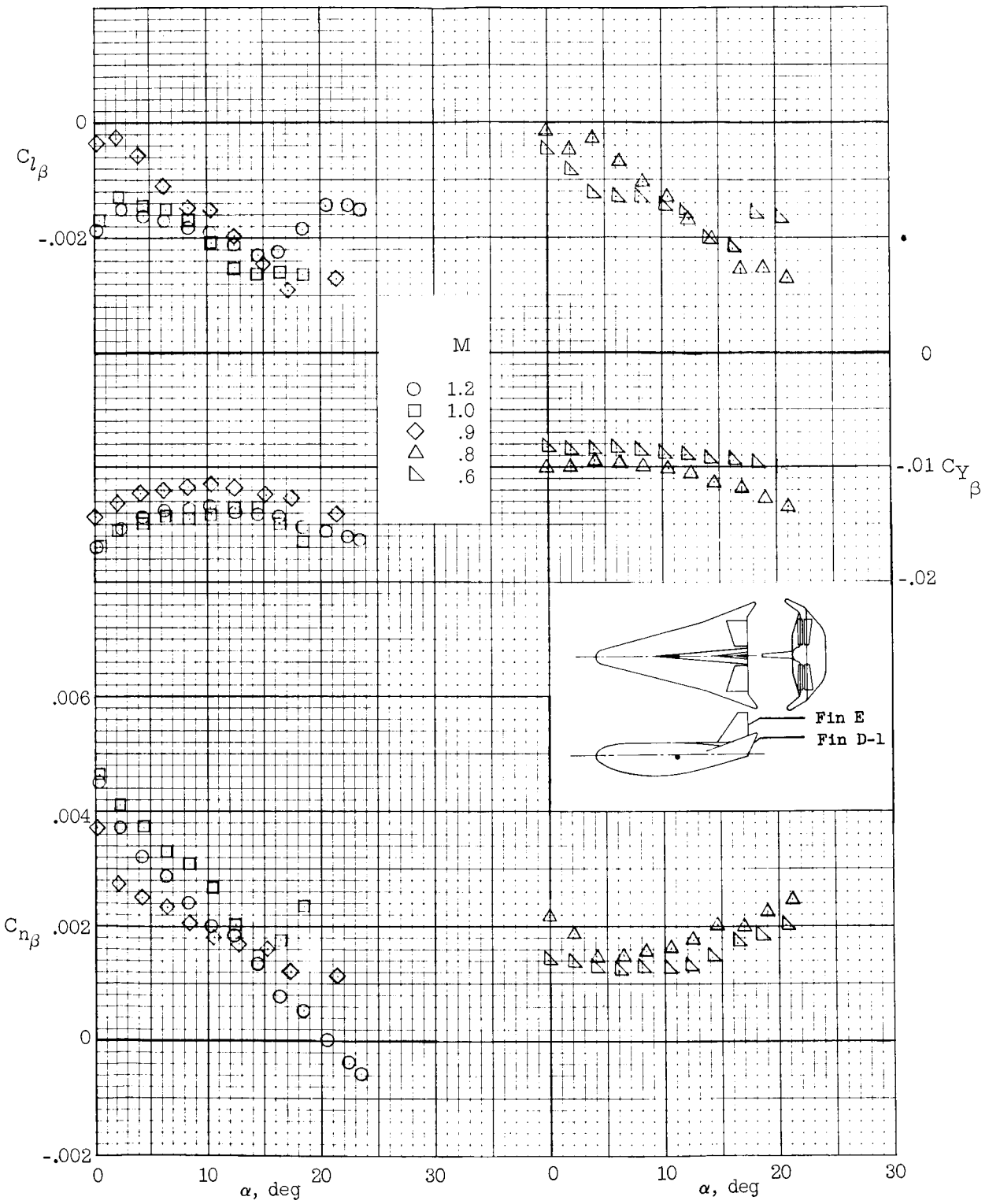

(b) $\delta_e = -5^\circ$.

Figure 7.- Continued.

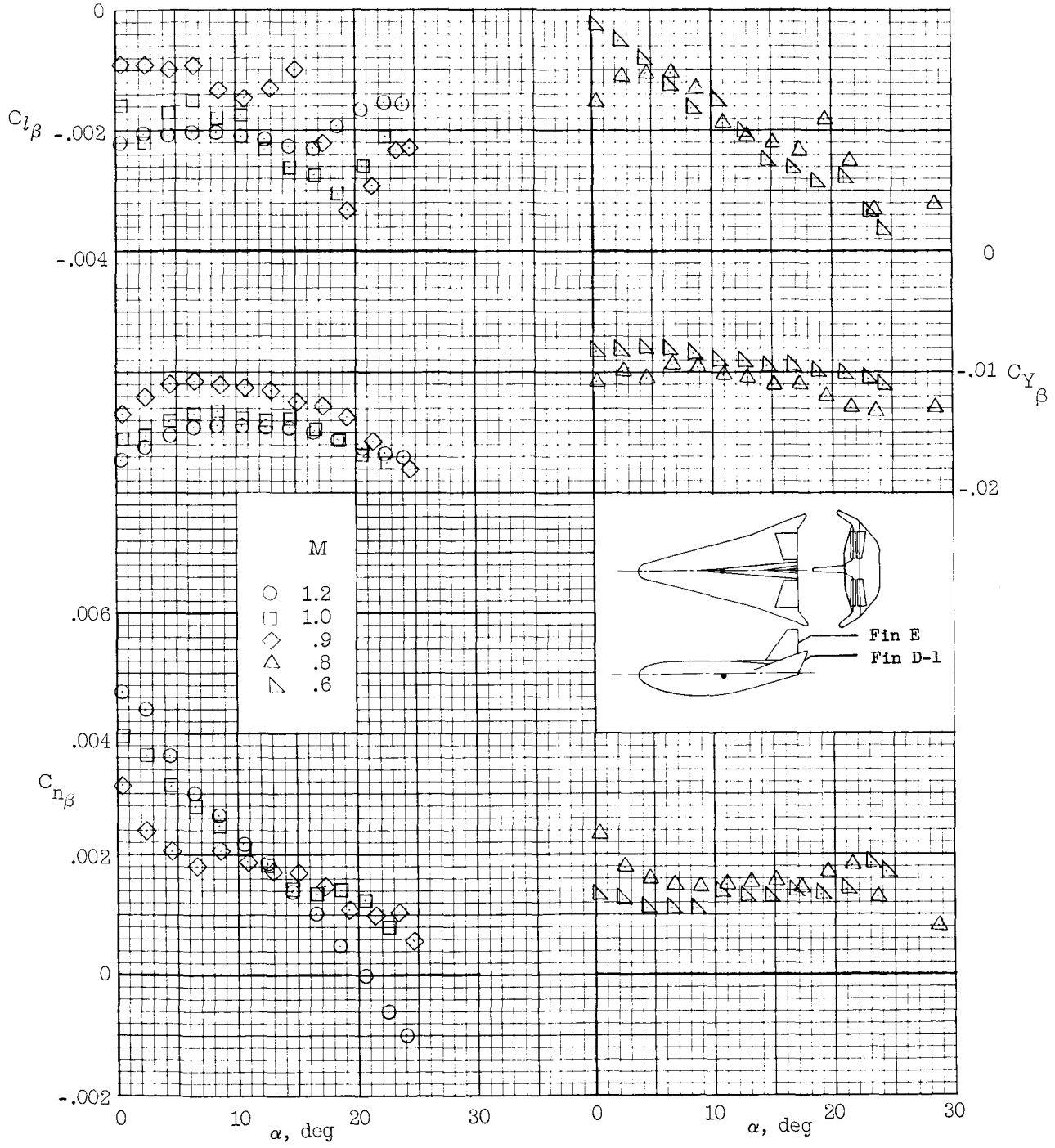

(c) $\delta_e = -10^\circ$.

Figure 7.- Continued.

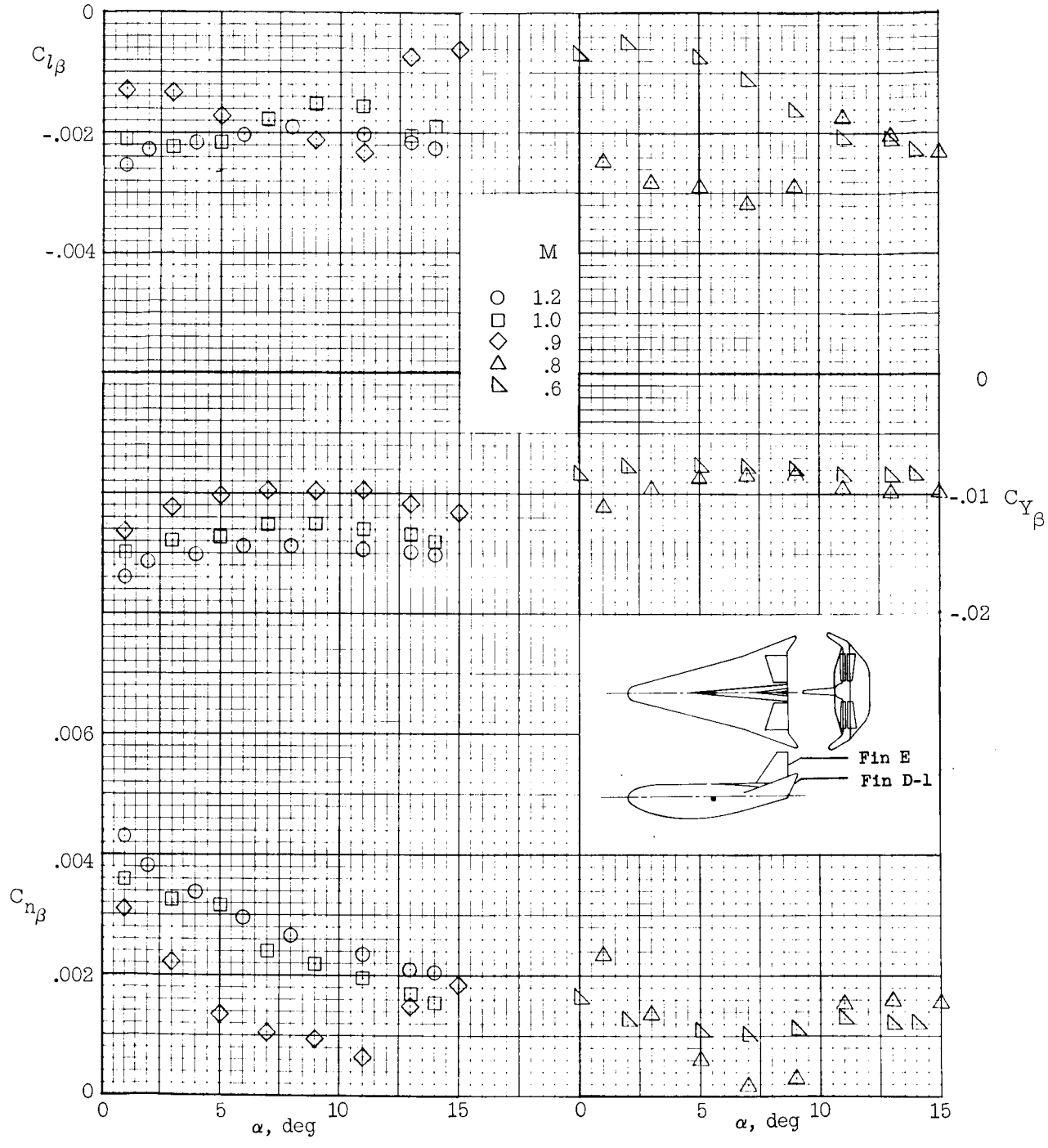

(d) $\delta_e = -15°$.

Figure 7.- Continued.

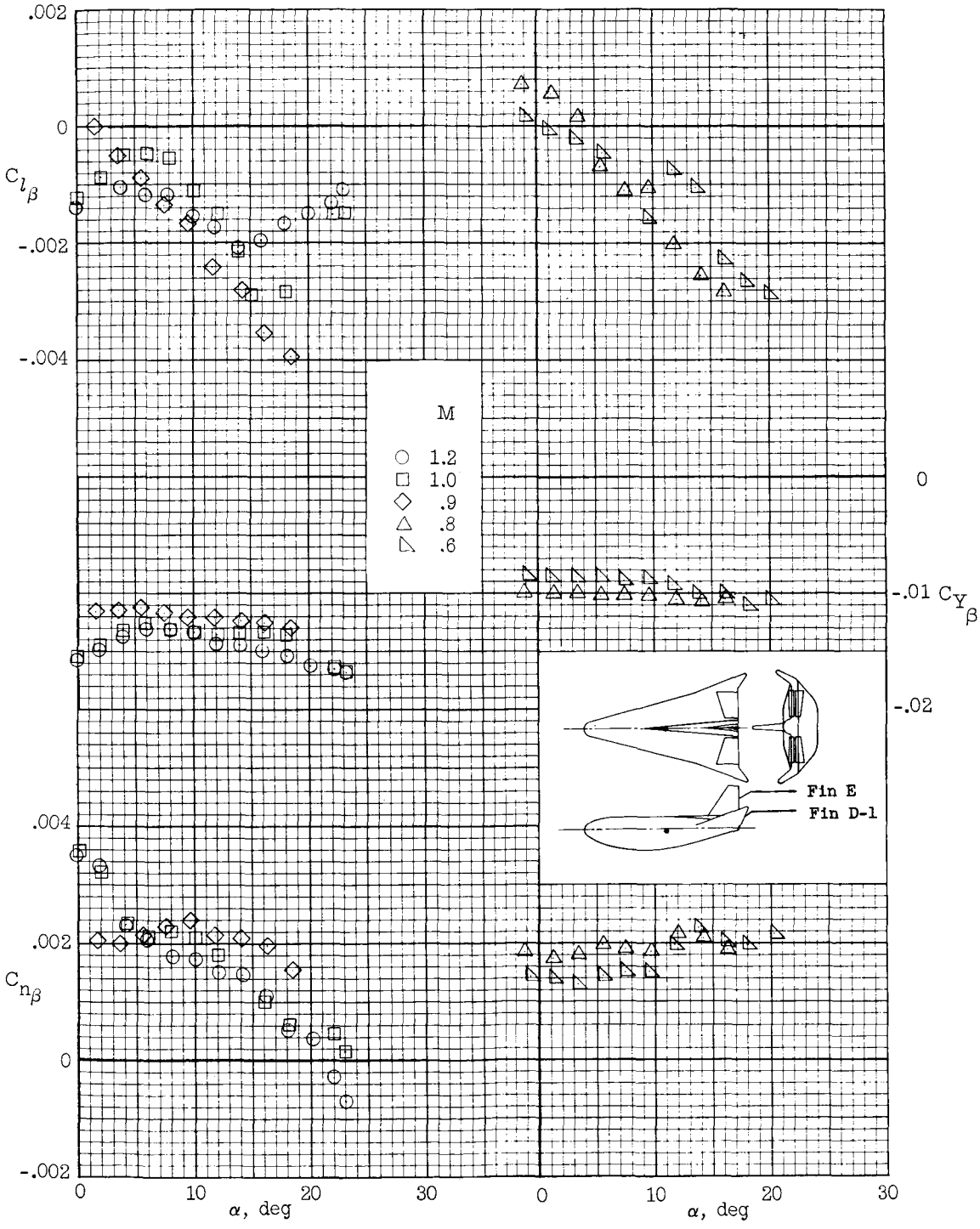

(e) $\delta_e = 10^\circ$.

Figure 7.- Continued.

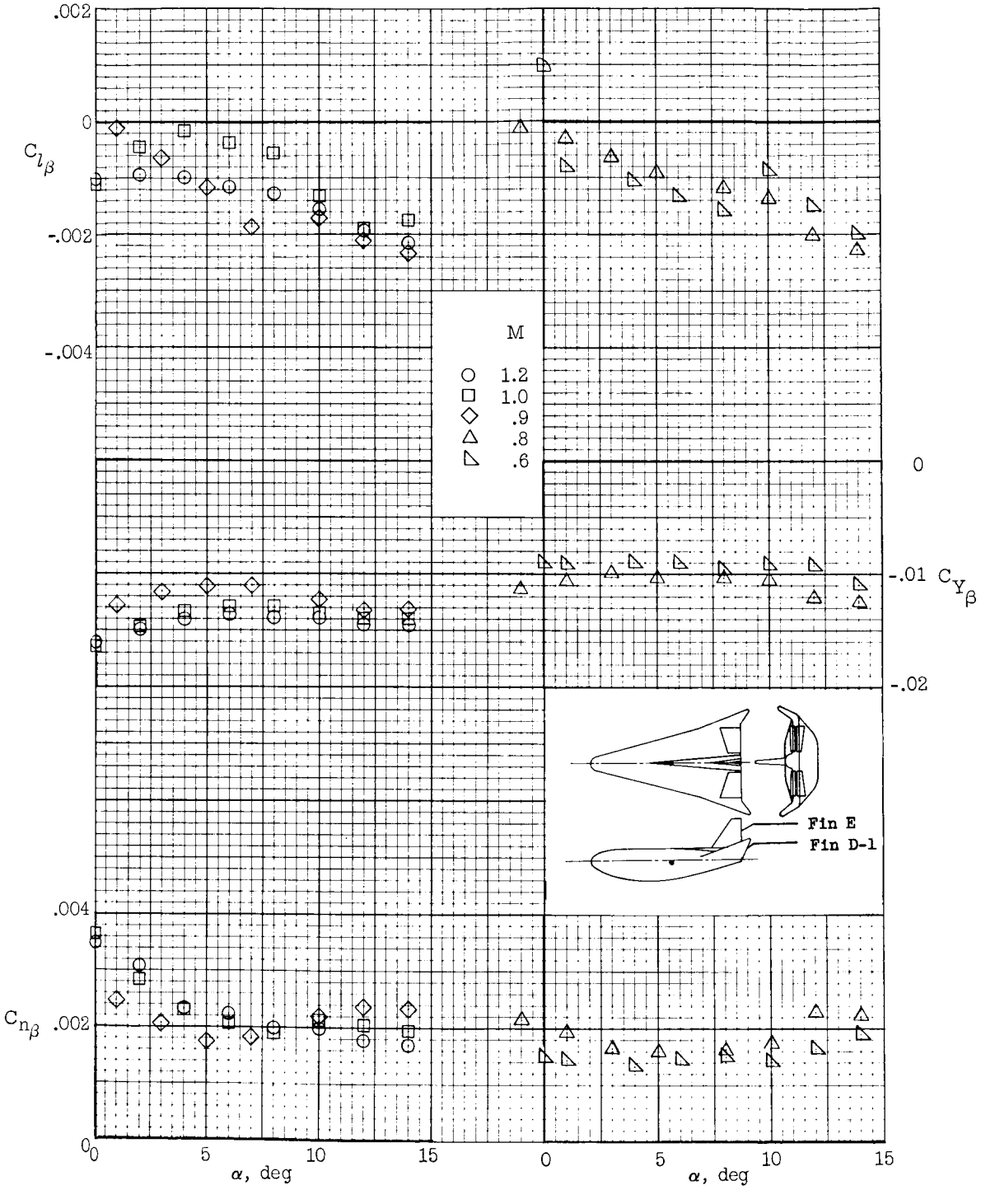

(f) $\delta_e = 15°$.

Figure 7.- Concluded.

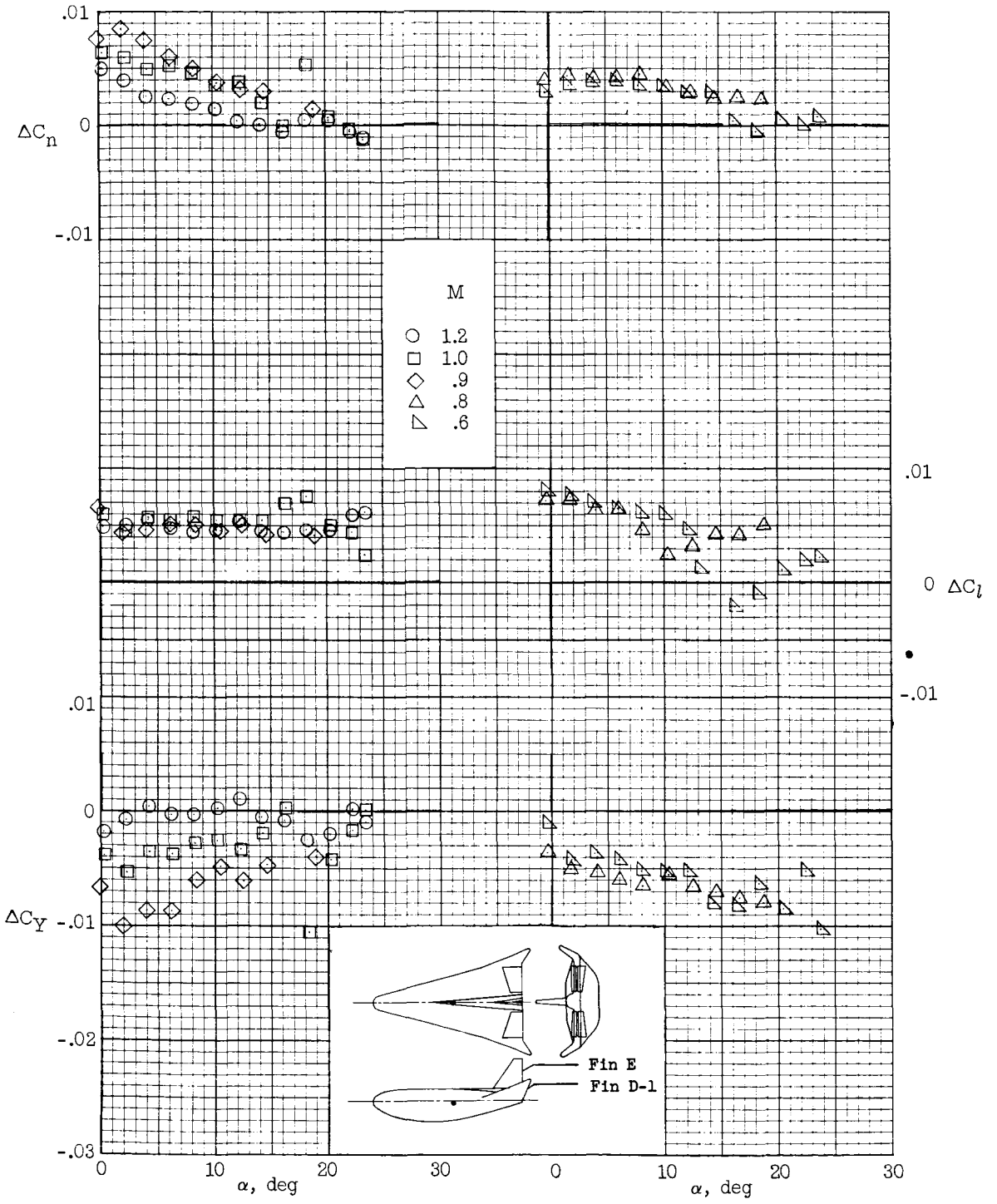

(a) $\delta_e = 0^o$; $\delta_a = -10^o$.

Figure 8.- Roll control of HL-10 model with center fin E, tip fins D-1, $\beta = 0^o$, and $\delta_r = 0^o$.

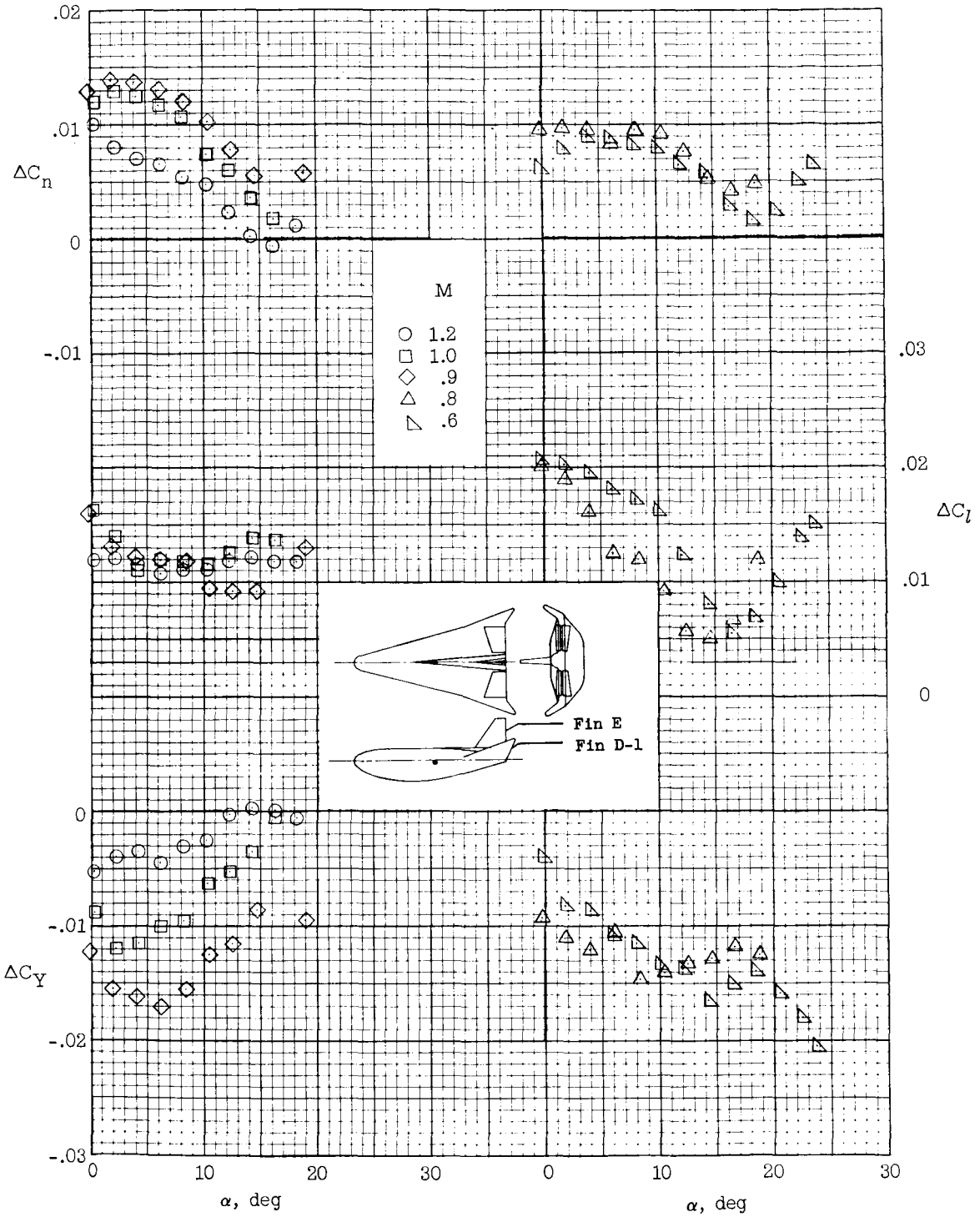

(b) $\delta_e = 0^\circ$; $\delta_a = -20^\circ$.

Figure 8.- Continued.

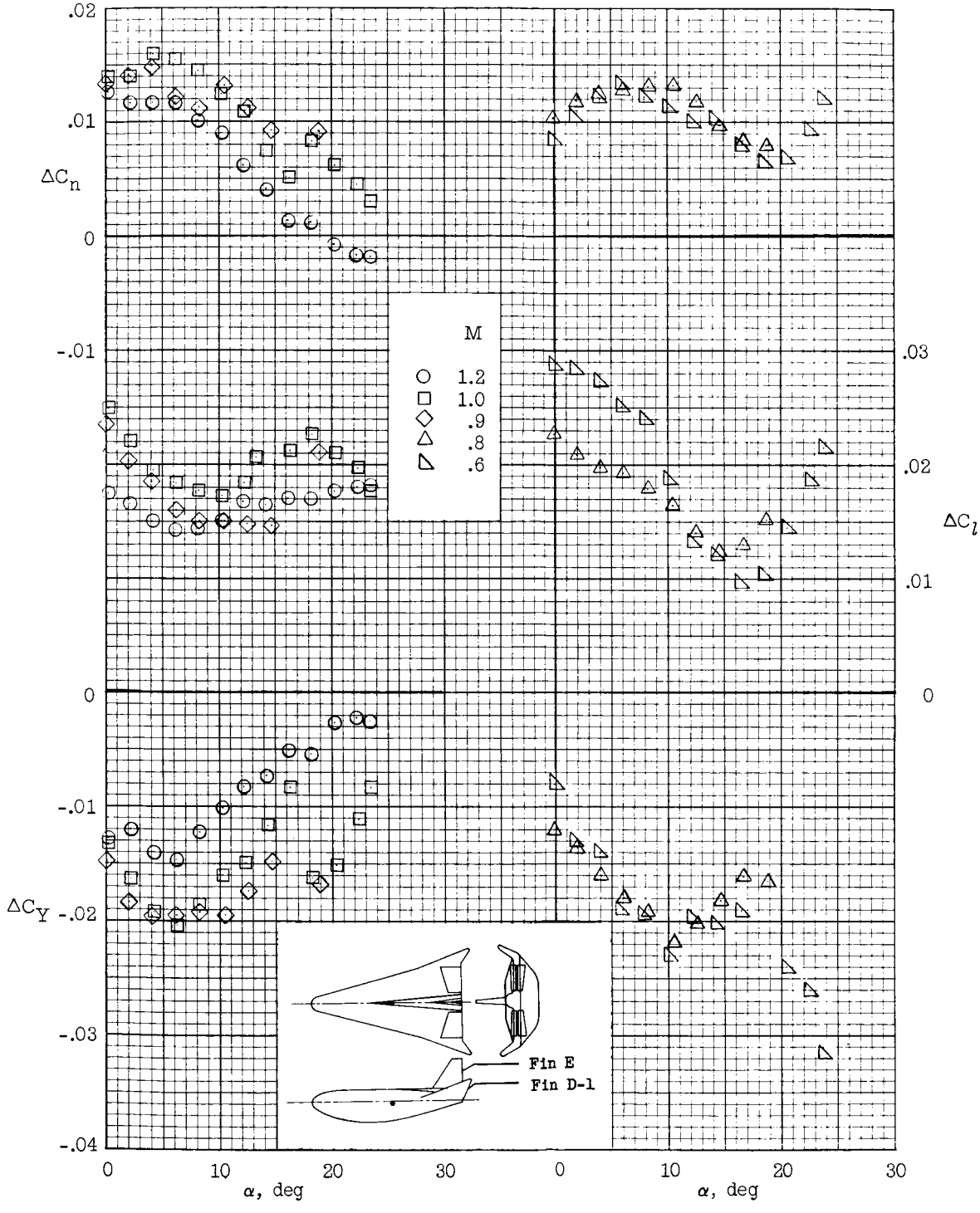

(c) $\delta_e = 0^\circ$; $\delta_a = -30^\circ$.

Figure 8.- Continued.

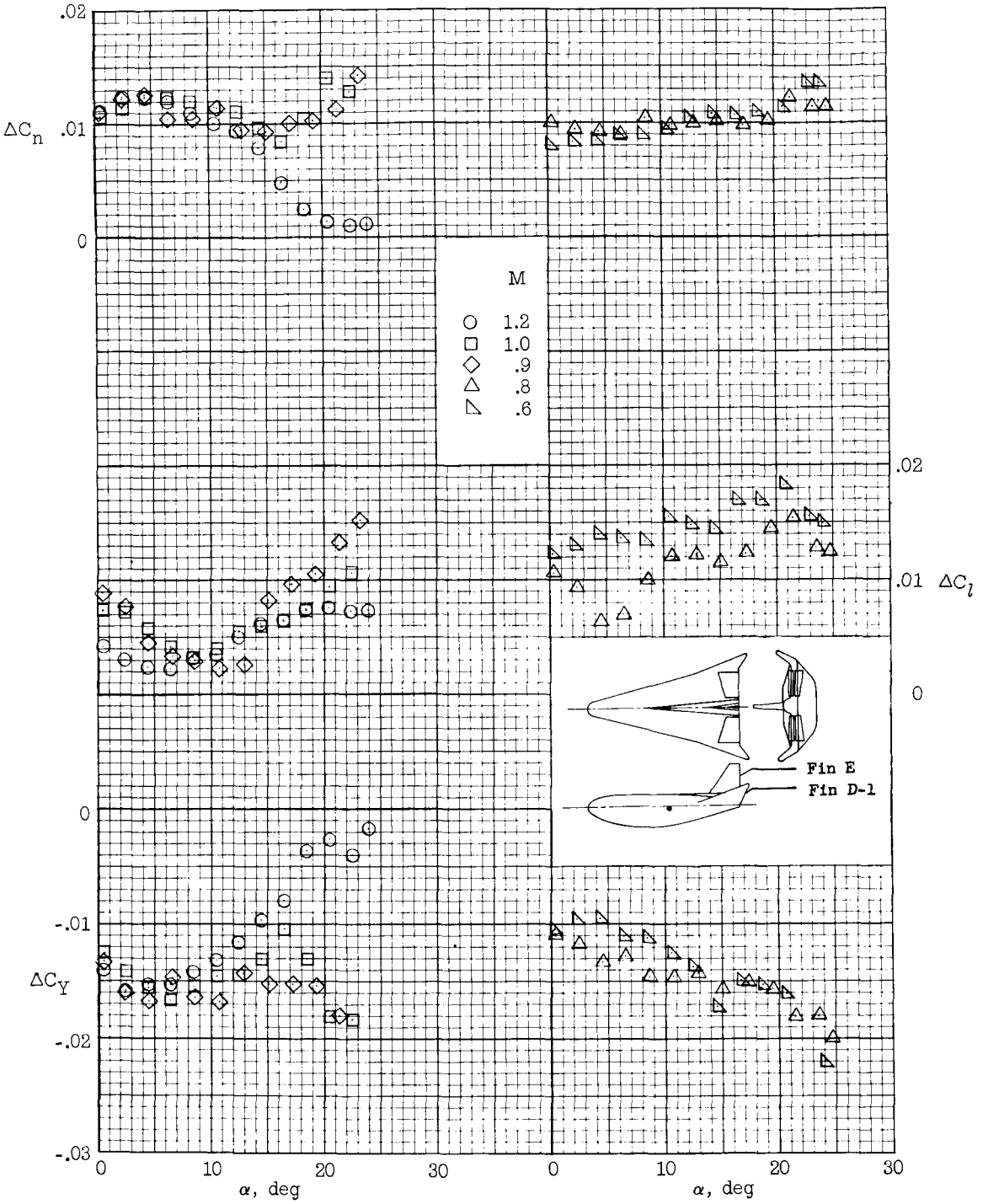

(d) $\delta_e = -10^\circ$; $\delta_a = -10^\circ$.

Figure 8.- Continued.

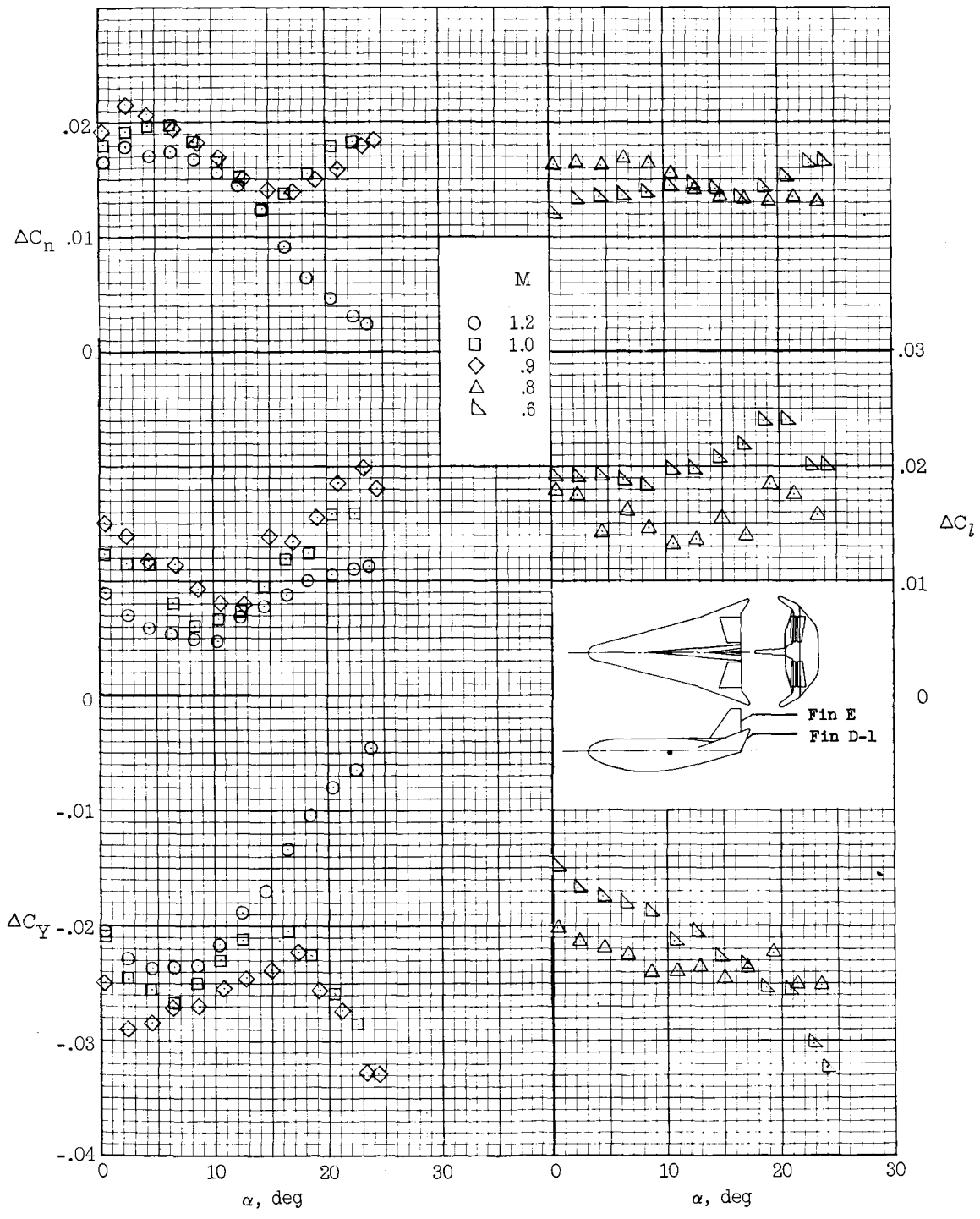

(e) $\delta_e = -10^o$; $\delta_a = -20^o$.

Figure 8.- Continued.

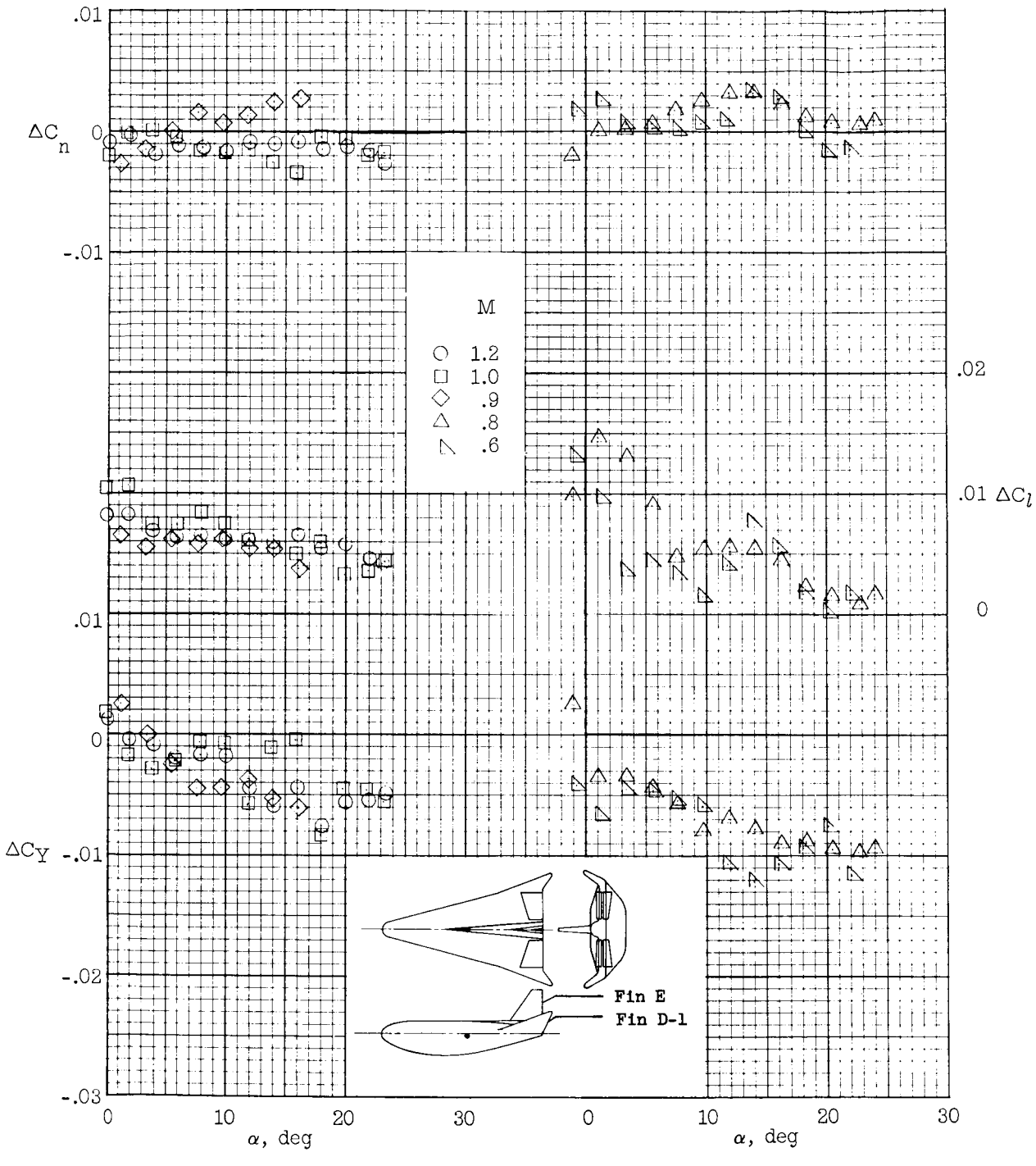

(f) $\delta_e = 10^\circ$; $\delta_a = -10^\circ$.

Figure 8.- Continued.

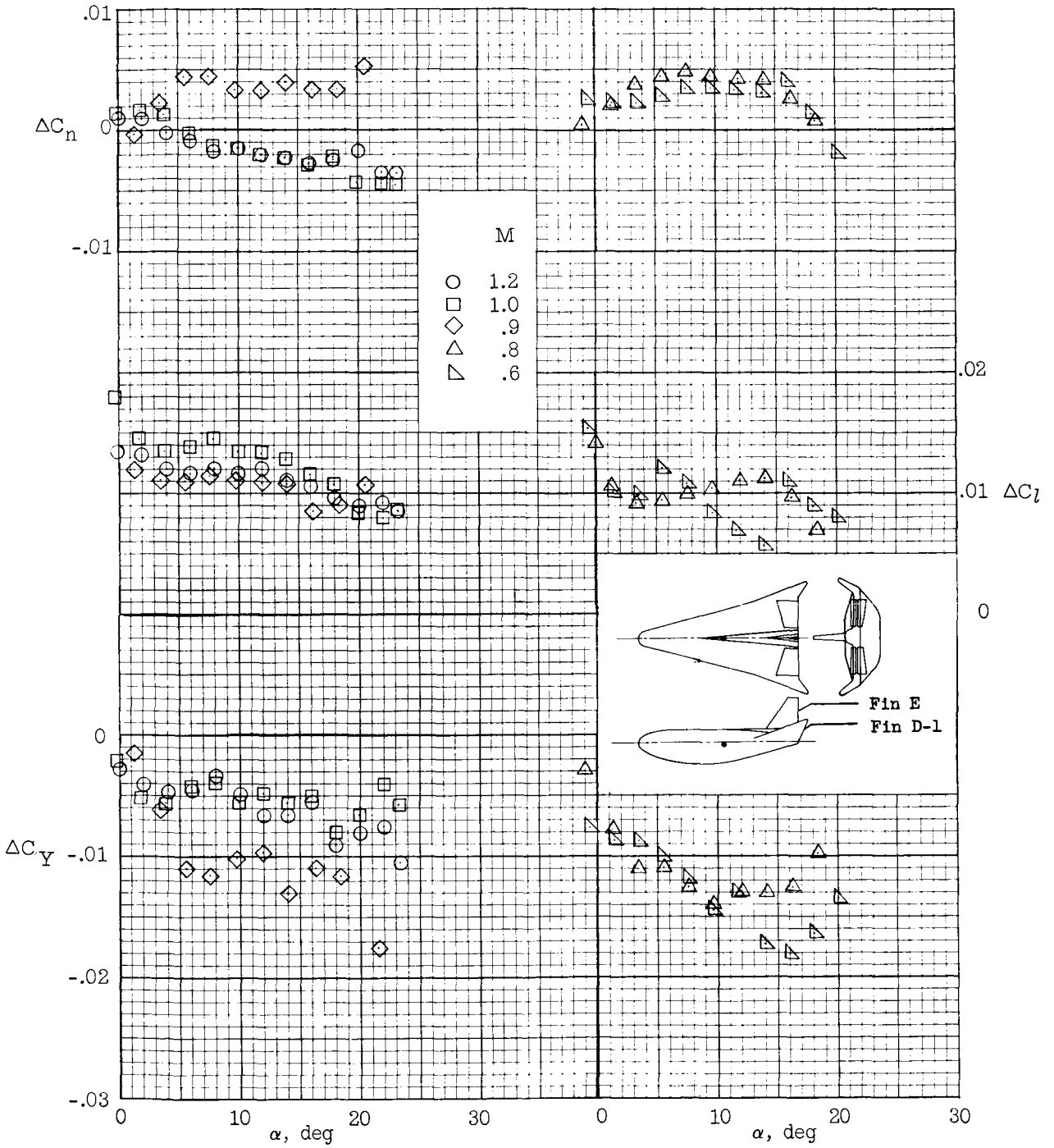

(g) $\delta_e = 10^\circ$; $\delta_a = -20^\circ$.

Figure 8.- Concluded.

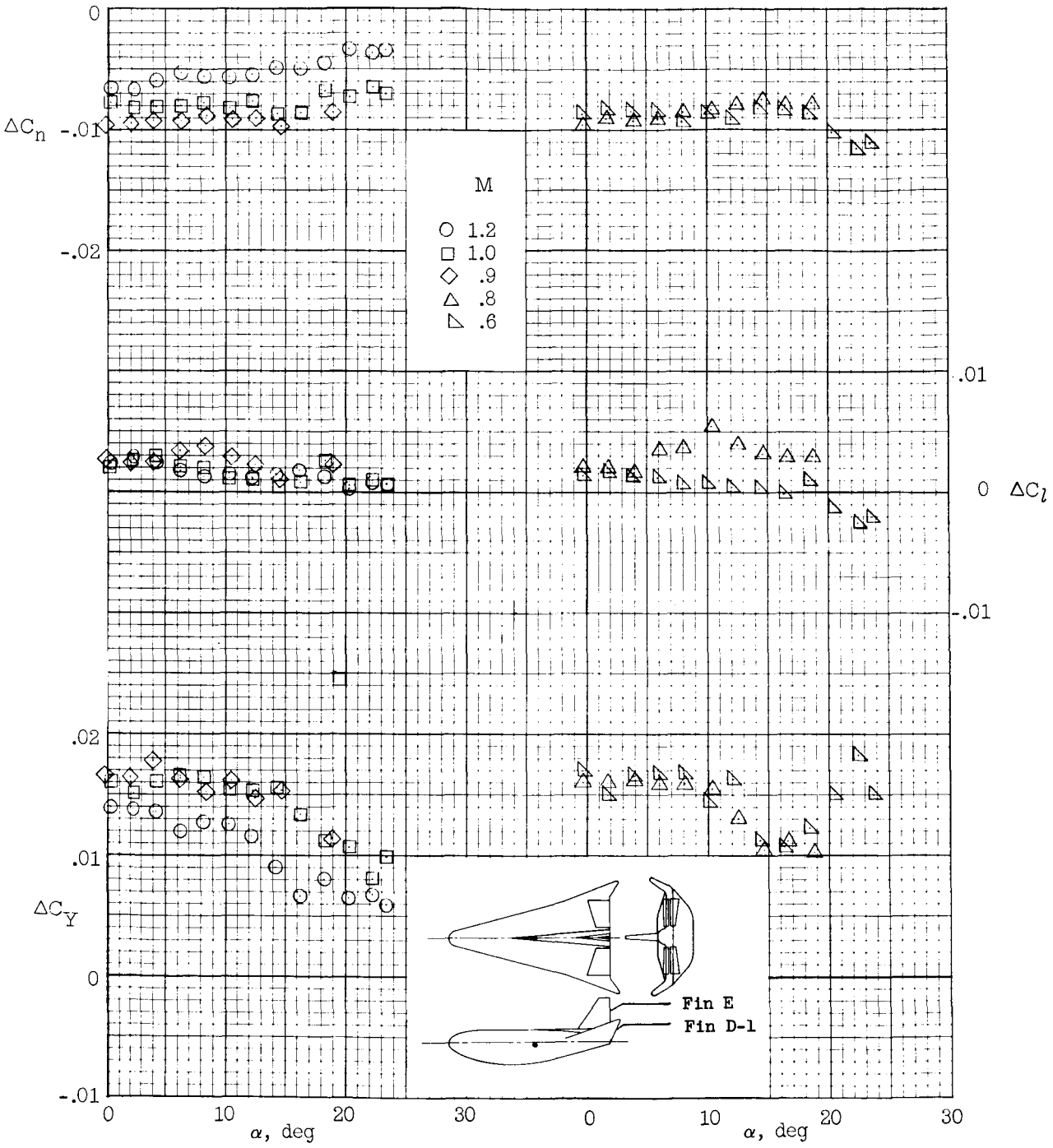

(a) $\delta_r = 22.5^\circ$.

Figure 9.- Yaw control of HL-10 model with center fin E, tip fins D-1, $\beta = 0^\circ$, $\delta_e = 0^\circ$, and $\delta_a = 0^\circ$.

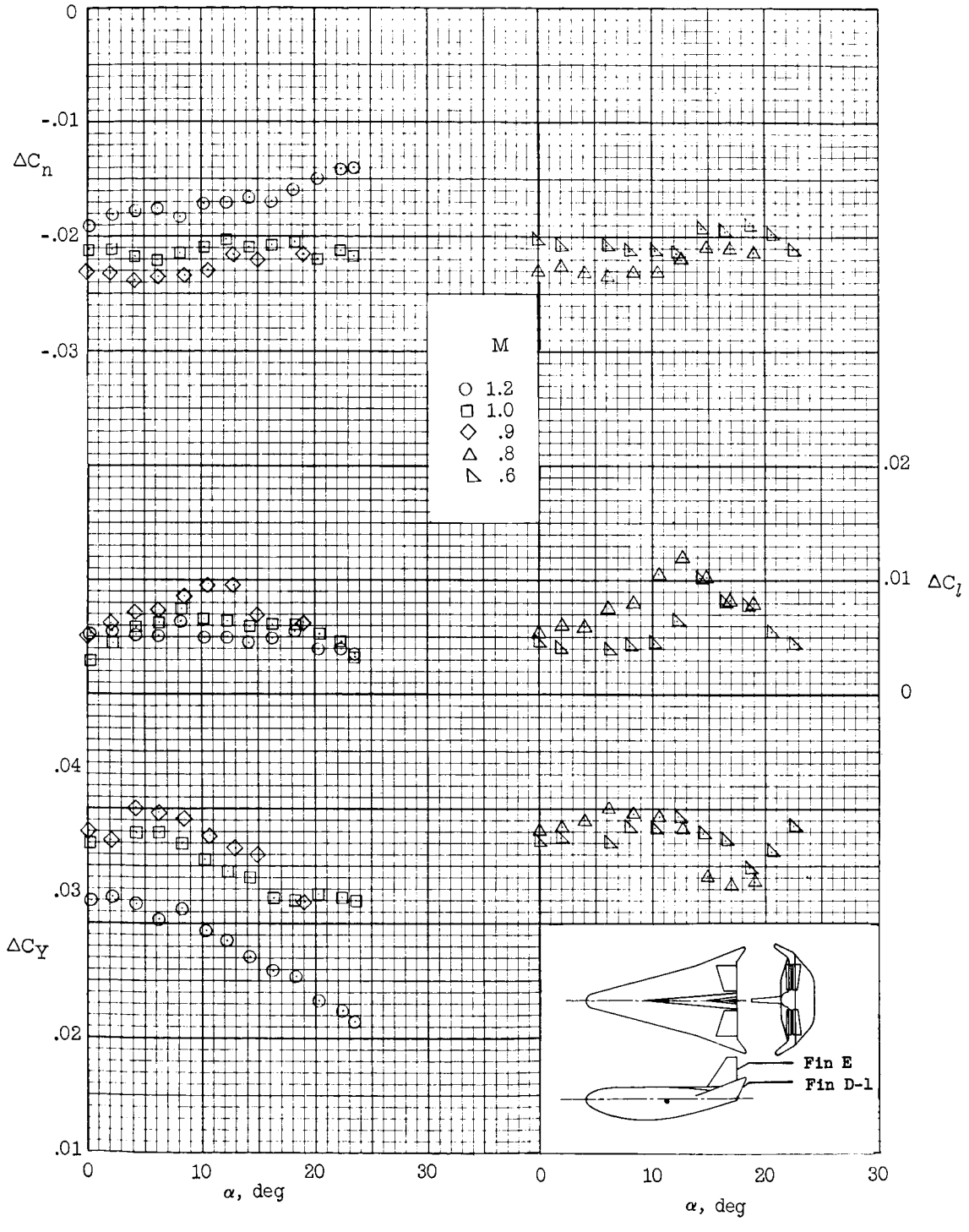

(b) $\delta_r = 45^\circ$.

Figure 9.- Concluded.

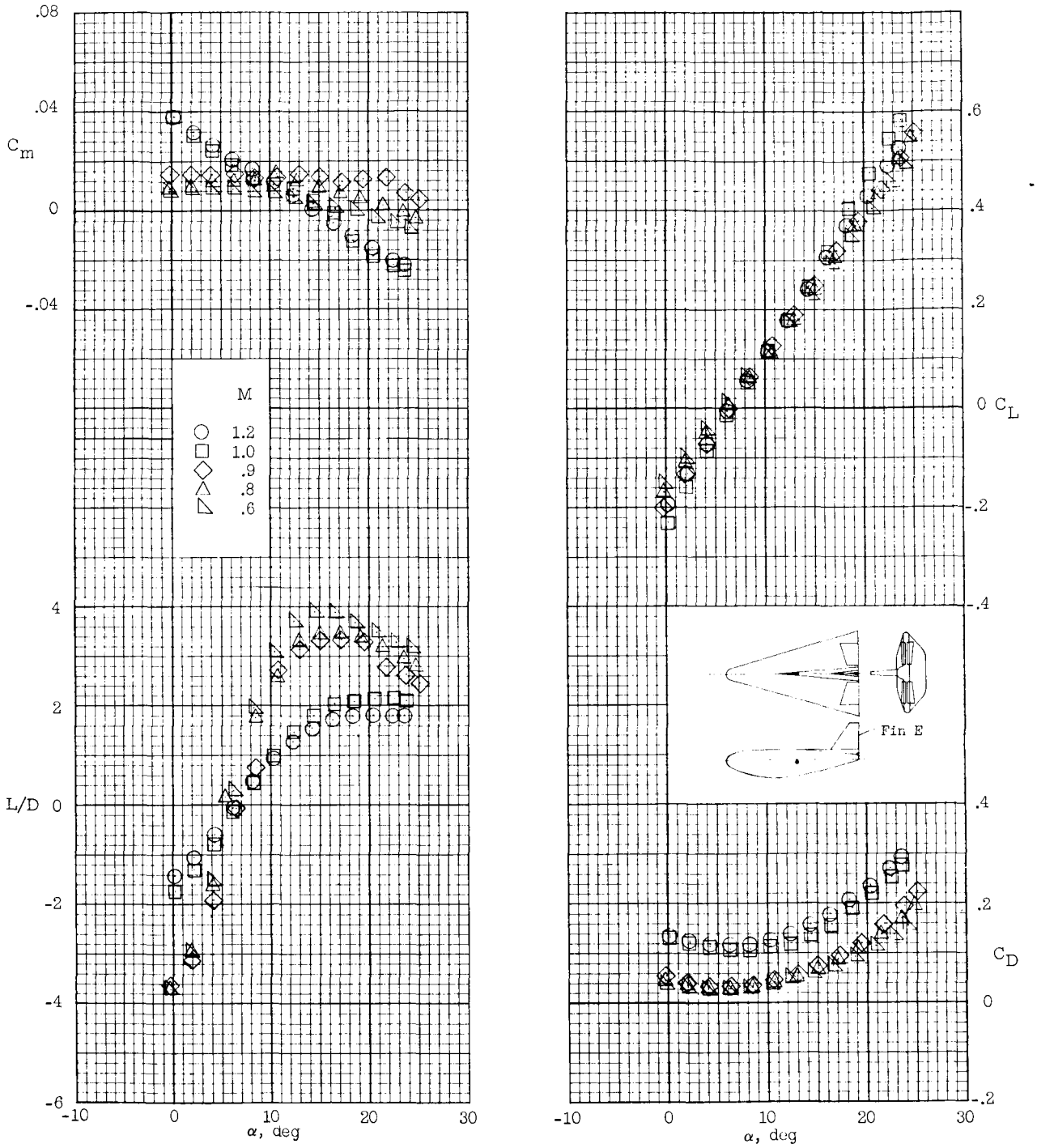

(a) $\delta_e = 0^o$.

Figure 10.- Longitudinal performance of HL-10 model with center fin E, $\beta = 0^o$, $\delta_a = 0^o$, and $\delta_r = 0^o$.

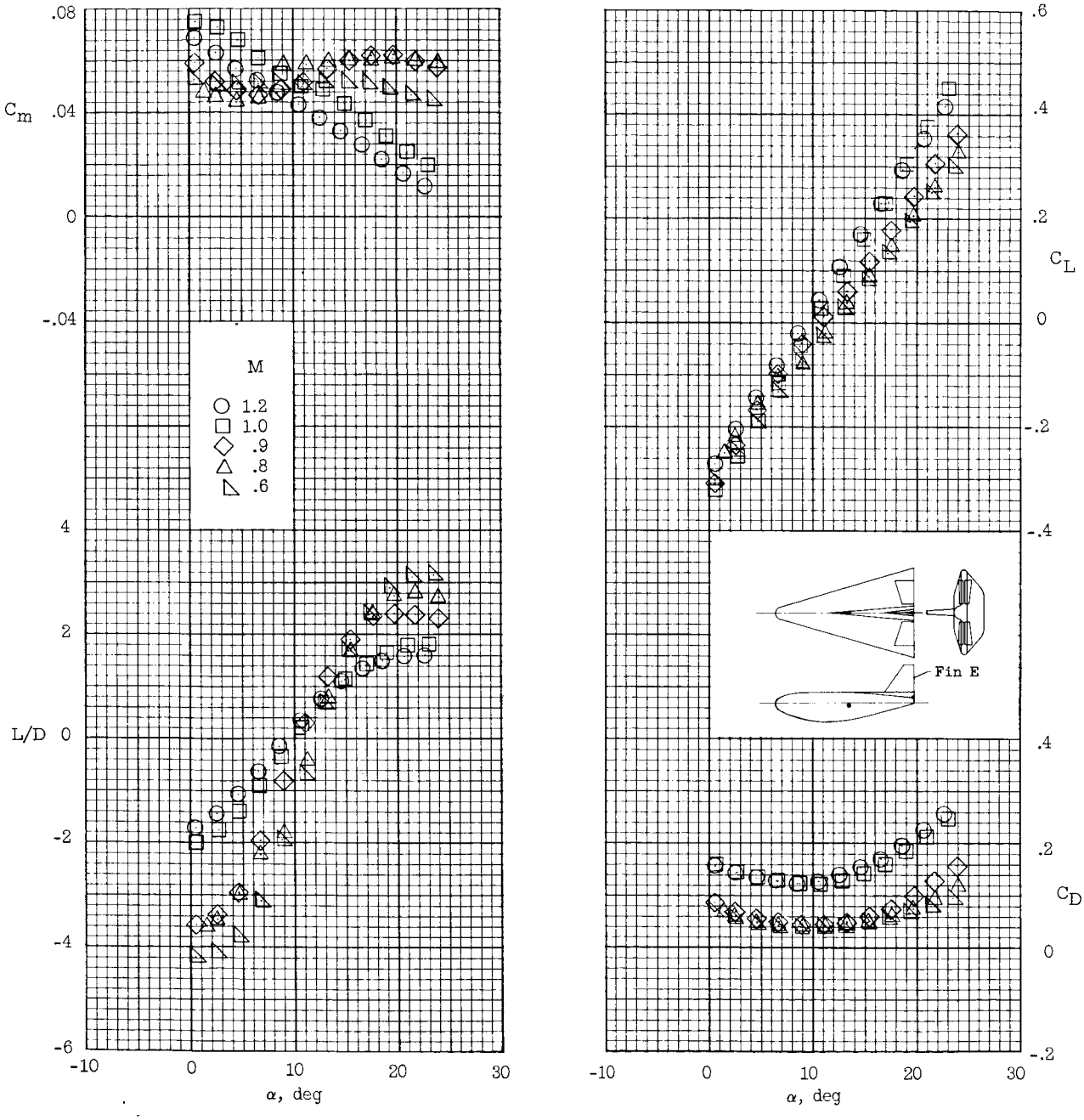

(b) $\delta_e = -15°$.

Figure 10.- Continued.

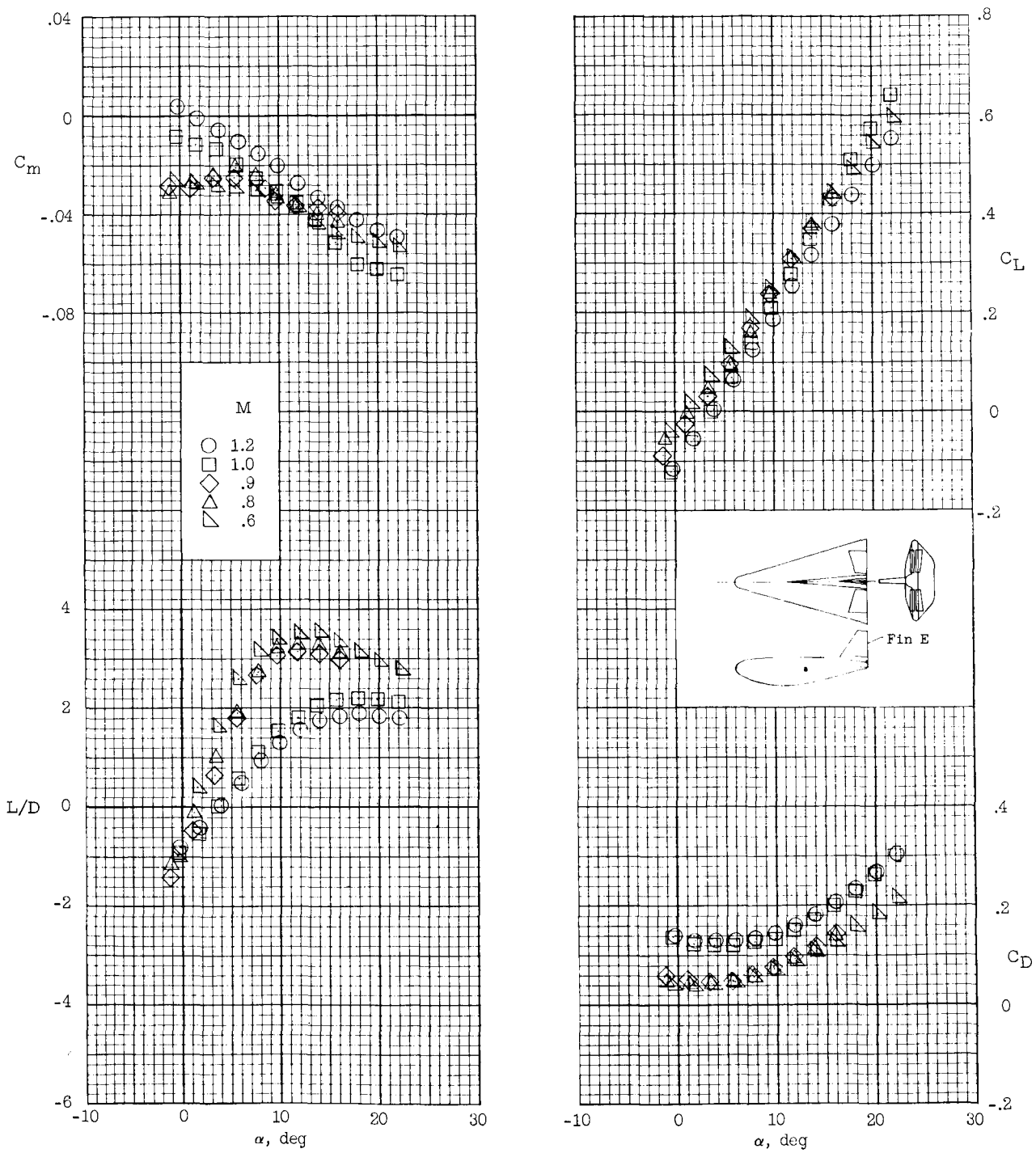

(c) $\delta_e = 15^\circ$.

Figure 10.- Concluded.

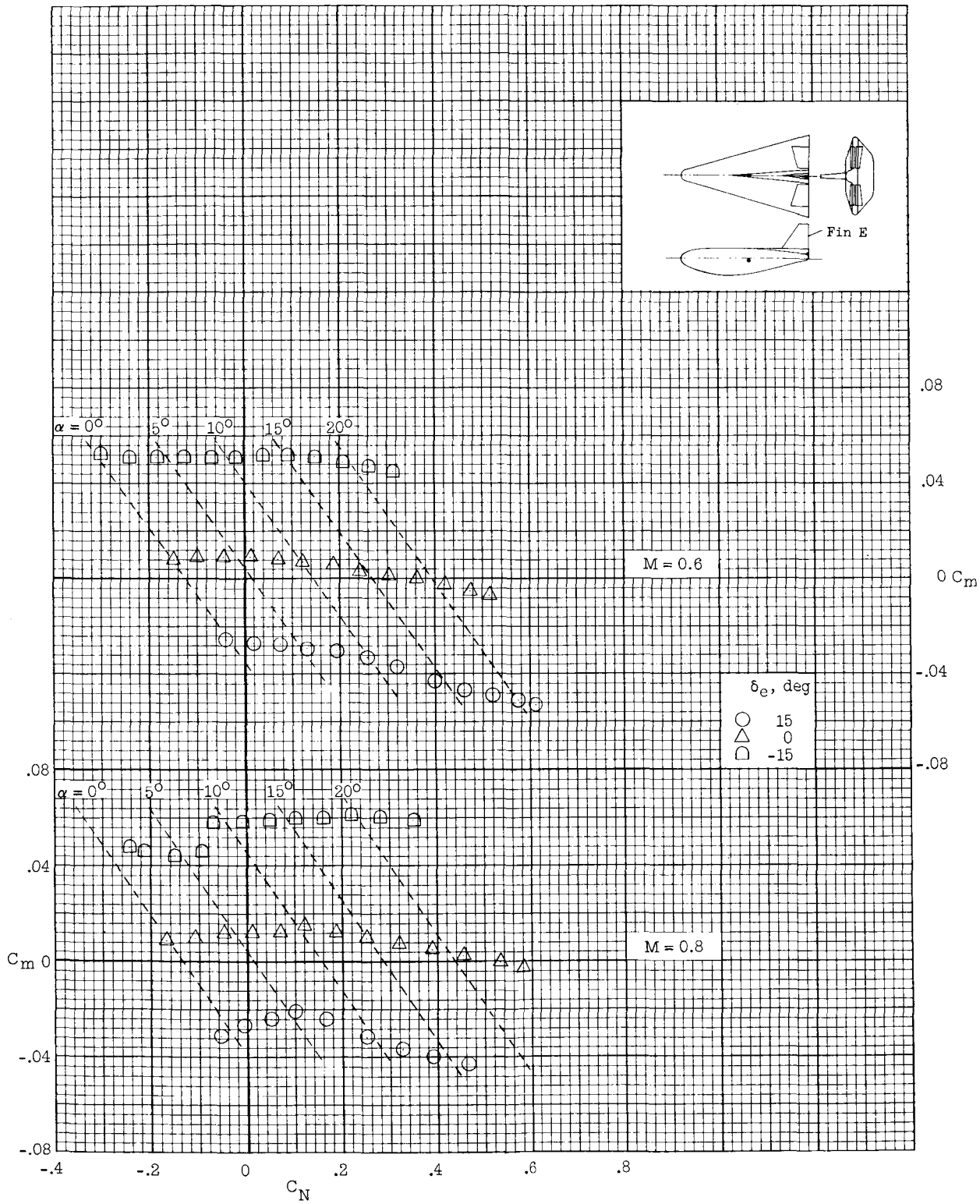

(a) M = 0.6 and 0.8.

Figure 11.- Longitudinal stability of HL-10 model with center fin E, $\beta = 0^\circ$, $\delta_a = 0^\circ$, and $\delta_r = 0^\circ$.

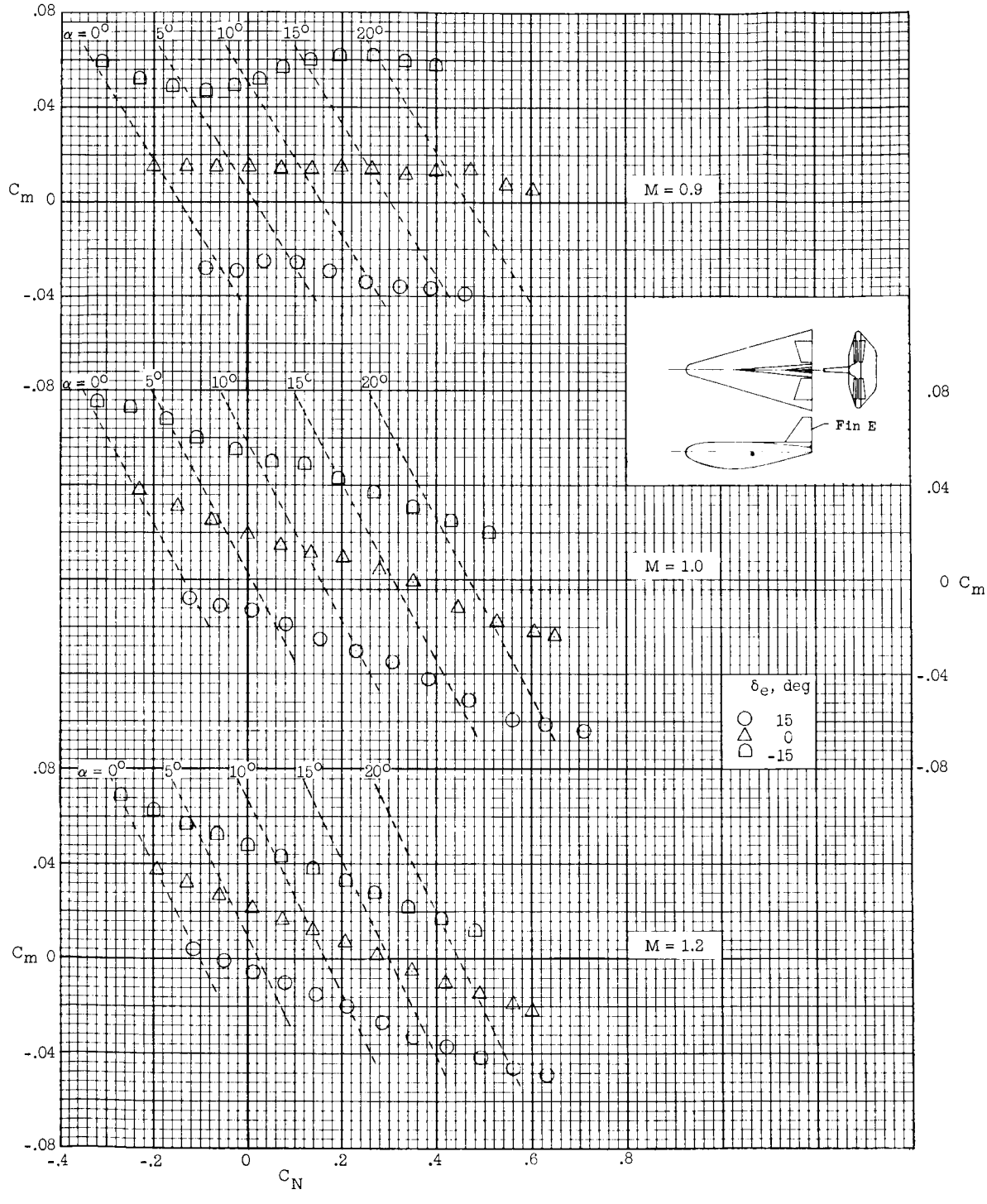

(b) M = 0.9, 1.0, and 1.2.

Figure 11.- Concluded.

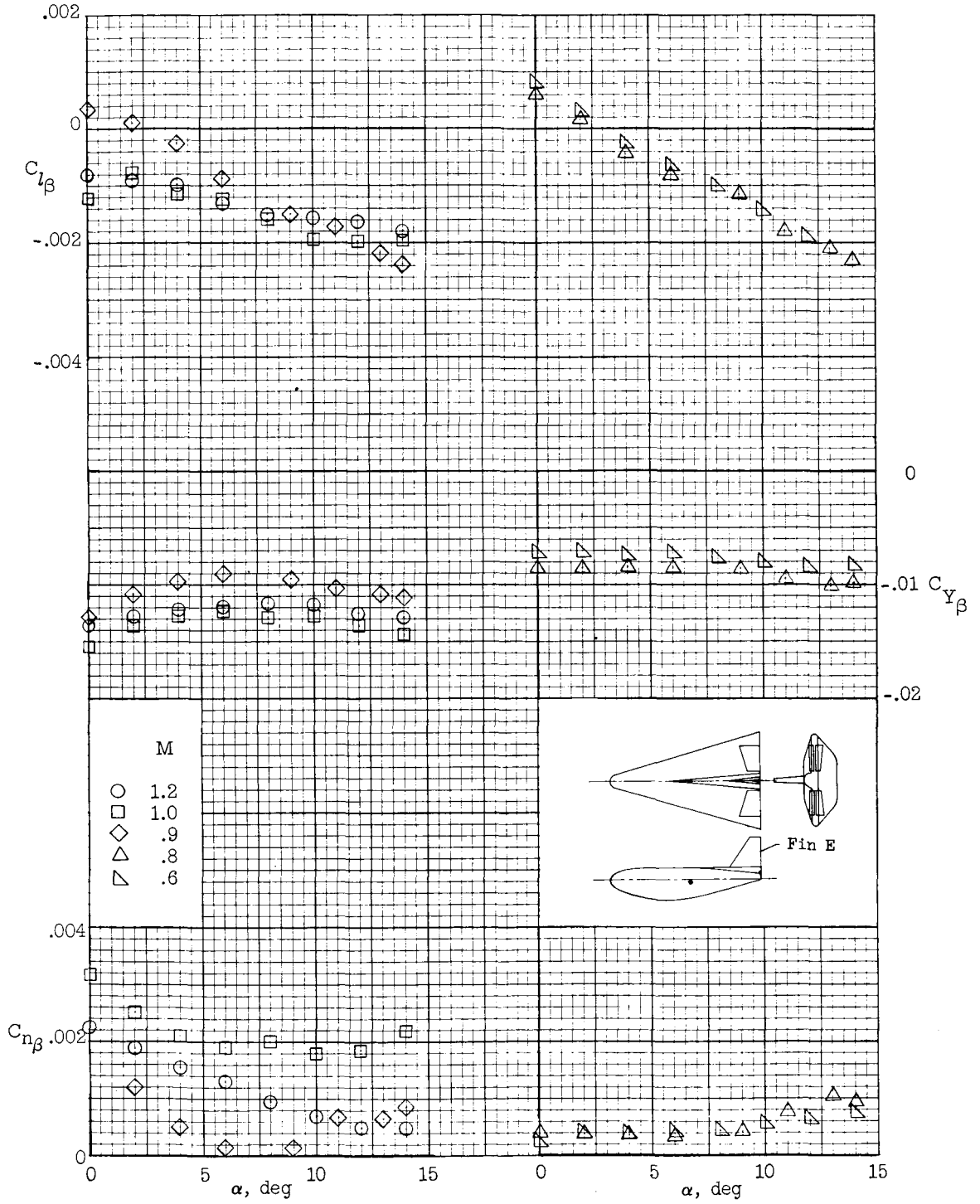

Figure 12.- Directional-lateral stability of HL-10 model with center fin E, $\delta_e = 0^\circ$, $\delta_a = 0^\circ$, and $\delta_r = 0^\circ$.

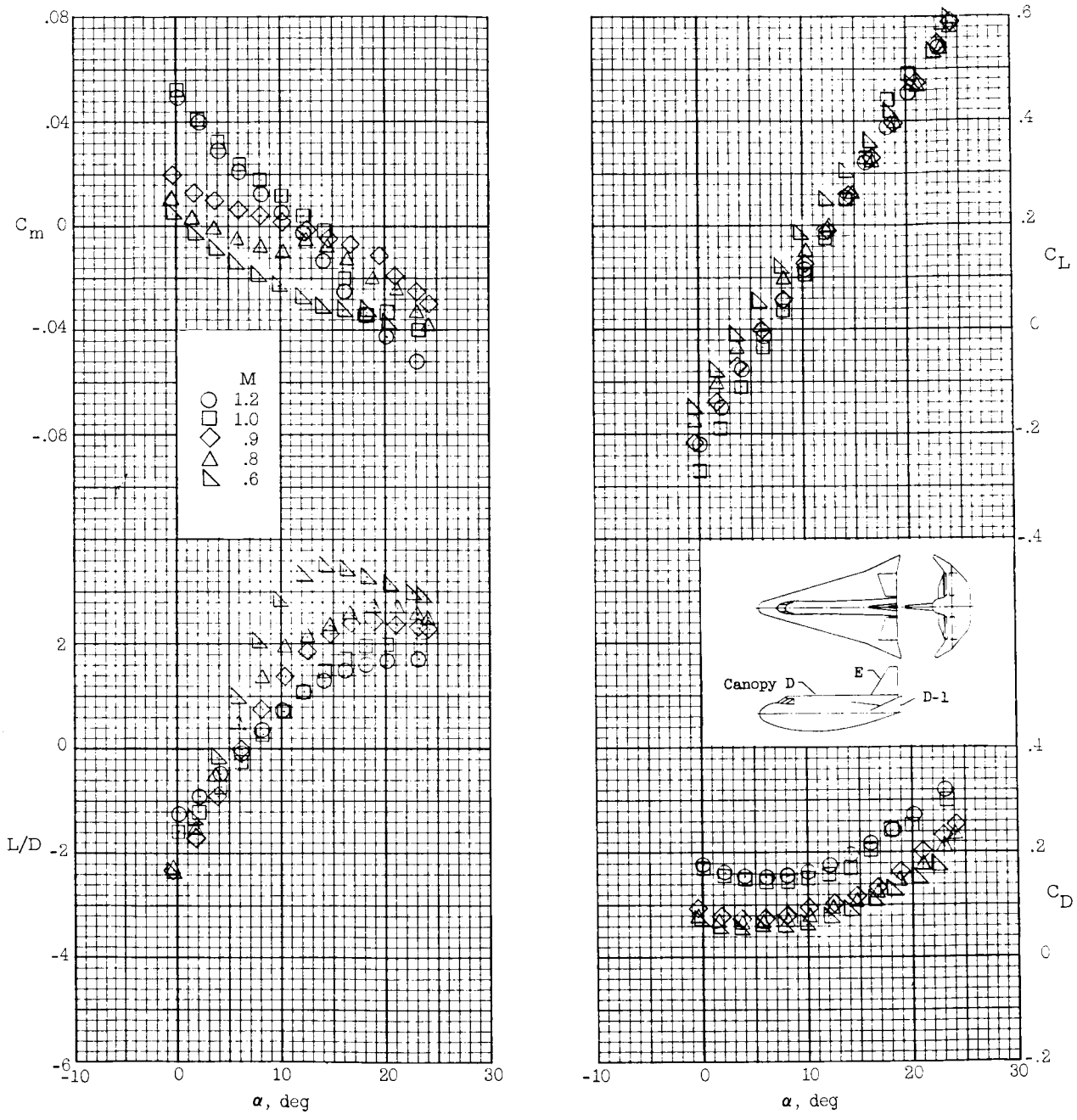

(a) Center fin E; $\delta_e = 0^o$.

Figure 13.- Longitudinal performance of HL-10 model with canopy D, tip fins D-1, $\beta = 0^o$, $\delta_a = 0^o$, and $\delta_r = 0^o$.

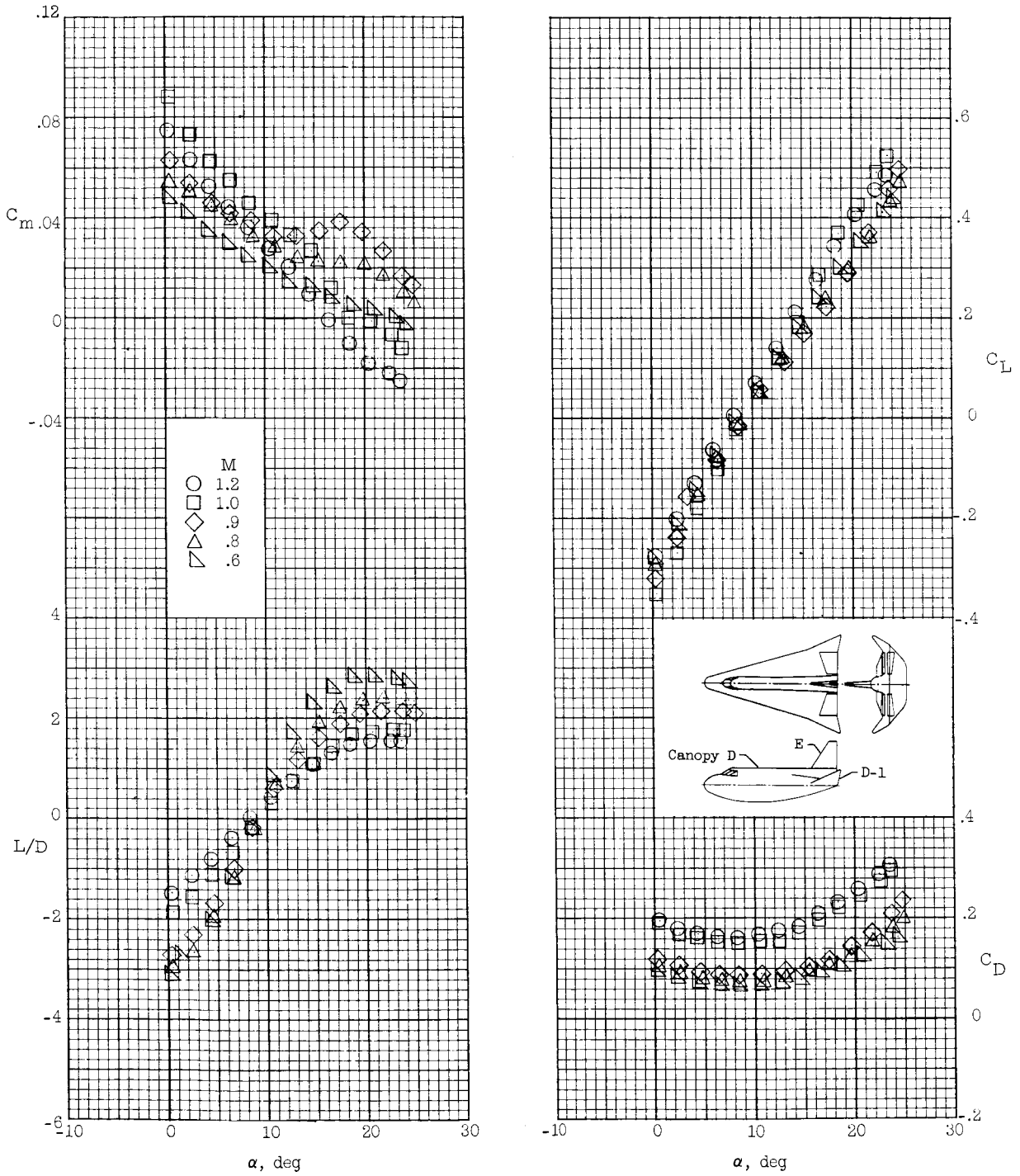

(b) Center fin E; $\delta_e = -10^\circ$.

Figure 13.- Continued.

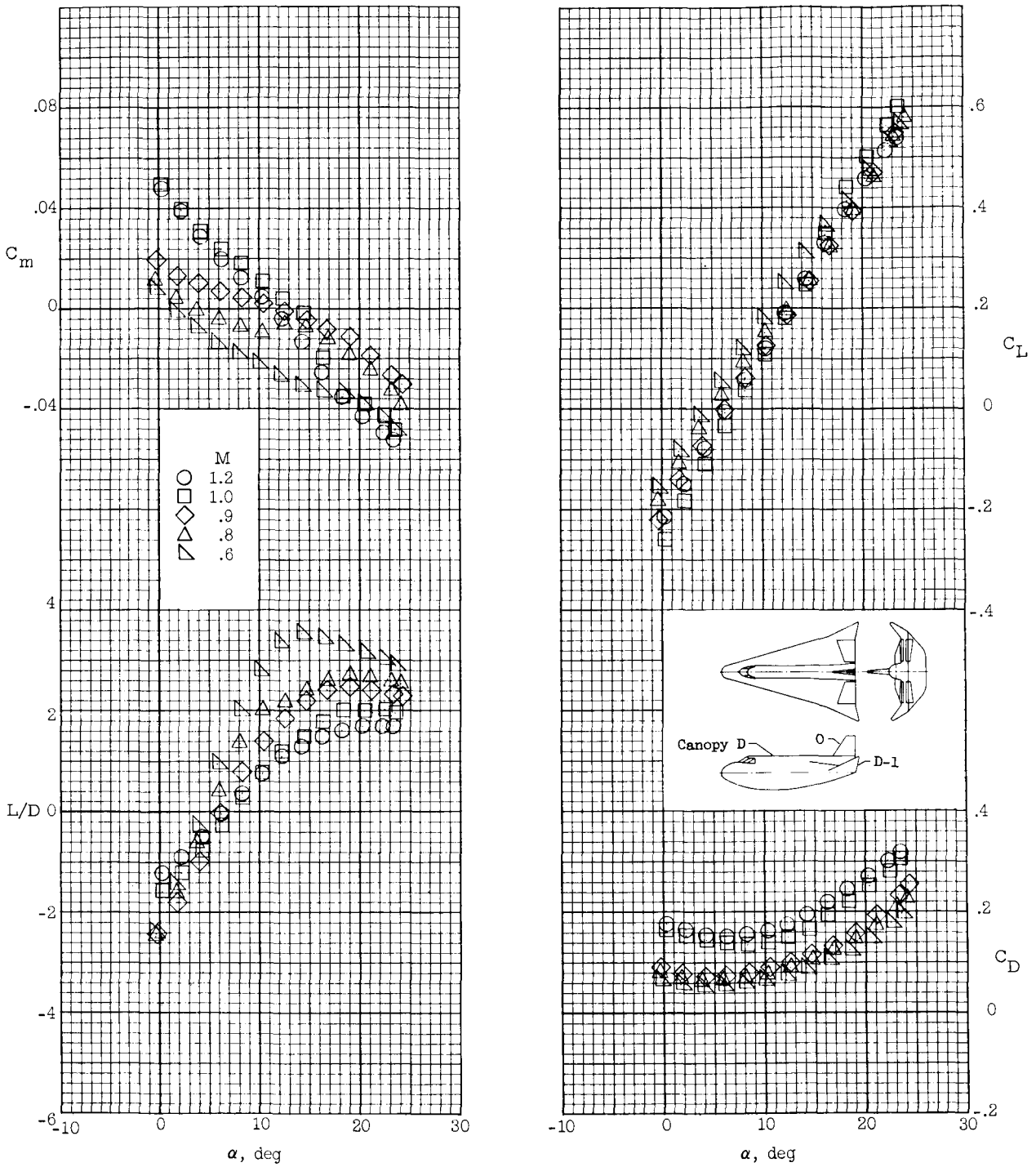

(c) Center fin 0; $\delta_e = 0^o$.

Figure 13.- Continued.

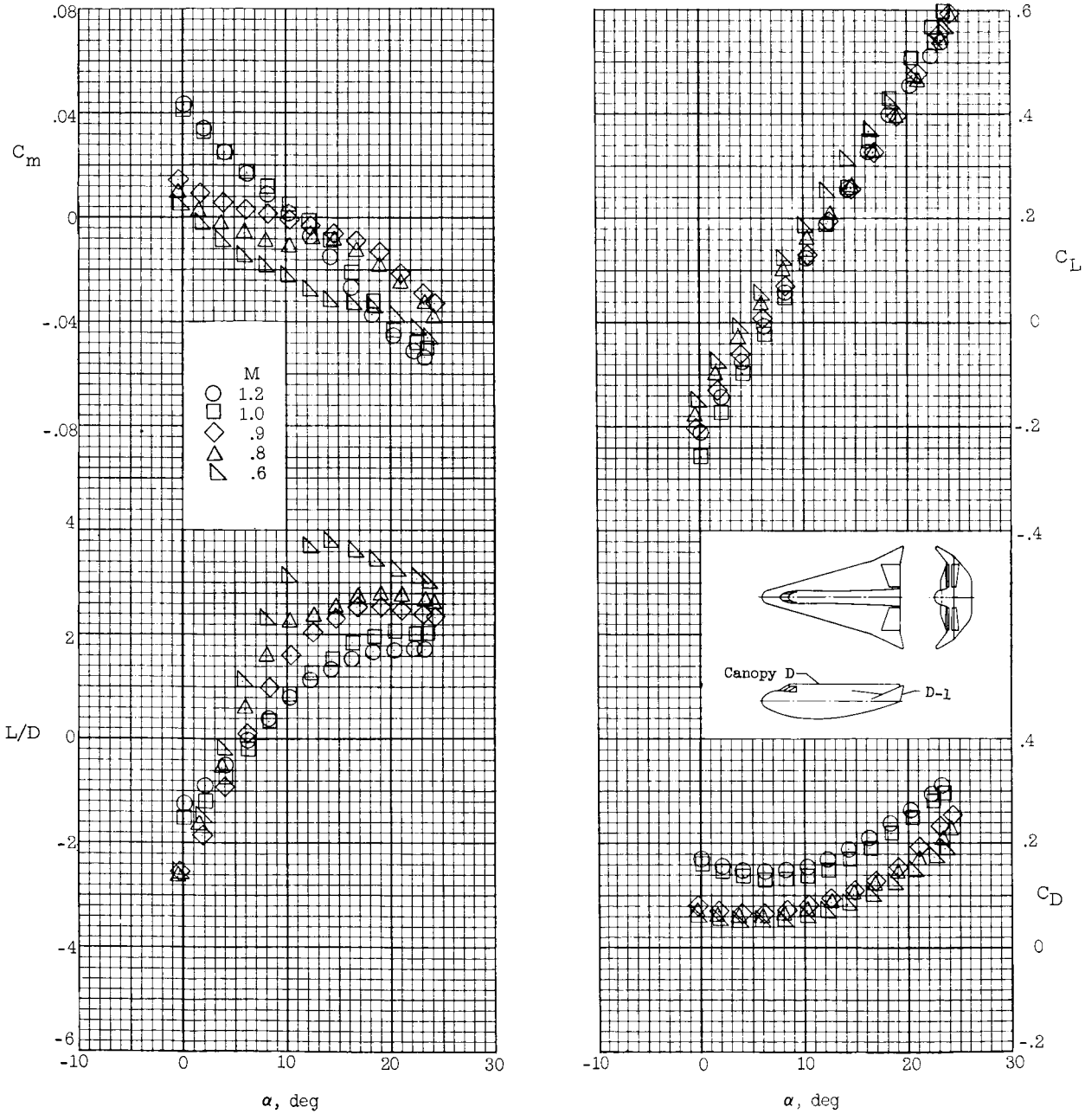

(d) No center fin; $\delta_e = 0^o$.

Figure 13.- Concluded.

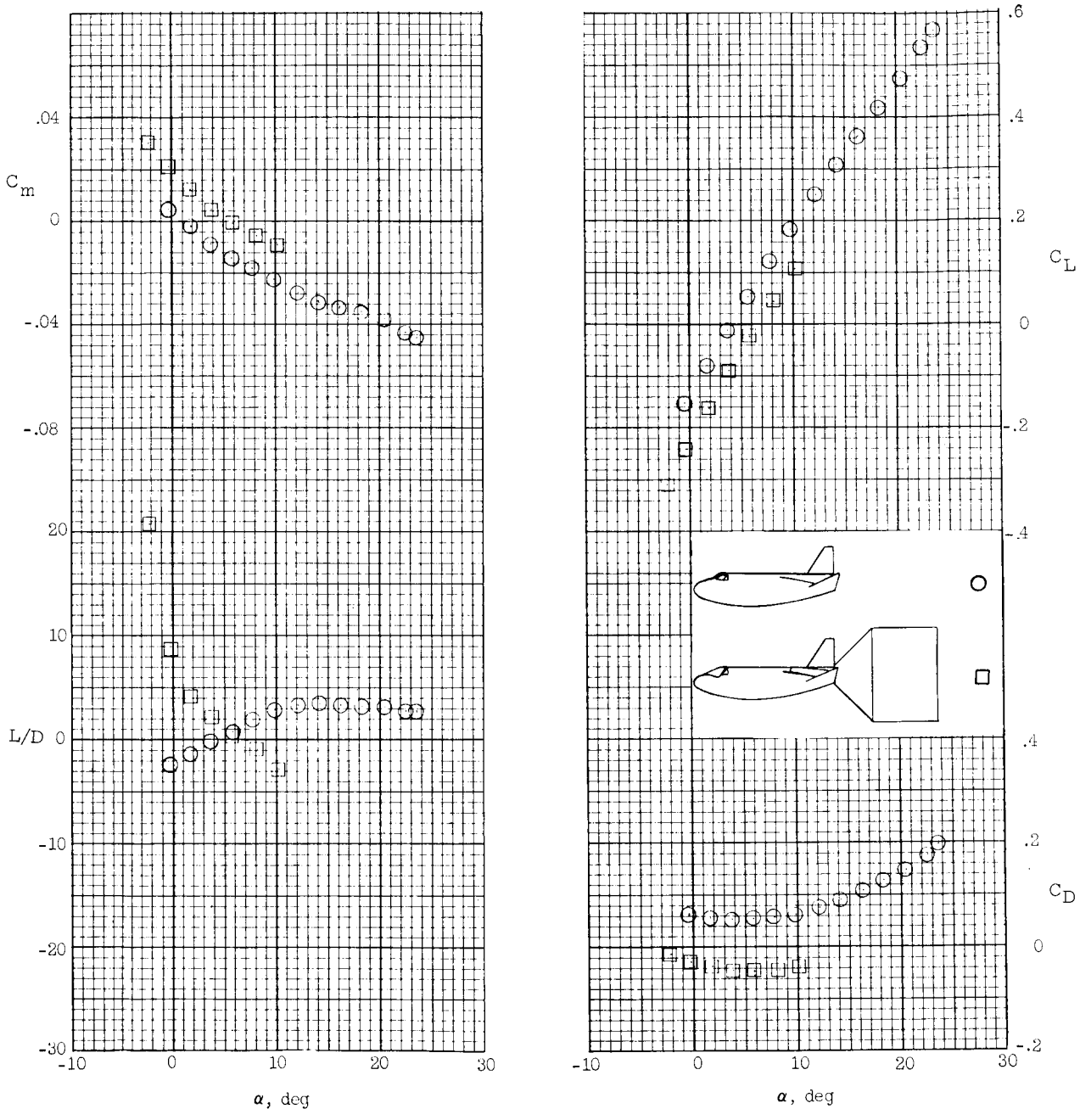

(a) M = 0.6.

Figure 14.- Effect of presence of launch vehicle on longitudinal performance of HL-10 model with canopy D, center fin E, tip fins D-1, $\beta = 0^o$, $\delta_e = 0^o$, $\delta_a = 0^o$, and $\delta_r = 0^o$.

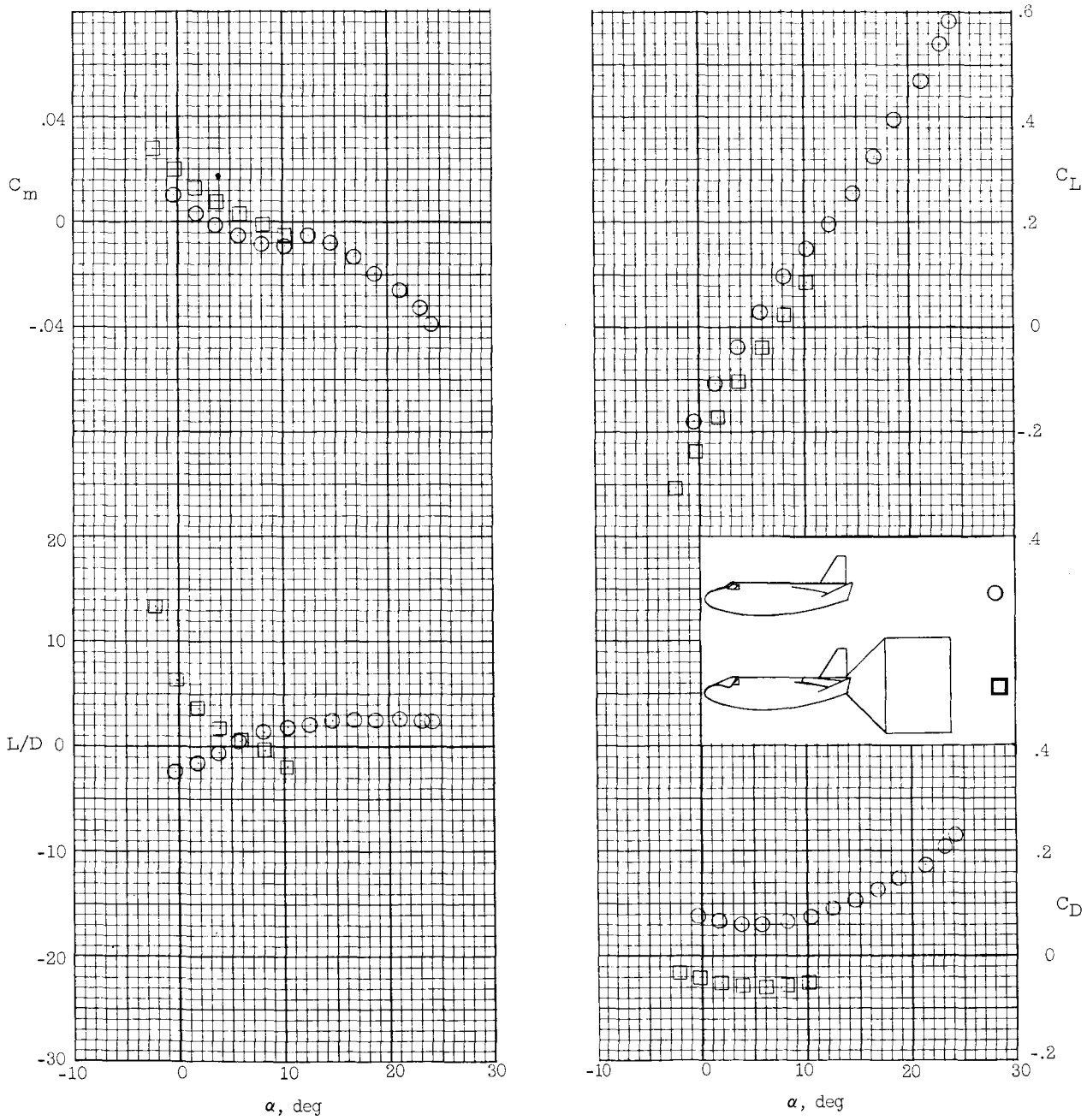

(b) M = 0.8.

Figure 14.- Continued.

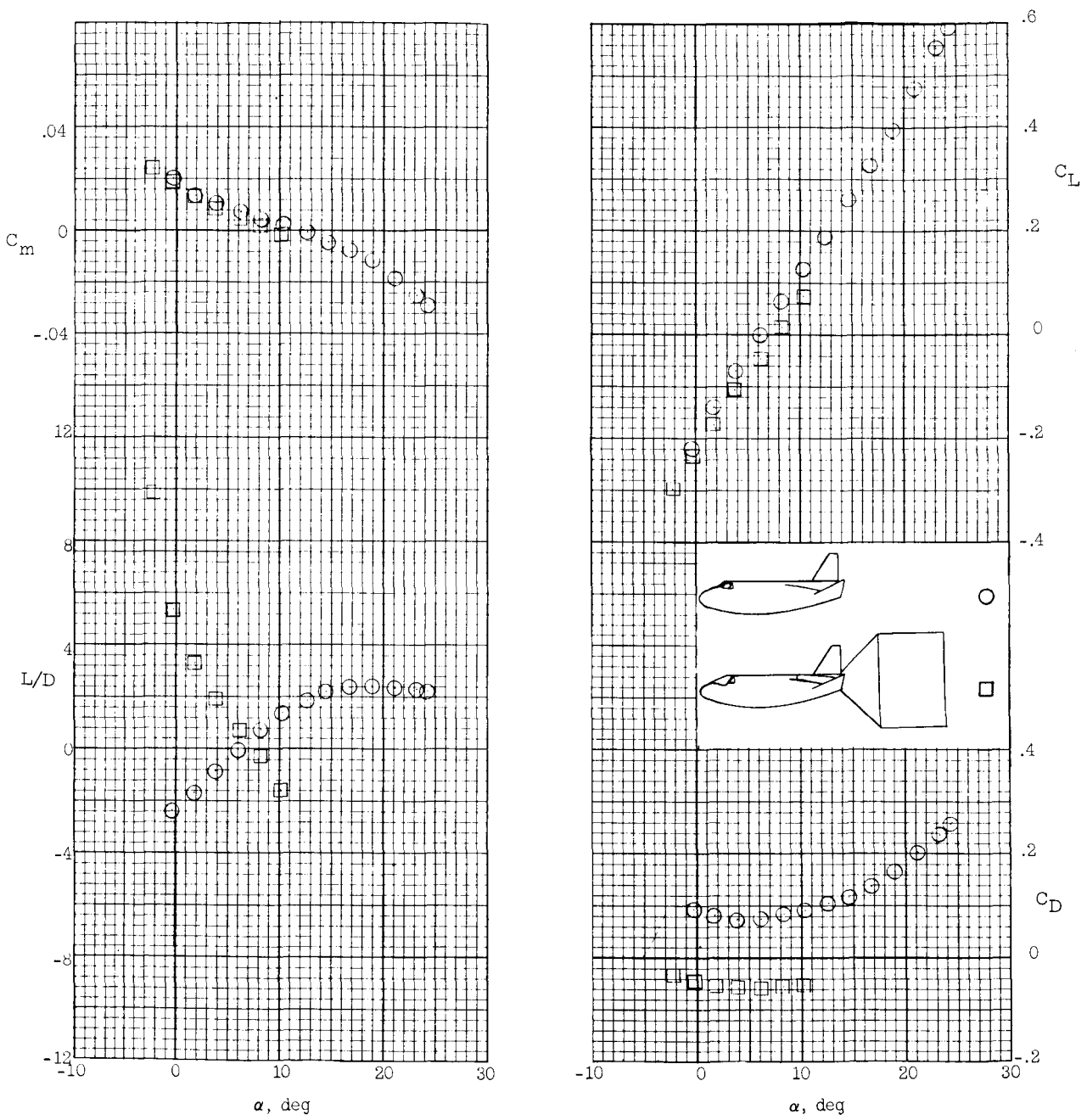

(c) M = 0.9.

Figure 14.- Continued.

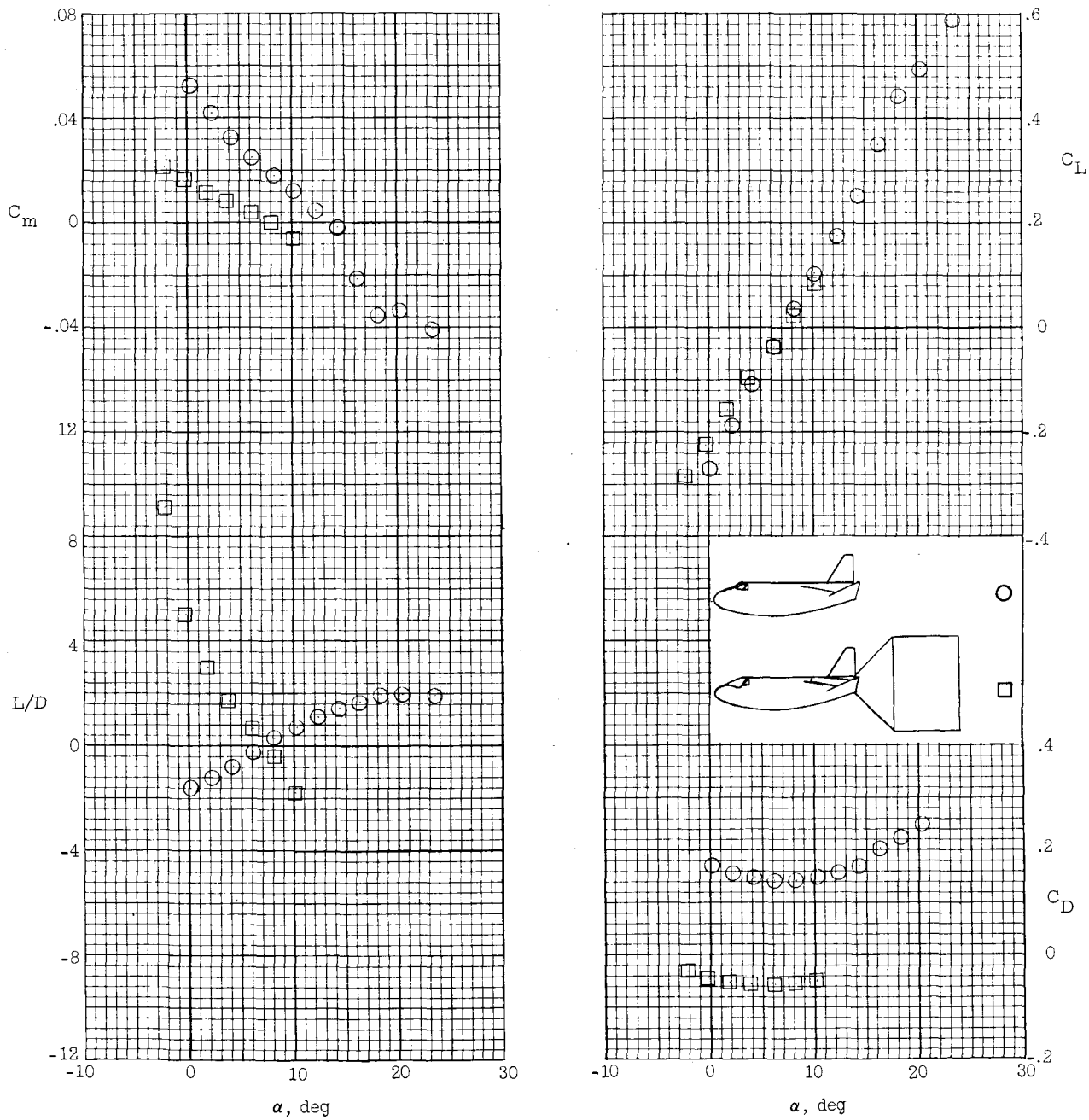

(d) M = 1.0.

Figure 14.- Continued.

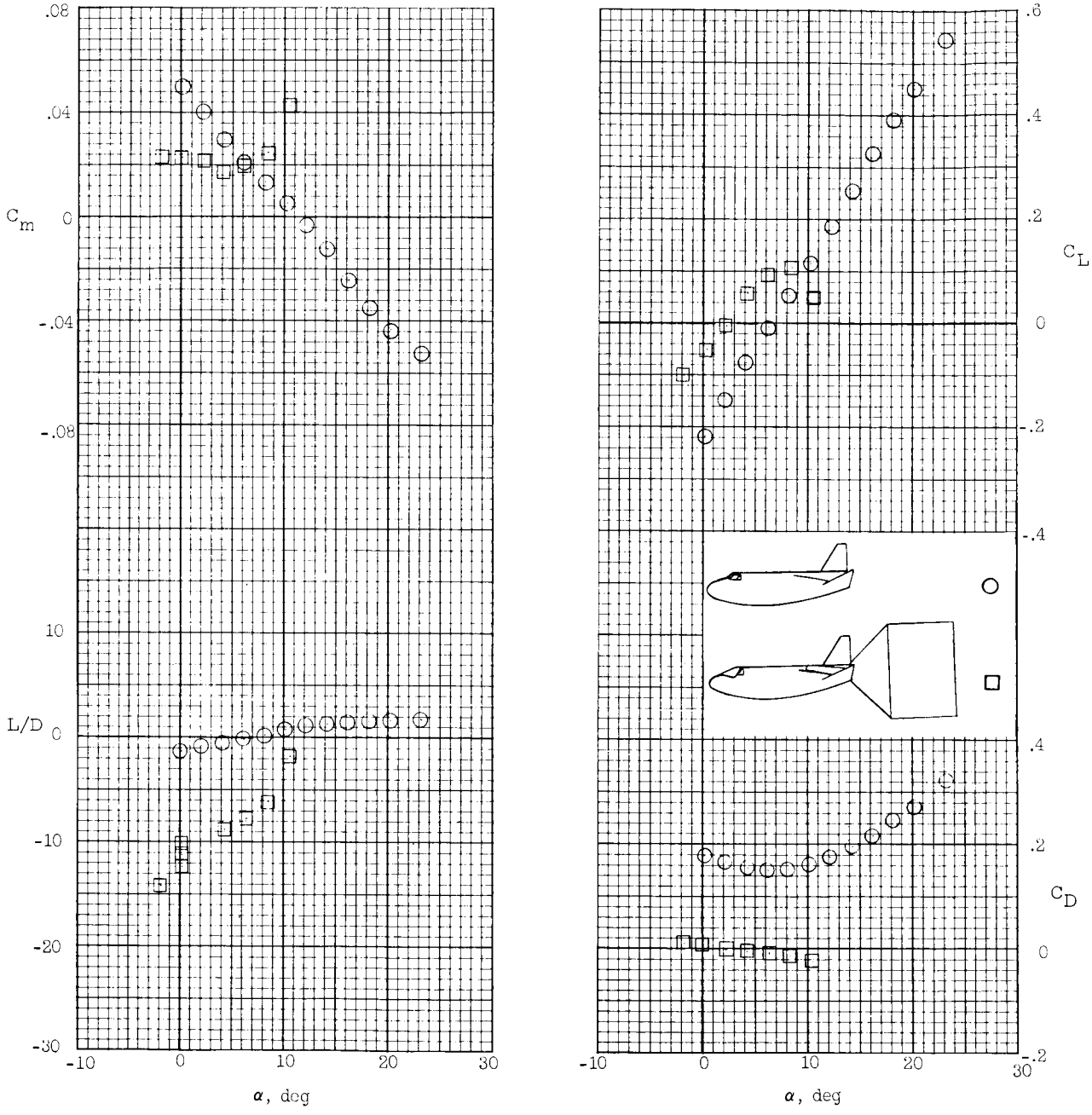

(e) M = 1.2.

Figure 14.- Concluded.

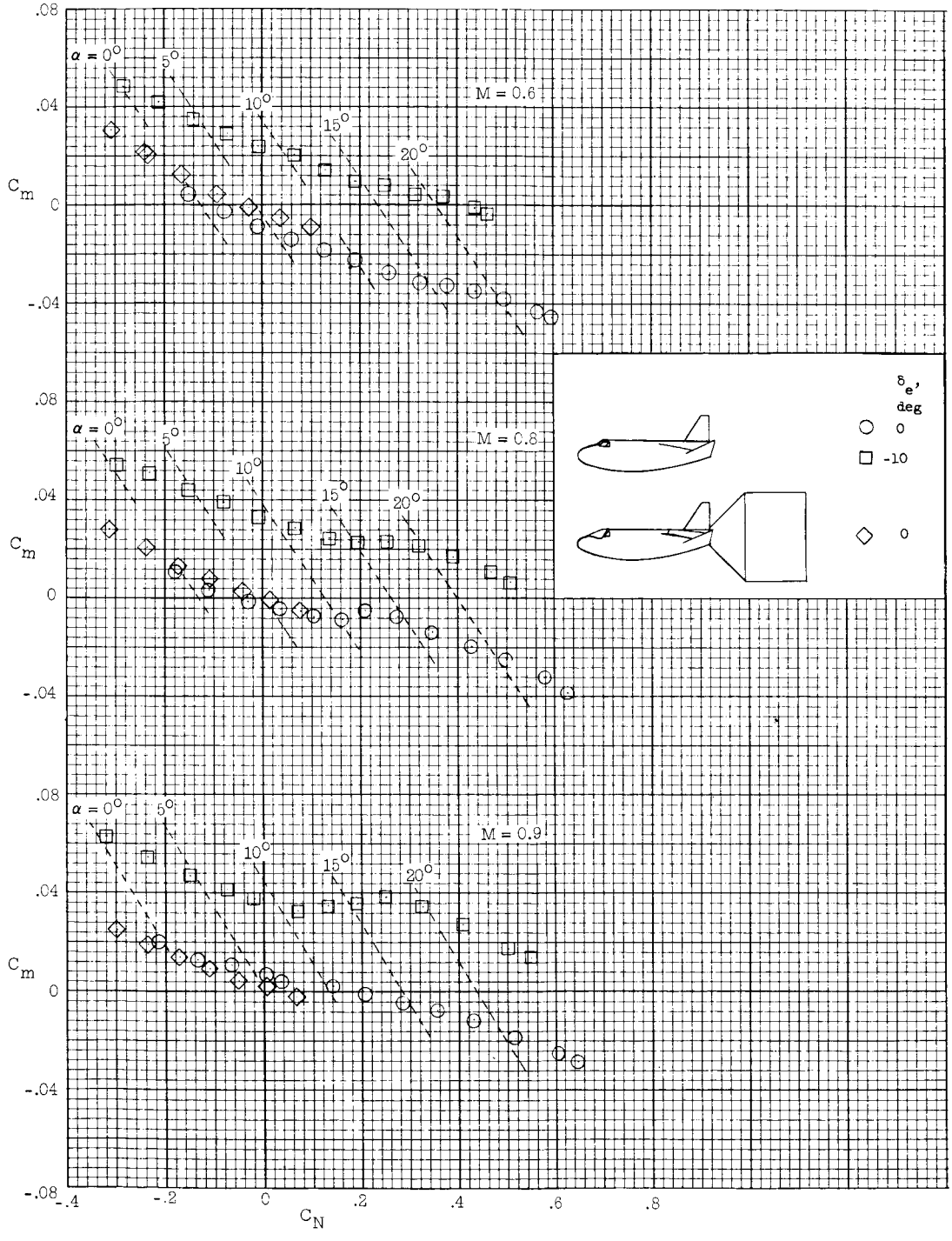

(a) M = 0.6, 0.8, and 0.9.

Figure 15.- Effect of presence of launch vehicle on longitudinal stability results with canopy D, tip fins D-1, center fin E, $\beta = 0^o$, $\delta_a = 0^o$, and $\delta_r = 0^o$.

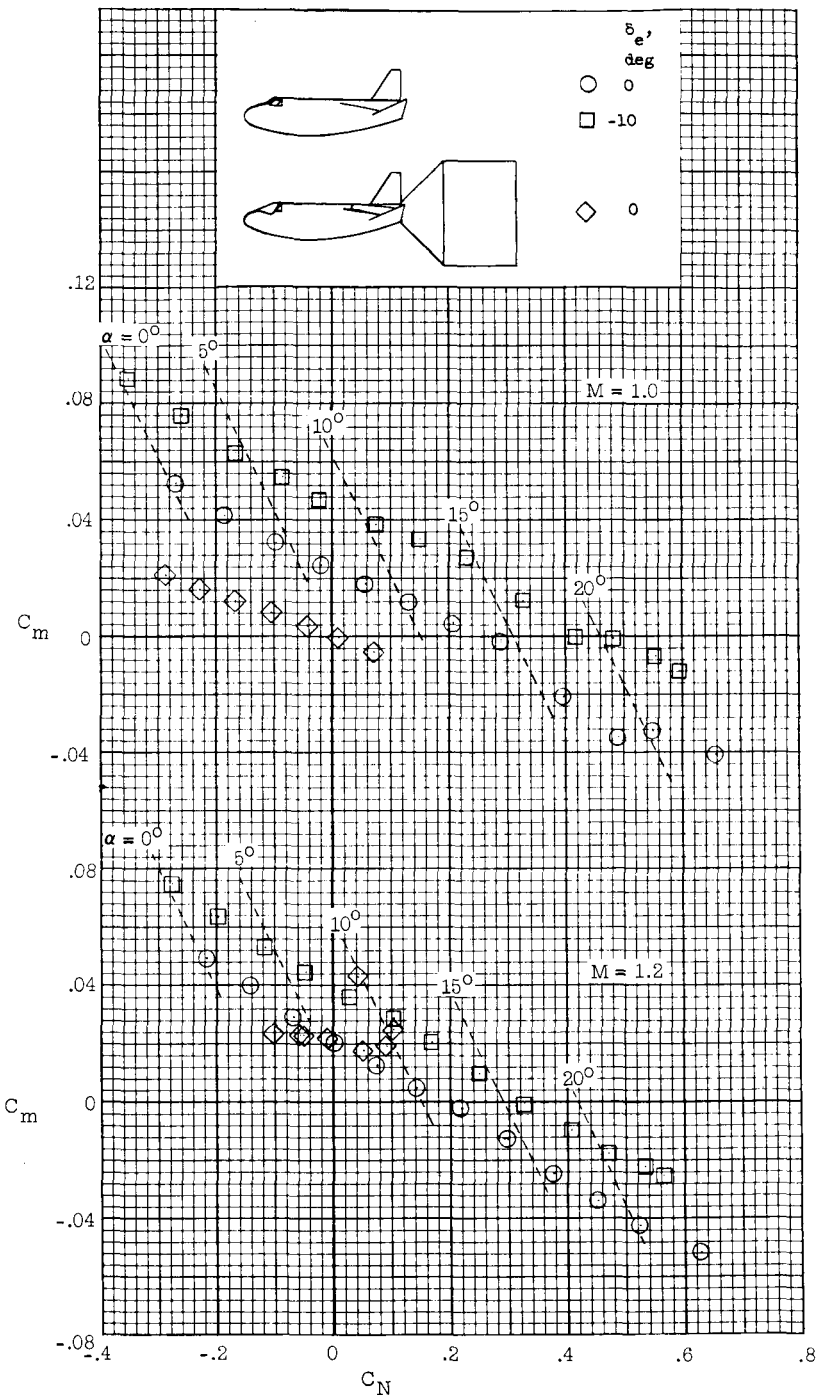

(b) M = 1.0 and 1.2.

Figure 15.- Concluded.

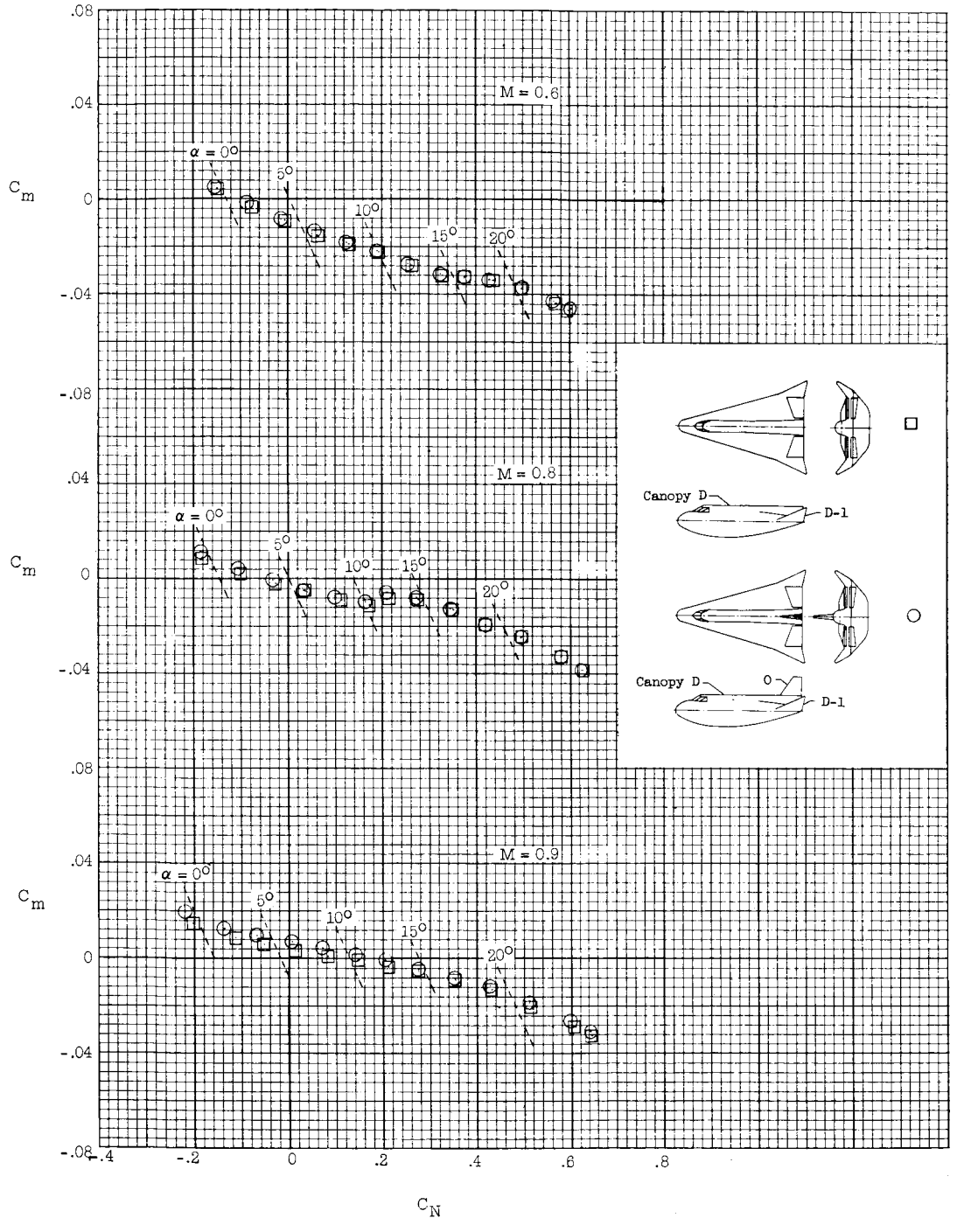

(a) M = 0.6, 0.8, and 0.9.

Figure 16.- Effects of center fin 0 on longitudinal stability results with canopy D, tip fins D-1, $\beta = 0^o$, $\delta_a = 0^o$, $\delta_r = 0^o$, and $\delta_e = 0^o$.

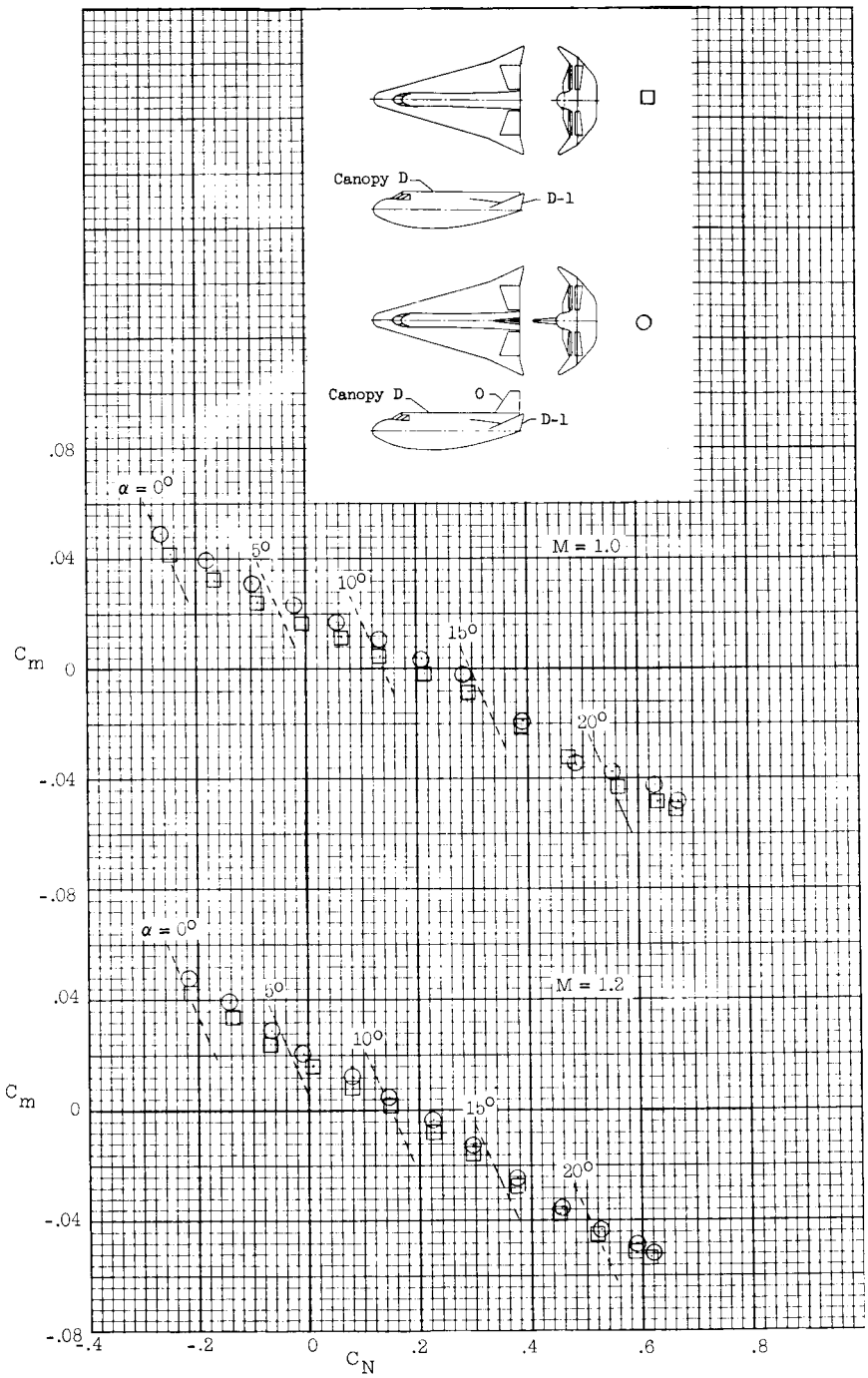

(b) M = 1.0 and 1.2.

Figure 16.- Concluded.

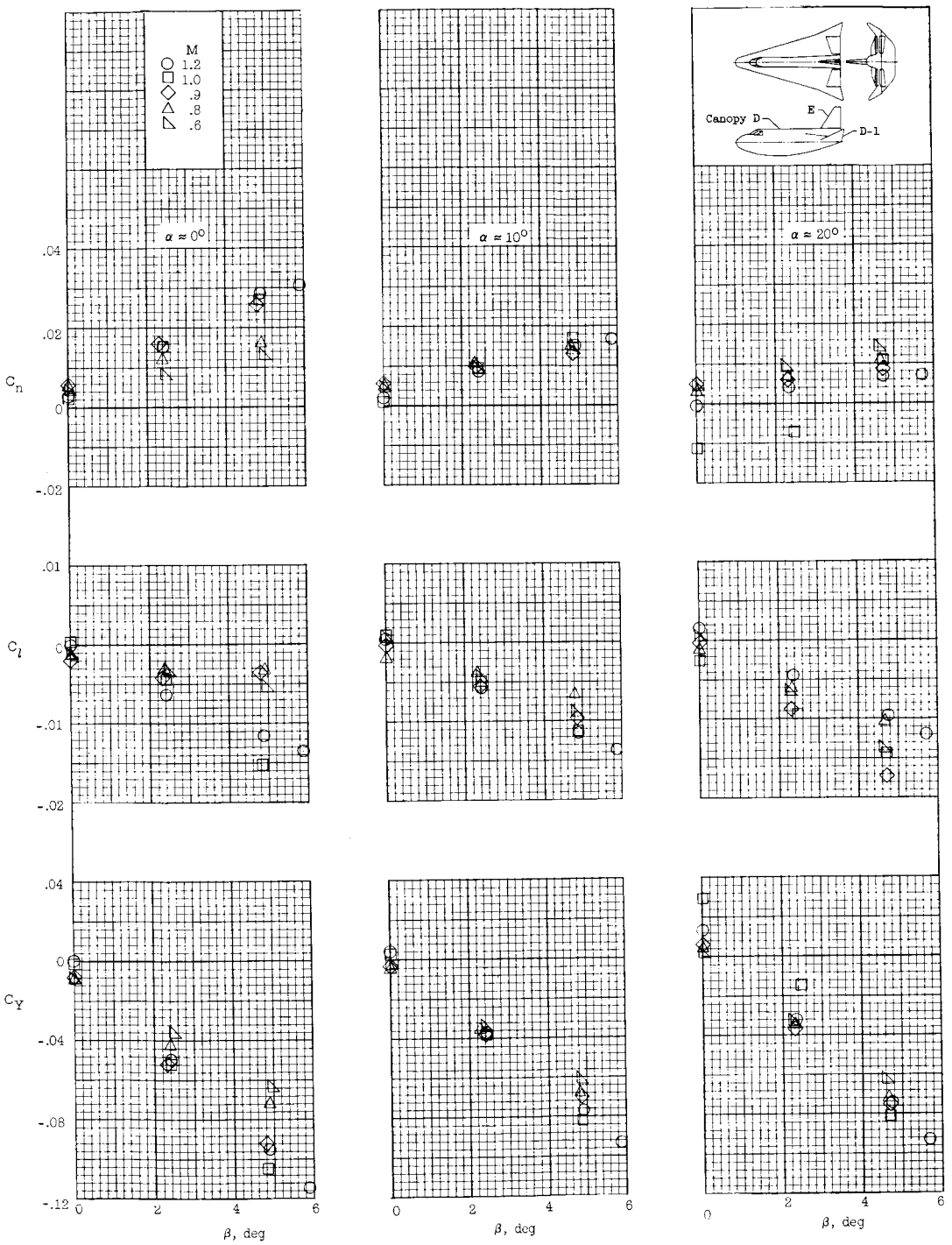

(a) Effect of β variation; center fin E.

Figure 17.- Directional-lateral stability of HL-10 model with canopy D, tip fins D-1, $\delta_e = 0^\circ$, $\delta_a = 0^\circ$, and $\delta_r = 0^\circ$.

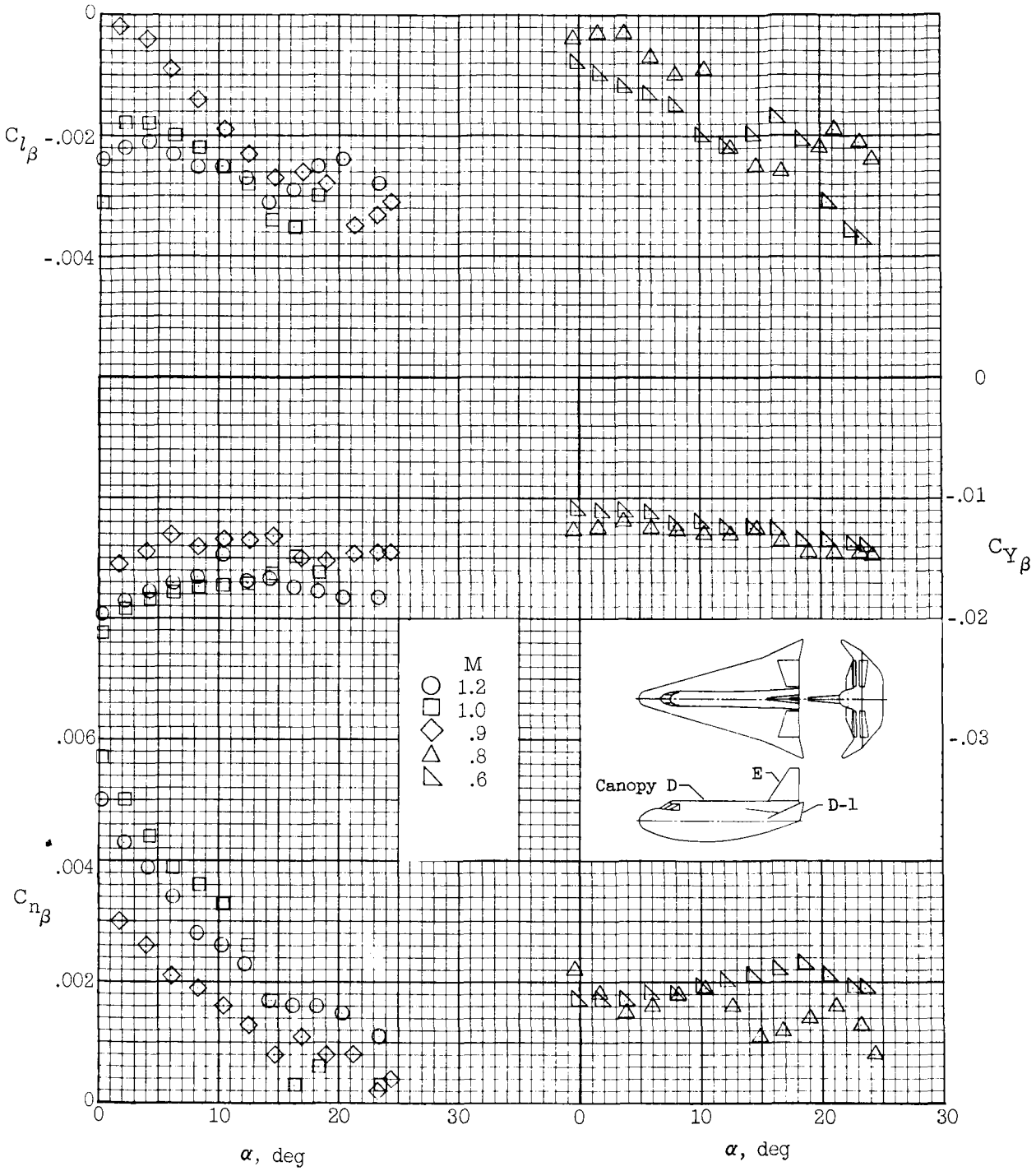

(b) Effect of α variation; center fin E.

Figure 17.- Continued.

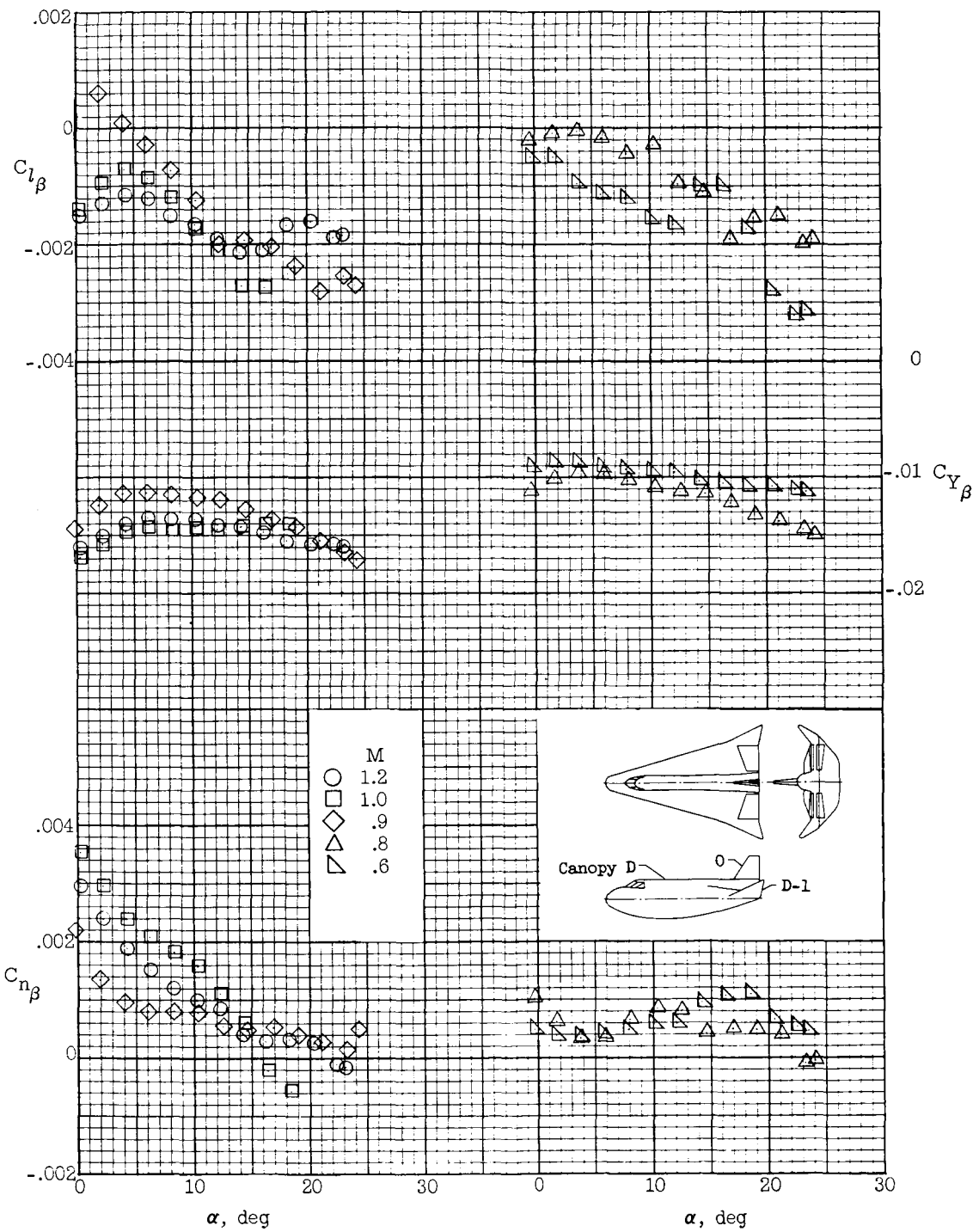

(c) Effect of α variation; center fin 0.

Figure 17.- Continued.

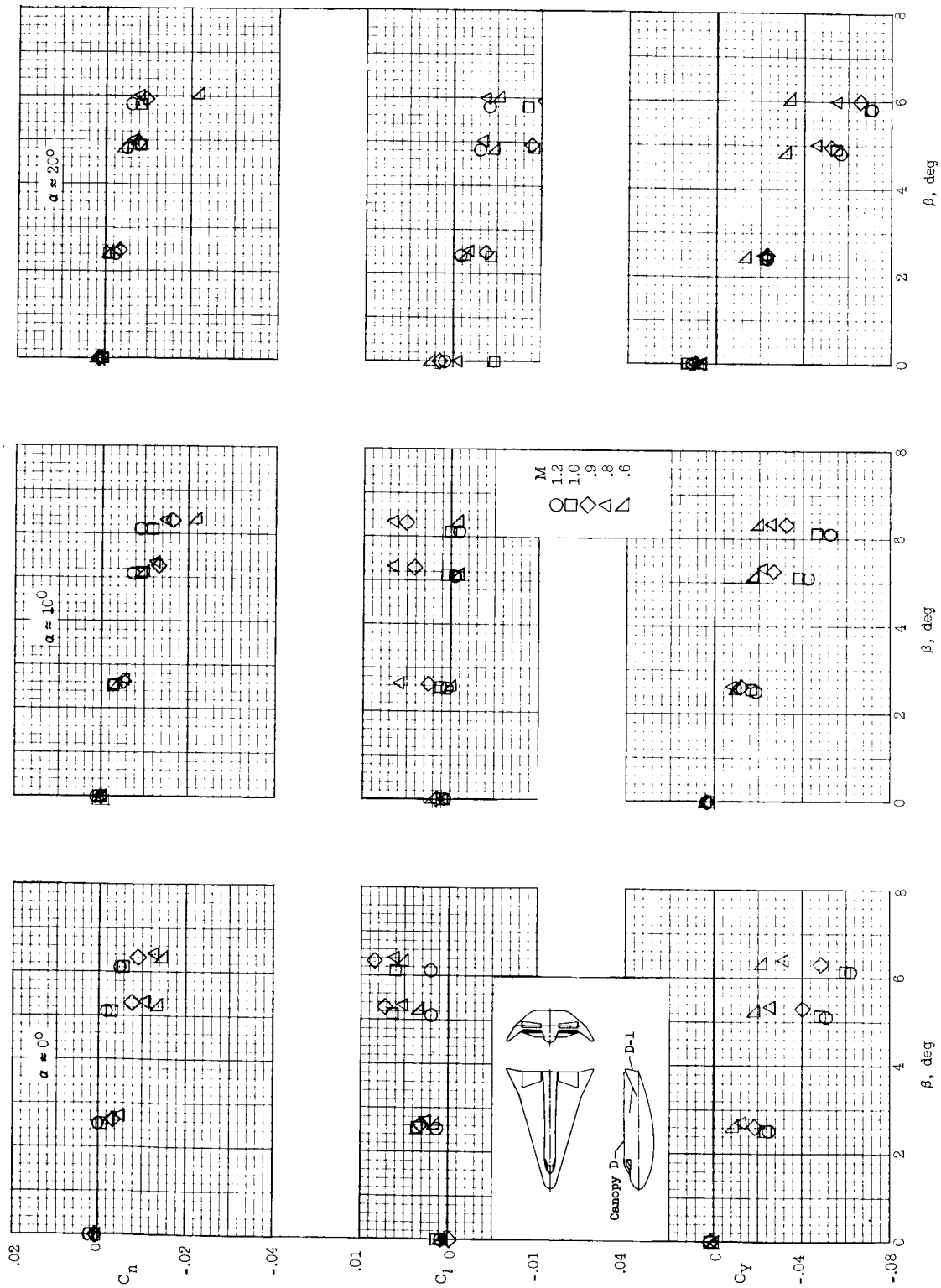

(d) Effect of β variation; center fin off.

Figure 17.- Continued.

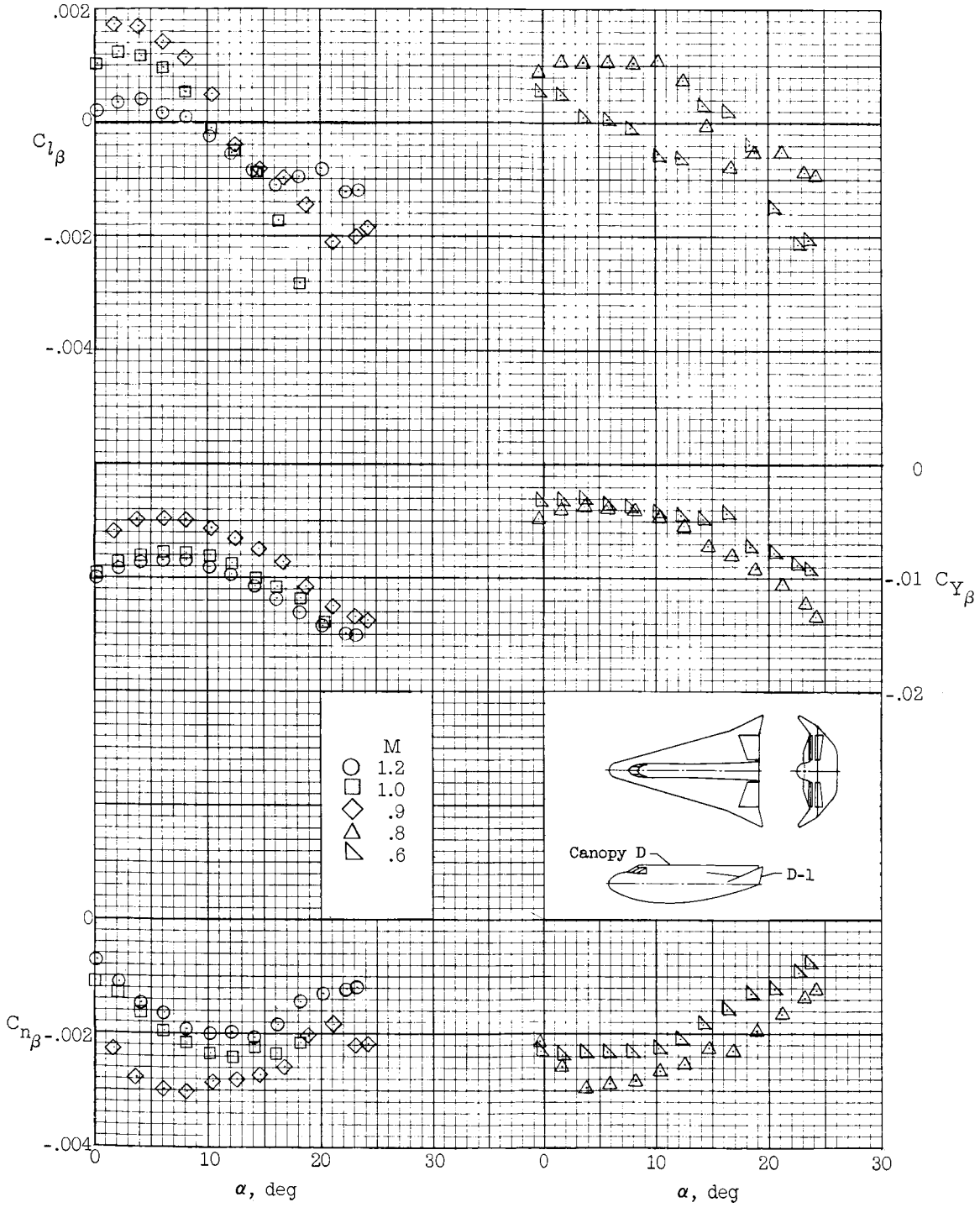

(e) Effect of α variation; center fin off.

Figure 17.- Concluded.

"The aeronautical and space activities of the United States shall be conducted so as to contribute . . . to the expansion of human knowledge of phenomena in the atmosphere and space. The Administration shall provide for the widest practicable and appropriate dissemination of information concerning its activities and the results thereof."

—NATIONAL AERONAUTICS AND SPACE ACT OF 1958

NASA SCIENTIFIC AND TECHNICAL PUBLICATIONS

TECHNICAL REPORTS: Scientific and technical information considered important, complete, and a lasting contribution to existing knowledge.

TECHNICAL NOTES: Information less broad in scope but nevertheless of importance as a contribution to existing knowledge.

TECHNICAL MEMORANDUMS: Information receiving limited distribution because of preliminary data, security classification, or other reasons.

CONTRACTOR REPORTS: Technical information generated in connection with a NASA contract or grant and released under NASA auspices.

TECHNICAL TRANSLATIONS: Information published in a foreign language considered to merit NASA distribution in English.

TECHNICAL REPRINTS: Information derived from NASA activities and initially published in the form of journal articles.

SPECIAL PUBLICATIONS: Information derived from or of value to NASA activities but not necessarily reporting the results of individual NASA-programmed scientific efforts. Publications include conference proceedings, monographs, data compilations, handbooks, sourcebooks, and special bibliographies.

Details on the availability of these publications may be obtained from:

SCIENTIFIC AND TECHNICAL INFORMATION DIVISION

NATIONAL AERONAUTICS AND SPACE ADMINISTRATION

Washington, D.C. 20546